The Dissertation Committee for Jacob Robert Adams certifies that this is the approved version of the following dissertation:

Organic Materials Development for Advanced Lithographic Applications

Committee:

C. Grant Willson, Supervisor

Brent L. Iverson

Christopher W. Bielawski

Alan Campion

Jennifer Maynard

Organic Materials Development for Advanced Lithographic Applications

by

Jacob Robert Adams, B.S. Chem.

Dissertation

Presented to the Faculty of the Graduate School of

The University of Texas at Austin

in Partial Fulfillment

of the Requirements

for the Degree of

Doctor of Philosophy

The University of Texas at Austin

August 2009

Dedicated in memory of Patricia Welsh Adams

Acknowledgements

I would like to thank my advisor, Professor Willson for his patience, understanding and guidance through the years. In my time in his group I have grown tremendously as a scientist and as a person.

Many members of the Willson group deserve a great deal of thanks for their assistance, friendship and entertainment throughout the years. Dr. Ryan Callahan and Professor Scott Grayson were invaluable colleagues for a first year graduate student and have remained both friends and valued confidants after they moved. Stefan Caporale and Dr. Bill Heath were both great friends and insightful scientists without whom I would have struggled mightily. The old men of the group, Dr. Brian Osborn and Dr. Matthew Pinnow, have provided valuable advice, guidance and many laughs both during their time as coworkers and since leaving. I would also like to thank the good people of IMEC in Leuven, Belgium, in particular Roel Gronheid, for being outstanding colleagues and valued teachers. I was fortunate enough to work with two amazingly bright and talented undergraduates, who both went on to their own graduate careers, Christy Steger and Will Durand. Yukio and Isao Nishimura provided frequent lithographic advice and the occasional Japanese lesson. Many thanks are due to Jeffrey Ryan Strahan and Börje Michael Jacobsson, who have been terrific colleagues and without whom this may never have been completed. Good luck to Chris Bates and Will Bell in their time at UT. To

each of the Drs. Polymer, I-IV, you may never have had a name but you played an invaluable role in my life, 'I will love you forever.' Perhaps most importantly, thank you to Margaret Rodgers for dealing with the bureaucracy and for never being unprepared to give a disapproving head nod or scolding looking and to Kathleen Sparks for keeping the group running smoothly while always finding time to chat, offer advice and listen to stories.

Finally, thank you to all of my family for all the love, support and patience. I couldn't have gotten luckier in the genetic lottery.

Organic Materials Development for Advanced Lithographic Applications

Publication No._____

Jacob Robert Adams, Ph.D.

The University of Texas at Austin, 2009

Supervisor: C. Grant Willson

The microelectronics industry strives for continued reduction in feature sizes to allow increased computing speed and power. This calls for continuous development of new materials. During the shift to 157 nm photolithography, it was discovered that fluorinated materials were necessary to provide sufficient transparency. Material design and synthesis to incorporate fluorine bearing norbornane based materials through an alternate means of polymerization to those used in traditional lithographic materials will be presented.

Step and Flash Imprint Lithography represents a low cost alternative to optical lithography for production of nanoscale features. Sub-20 nm features have been produced using commercial tools however the contact between the imprint template and resist formulation leaves the template prone to fouling. A new imprint resist designed to facilitate wafer reworking and template cleaning is presented.

The small amount of power available from deep ultraviolet light sources necessitates the use of systems that behave in a catalytic manner that is referred to as gain. The use of small molecules for gain necessitates a reliance on diffusion through the resist film and results in image bias. A polymeric material that undergoes depropagation catalyzed by a single photochemical event and causes a solubility change due to this event represents a system that possesses gain while removing diffusion bias. Progress towards such a system is presented.

Table of Contents

List of Tables

List of Figures

CHAPTER 1 INTRODUCTION TO PHOTOLITHOGRAPHY

The term revolution is most frequently associated with political events such as the American, French and Bolshevik revolutions. Ultimately, all political revolutions fail. The American and French revolutions, which ushered in personal liberties, have been eroded by socialism and its intrusion on individuals' liberties by replacing personal will and responsibility with government mandates. Counter to their own hopes, the Bolsheviks successfully proved that the populace cannot be relied upon to work toward the improvement society as a whole at the expense of one's own greed, particularly for power. More long lasting revolutions occur without political motives and in spite of politicians' attempts to handicap them. The industrial revolution touched nearly every aspect of modern day life and seems in no hurry to go away despite the hippy generation's best efforts. More recently the term has been attached to the 'digital revolution'. This seems appropriate as the 'information age' accompanying the digital revolution likely has had a broader effect on the world, reaching even remote areas largely unaffected by the industrial revolution, than all of the aforementioned movements and looks poised to remain a part of the human experience far into the future.

Early computational devices began appearing in the 19th century and were mechanical or electro-mechanical machines. The first fully electronic computational devices began to appear in the early 1940s. They were physically very large and relied on vacuum tube technology. An early example, the Electronic Numerical Integrator and Computer (ENIAC), required approximately 18,000 vacuum tubes and occupied a space of 680 square feet. ENIAC and others demonstrated both the potential of computers and the necessity to find a small, fast and efficient replacement for vacuum tubes.

This replacement, which ushered in the digital revolution, was soon found in the transistor. The invention and early evolution occurred over the period from 1947-1952 at Texas Instruments. William Shockley is most often credited with this invention. While the original patents for transistors do not include his name, he shared the Nobel Prize in Physics in 1956 with two colleagues. The credit stems from the fact that the most effective transistors produced during this time, which evolved into early generation technologies, are attributed to Shockley's work.

Transistors rely on semiconducting materials and can function as a rectifier, an amplifier and an electronic switch. Transistors rapidly replaced vacuum tubes because they are cheaper, longer lasting, consume less space, function more efficiently and perform more reliably. This allowed for smaller and more powerful electronic devices to be produced.

As technology progressed more complex electronic devices began to push the transistor to its performance limits. Soldering together an entire electronic device with a large number of transistors increased the likelihood of a bad connection. As complexity increased, the number of transistors caused an increase in the physical length of the wiring between transistors, adversely affecting the speed of the device.

The introduction of the integrated circuit (IC) in 1959 by both Jack Kilby of Texas Instruments and Robert Noyce of Fairchild Semiconductor overcame these limitations. ICs incorporate passive devices, such as resistors and capacitors, and active devices, transistors. The IC design removes the mechanical issues due to soldering, thus allowing devices to be miniaturized. The transistor started the digital revolution but the IC increased its pace as semiconductor manufacturers fought for market share by designing smaller and more complex devices.

THE DRIVE TO SMALLER DEVICES

Like any new technology, there were dramatic improvements in the initial utility and capability of ICs. To a casual observer, the initial growth may have seemed like an enormous leap in manufacturing ability that would represent an unsustainable growth rate. Industry insiders noticed that consumer demand and subsequent competition for consumer dollars would necessitate the industry to continue to grow at this rate. The most notable observation from this early period in IC manufacturing came from Gordon Moore who co-founded and later became the CEO of Intel Corporation. Moore's 1965 observation published in Electronics Magazine stated:

> *'The complexity for minimum component costs has increased at a rate of roughly a factor of two per year... Over the longer term, the rate of increase is a bit more uncertain, although there is no reason to believe it will not remain nearly constant for at least 10 years.'*[1]

This statement has come to be known as Moore's Law. Moore sketched this observation to show that the manufacturing costs for transistors would decrease such that continually more complex products could be offered at the same price due to a reduction in the cost per transistor (Figure 1.1).

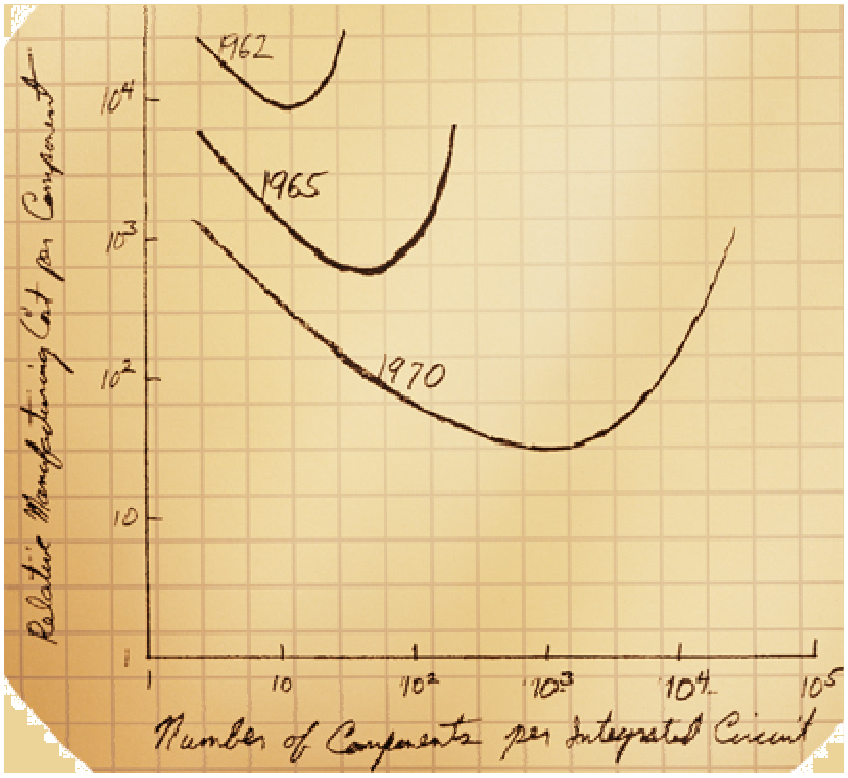

Figure 1.1 Moore's sketch of the decreasing cost to manufacture components and its impact on number of components per IC[1]

This observation is now more frequently evaluated in terms of increasing the number of transistors on an IC, which is projected to double every 18-24 months. Figure 1.2 shows commercially available Intel processors from a three and a half decade period to demonstrate the increase in the number of transistors per IC.

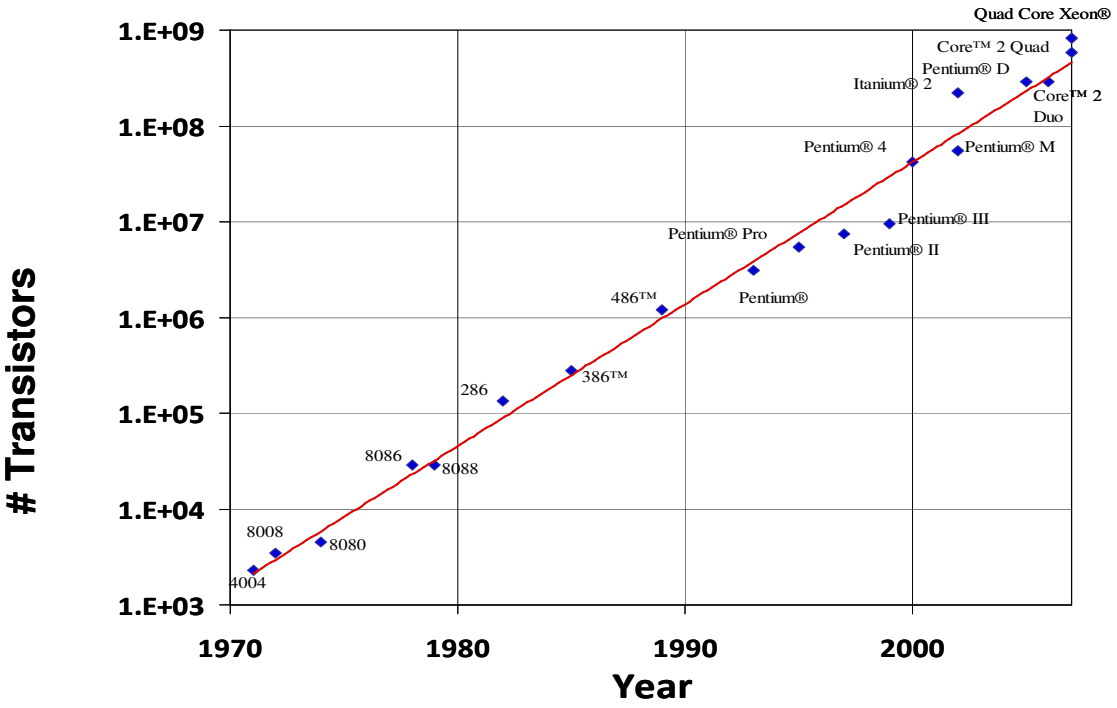

Figure 1.2 Exponential growth of transistors over time in an IC[2]

The number of transistors on an Intel processor has increased from 29,000 in 1978 to 42,000,000 in 2000.[2] If consumer demand and corporate innovation in the auto industry had followed this trend with respect to average fuel economy which was 18 miles per gallon (MPG) in 1978[3] a car would have traveled just over 26,000 MPG in 2000. As is, the automobile industry had reached a stunning 27.5 MPG by 2000 thus falling a mere three orders of magnitude short.

To keep pace with Moore's Law, the semiconductor industry must constantly be innovating in the areas of chemistry, physics and engineering. Photolithography is an area in which these three fields overlap.

THE PHOTOLITHOGRAPHIC PROCESS

Photolithography is a multi-step process used to pattern silicon wafer substrates. The term comes from Greek roots with *photo-* meaning light and *–lithography* meaning

to write with stone. The term may not translate perfectly as photolithography is used to mean writing with light, which happens to be far faster than using stone.

The photolithographic process (Figure 1.3) begins with a coated silicon wafer. A photoresist material, so named because of its light sensitivity (*photo-*) and its resistance to subsequent etch steps (*-resist*), is spin coated on the wafer after which a post-apply bake (PAB) is used to remove residual solvent. A chromium coated quartz photomask in which the desired feature pattern has been etched is used for the exposure step. The areas in which light passes through the mask and irradiates the film undergo a chemical change which is further driven by a post-exposure bake (PEB). A development step dissolves away the exposed areas in the case of a positive-tone photoresist and the opposite for negative-tone. Only positive-tone resists will be discussed from here on. The pattern is transferred through the substrate to the silicon wafer using a reactive ion etch (RIE) and finally the remaining resist is stripped leaving the desired features.

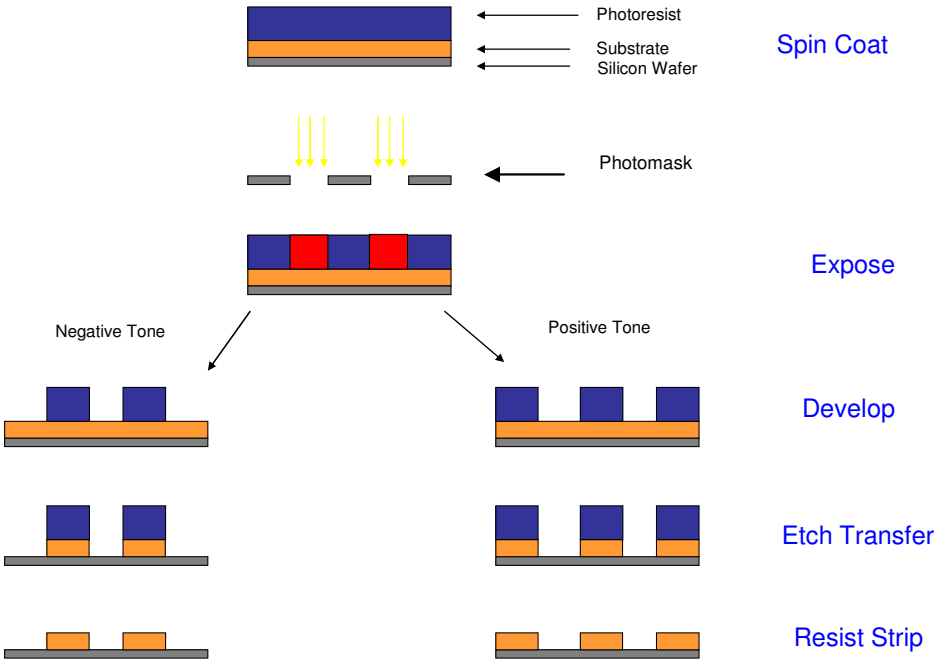

Figure 1.3 The photolithographic process

Subsequent processing steps followed by additional photolithographic procedures build the multilayer devices that serve as CPUs and memory devices.

Photoresist Formulation and Spin Coating

For industrial uses, photoresists are purchased from vendors as multi-component formulations in solution. The primary components of a photoresist are an acidic, aqueous basic soluble polymeric material, which has been protected to change its solubility, and a photoacid generator (PAG) dissolved in a low-volatility, low-viscosity non-toxic organic solvent. The photoresist is dispensed onto the coated silicon wafer and the wafer is spun at high speeds to distribute the resist across the wafer.

Post Application Bake and Exposure

After spin coating the wafer is transferred to a temperature controlled hot plate to drive off residual solvent and promote better adhesion to the substrate. The PAB is performed at a temperature below the glass transition temperature (T_g), typically 90-130 ^oC for 30-90 s. After the PAB, the wafer is transferred to an exposure tool. Exposure is performed through the photomask in a step and repeat fashion many times across the wafer. In the areas exposed to light the PAG produces an acid ($PAGH^+$).

Post Exposure Bake and Development

The exposed wafer is subjected to an additional bake step to provide the energy of activation for the acidolysis of the protecting group. The acid catalyzes deprotection of the protected polymer thus switching its solubility. The time and temperature of the PEB is dependant on the protection chemistry for each resist. For acetal protecting groups the PEB is typically about 90 ^oC while for *tert*-butyl carbonate (*t*-BOC) and *tert*-butyl esters it is typically about 110-130 ^oC. The wafer is then immersed in 0.26 N

tetramethylammonium hydroxide (TMAH). This dissolves the exposed areas of the photoresist film leaving a three-dimensional image that provides access to the substrate.

Reactive Ion Etch and Resist Stripping

The image is then transferred into the substrate through an RIE process. A high electric field is applied over a gas at low pressure to generate ions that are used to etch the silicon substrate. The photoresist is required to *resist* this etch process to provide high fidelity image transfer. After etching to the desired depth, the remaining photoresist is stripped away. A different etch chemistry is used that selectively removes the photoresist without affecting the underlying substrate. This whole process is repeated many times to construct the final device.

Projection Lithography

Current photolithography is generally performed with projection printing utilizing ultraviolet (UV) light. In projection printing light passes through a reticle or mask and is focused on the wafer through a 4:1 reduction lens system (Figure 1.4). The wavelength of light utilized is critical as shorter wavelengths of light allow smaller features to be printed. The direct proportionality of this relationship is described by the Rayleigh equation (Equation 1.1). Other factors governing the minimum feature resolution are the numerical aperature (NA) of the lens and a resist dependent factor known as the "*k* factor."

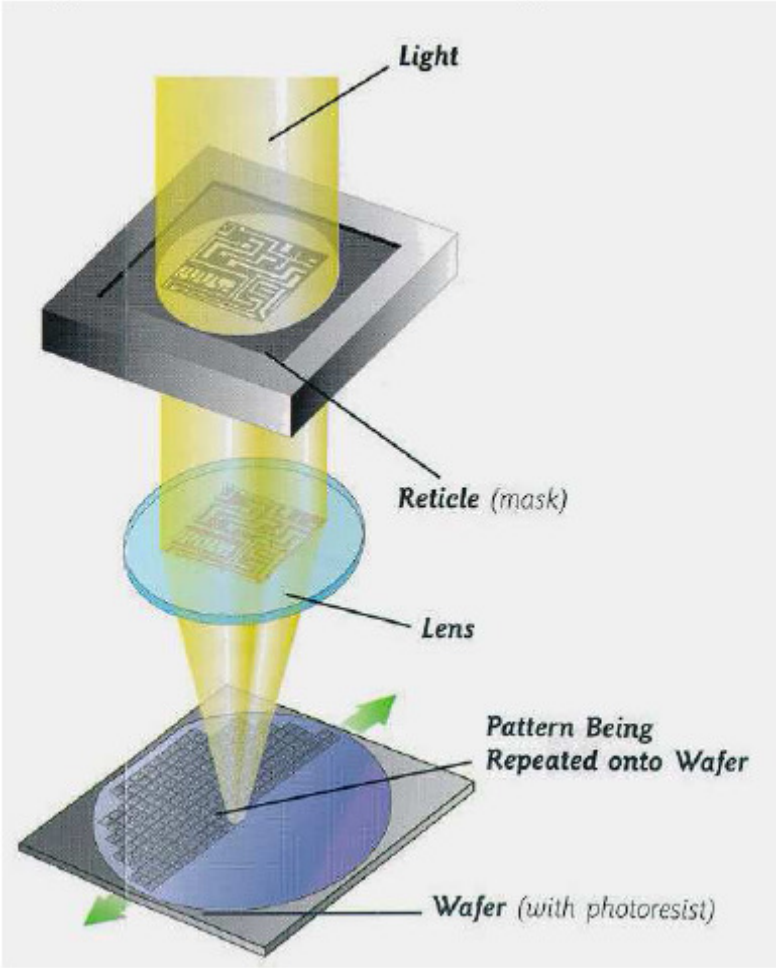

Figure 1.4 Schematic of Projection Lithography

$$R = k\frac{\lambda}{NA}$$

Figure 1.5 The Rayleigh relation

This relationship has led photolithographers to drive toward the use of ever shorter wavelengths of light and even higher numerical aperture for the production of transistors. Lithographers are restricted to wavelengths of light that can be produced with enough power using commercially available light sources. Shorter wavelengths have

enabled production of memory with decreased feature size as shown in Figure 1.6 (*eg.* 4K/7000 = 4K Dynamic Random Access Memory (DRAM)/ 7000 nm feature size). The reduction in the wavelength of light presents challenges that must be addressed in respect to maintaining etch resistance and transparency for each new generation.

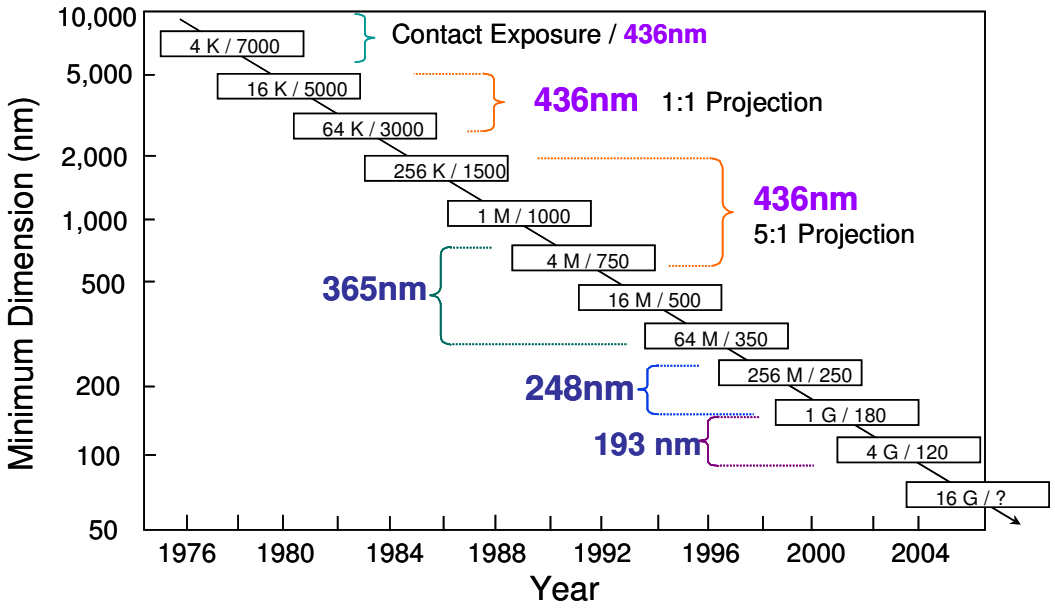

Figure 1.6 Minimum dimensions in DRAM related to wavelength of light used through time

EARLY PHOTORESIST MATERIALS

The earliest generations of resist materials were bisarylazide negative tone materials.[59] However these were replaced by the novolac-diazonapthoquinone (DNQ) resists originally developed by the Kalle Corporation in Germany and discussed in chapter 4. This resist system served the lithography industry through both the 436 and 365 nm generations. As lithographers looked to target future generations of materials it became obvious that with the low amounts of power available from mercury discharge sources for exposure in the deep-UV (DUV), novolac/DNQ resists would be too highly absorbent and would prevent effective imaging of the system.

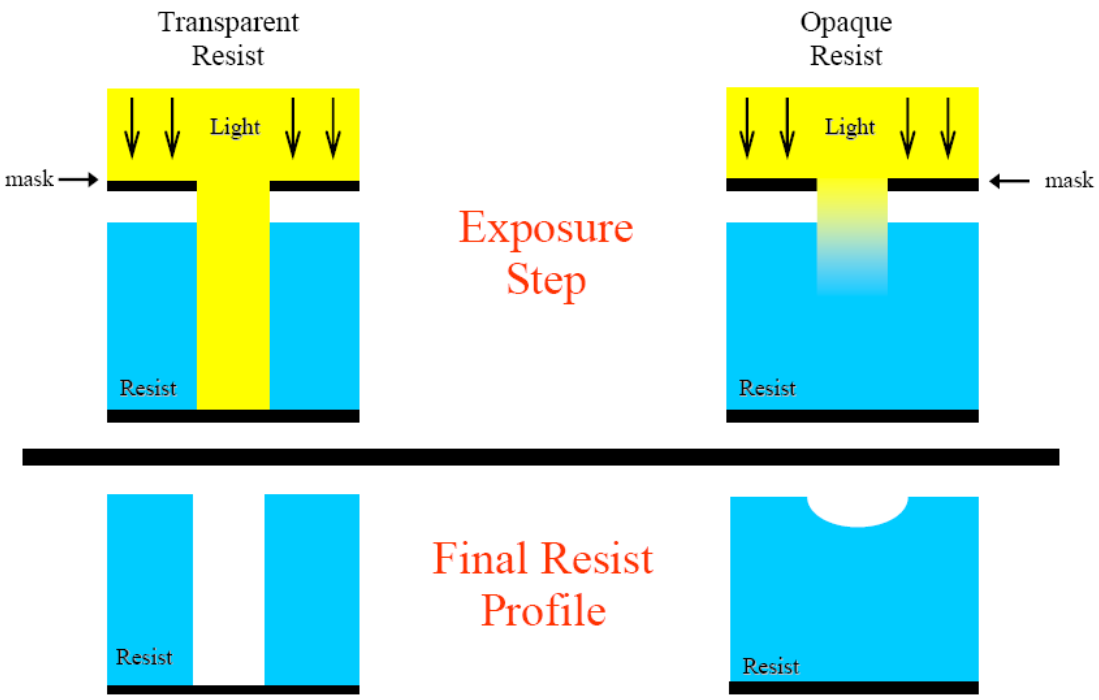

Figure 1.7 Non-transparent resist do not allow effective feature formation

INTRODUCTION TO CHEMICAL AMPLIFICATION

A fundamental change in resist chemistry would be needed to make efficient use of the limited power available in the DUV. The use of PAGs and their subsequent interaction with the resist film discussed above and in more detail in chapter 4 allowed for the efficient use of light in *t*-BOC protected polyhydroxystyrene (PHOST). Thermal deprotection of this material occurs around 200 ^{o}C but in the presence of acid the deprotection occurs very rapidly at 100 ^{o}C (Figure 1.8). This temperature difference allows for selective deprotction and thus selective dissolution of the resist film.

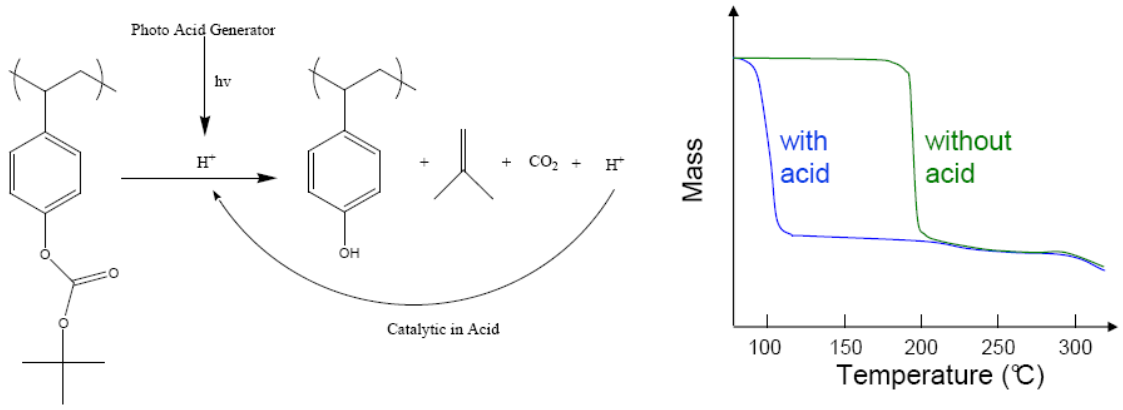

Figure 1.8 Acidic catalyzed thermolysis of t-BOC protecting group

This system served well for the purposes of 248 nm lithography; however, when the next step down in wavelength was investigated, it was noted that the aromatic PHOST was too strongly absorbing. A resist redesign was called for again. As it was desirable to use a chemically amplified system for subsequent generations a modular approach to looking at photoresists is useful (Figure 1.9).

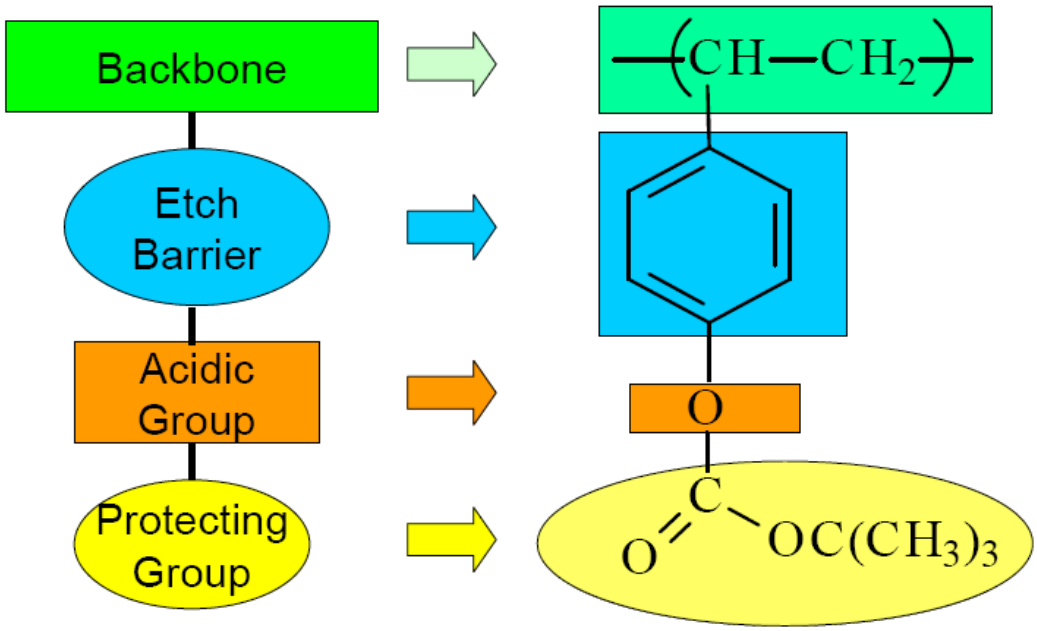

Figure 1.9 Modular approach to resist design

The resin must be a polymeric material to provide sufficient stability at processing temperatures. The resist polymers are typically in what polymer chemists would define as a low molecular weight (MW) range. It is important for these materials to dissolve cleanly without undergoing swelling that often accompanies dissolution of high MW polymers. A solubility switching unit is required. This is typically an acidic functionality that is protected with an acid labile functional group as previously described.

The key feature to be altered for 193 nm lithography is the etch resistant scaffold. Onishi devised a formula to predict the ability of a material to withstand the harsh conditions of RIE (Equation 1.2) where V is the etch rate, N the total number of atoms, N_C the number of carbon atoms and N_O the number of oxygen atoms.[4] Evaluation of this parameter led to the conclusion that transparent bridged cyclic aliphatics such as norbornane and adamantane could be used to replace aromatic functionality. This observation led to the production of a new generation of materials.

$$V \alpha N/(N_C-N_O)$$

Figure 1.10 Onishi's relationship of etch rate to molecular formula

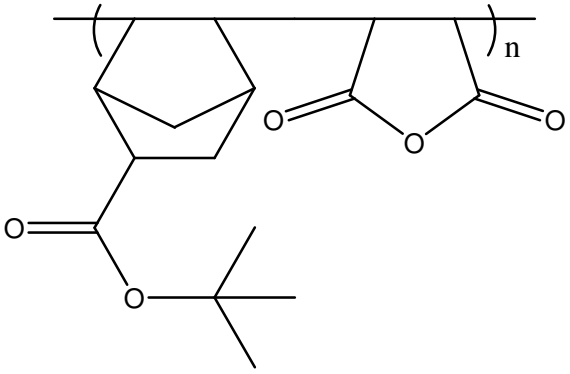

Figure 1.11 Example of a 193 nm resist, a cyclic olefin-maliec anhydride (COMA) resist

Lithographers always try to evolve the current generation technology while preparing for coming technologies. The microelectronics industry is currently at a large hurdle as several technologies are competing to replace 193 nm lithography and some perspective technologies have already failed.

DISSERTATION STRUCTURE

For several years the leading candidate to replace 193 nm lithography was 157 nm lithography. Nearly all materials are highly absorbing at 157 nm. Notably fluorine substitution significantly reduces the absorbance of hydrocarbons at 157 nm. Materials containing fluorinated alicyclic structures therefore became of great interest for this emerging technology. Chapter 2 discusses efforts to overcome difficulties in the polymerization of some of these materials.

A low cost, high fidelity new generation technology called Step and Flash Imprint Lithography is emerging as an alternative to other less production ready next generation technologies. Material for this application, which is designed to overcome one of the key problems will be described in Chapter 3. Chapter 4 will discuss initial efforts to harness the power of chemical amplification while removing the need for small molecule diffusion through a film and its potential to reduce printing error incurred in current technology.

CHAPTER 2 POLYACETALS FOR USE IN PHOTOLITHOGRAPHY

INTRODUCTION TO 157 NM LITHOGRAPHY

Creating smaller resist features has necessitated the use of smaller wavelengths of light as dictated by the Rayleigh relation. Each new exposure wavelength has called for a fundamental photoresist redesign. The shift from the visible region into the UV necessitated a paradigm switch from non-chemically amplified resists (NCAR) to chemically amplified resists (CAR) as available light sources could not generate sufficient power to efficiently induce a solubility switch. The shift from 248 nm to 193 nm lithography required the removal of aromatic substituents which were too strongly absorbing at 193 nm. Aromatic substituents were replaced by bridged cyclic aliphatics, which are sufficiently transparent and provide a great enough etch resistance to enable image transfer. The transition to 157 nm exposure wavelength presented a new challenge in that most organic compounds including simple hydrocarbons are strongly absorbing at 157 nm.[5] The transition is further complicated because components of air such as O_2, CO_2 and H_2O are strongly absorbing in the far-UV. This necessitates that exposures be performed be performed in a nitrogen purged system.

Historically, photoresist films have possessed an absorbance of approximately 0.4-0.7 μm^{-1} for the given exposure wavelength. Thus, the search for resist materials with an absorbance value in this range was targeted for 157 nm lithography. The early search for suitable materials was not particularly encouraging; previous generations of materials such as polynorbornenes, polyacrylates and polystyrenes were found to be far too strongly absorbing. It was noted that certain silsesquioxanes and fluorinated hydrocarbons showed promise due to their low absorbance at the exposure wavelength.[6]

The absorbance of acidic moieties used in earlier generations of photoresists, phenols and carboxylic acids, presented another problem as they were highly absorbing at 157 nm. Fortunately, a candidate for replacement, hexafluoroisopropanol (HFIPA), was identified. With a pK_a~ 11, HFIPA is nearly as acidic as phenol thus it was targeted as a transparent solubility switching unit. It was shown that a variety of protecting groups which had been utilized for previous generations of materials were effective for this functionality including, acetals, *t*-BOC and *t*-butyl.[7]

SELECTING TARGET MATERIALS FOR 157 NM LITHOGRAPHY

The vacuum-UV gas phase spectra of fully hydrogenated potential monomeric materials were acquired to speed the screening of materials. It has been shown the gas phase absorbance of hydrogenated monomers could be used to predict the relative absorbance of polymeric materials.[8] Norbornanes were initially investigated for use at 157 nm due to their etch resistance, generally facile synthetic availability and potential for fluorinated substitution. A study of selective fluorination of norbornane was undertaken.[9] Indeed, fluorination of norbornane in both quantity and position did have a dramatic effect in suppressing absorbance (Figure 2.1). As would be expected, greater degrees of fluorination are favorable and conveniently the more easily accessible 2-position of the norbornane ring has a greater effect on absorbance than the less easily fluorinated 7- position.

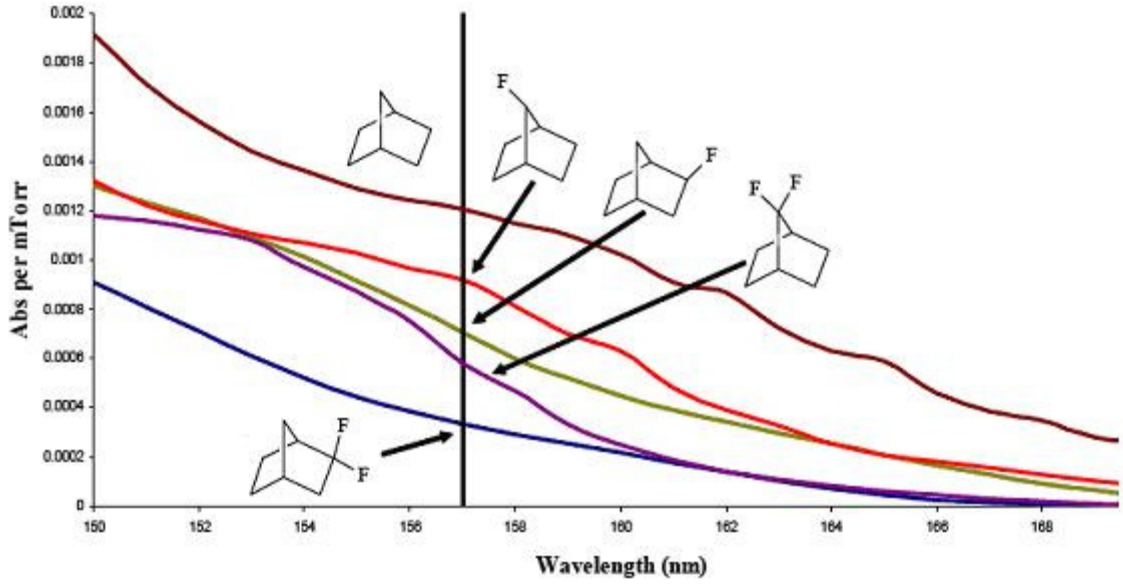

Figure 2.1 Impact of mono- and difluorination and position on absorbance at 157 nm[9]

A simple but very useful model, Simple Transmission Understanding and Prediction by Incremental Dilution (STUPID), was developed for the prediction of the absorbance of fluorine-bearing norbornane-based compounds was developed by Dammel.[10] The STUPID model assigns numerical values to each carbon in a potential monomer based upon its substitution with fluorine or proximity to fluorinated substituents. The model, while not absolutely accurate, is surprisingly useful for predicting the potential viability of fluorine substituted norbornane materials.

EARLY RESIST DESIGN

Knowing that fluorination decreases absorbance, higher degrees of fluorination were more transparent and a highly fluorinated acidic functionality was available, lithographers began the task of searching for suitable materials. An early target material was the monosubstituted, 2-Bicyclo[2.2.1]hept-5-en-2-ylmethyl-1,1,1,3,3,3-hexafluoro-propan-2-ol (NBHFA) (Figure 2.2). In spite of bearing only a single substituent

containing a methylene spacer between HFIPA and the ring, the material was surprisingly transparent ($A_{157\ nm}$~ 1.15 μm^{-1}).[11,12] PolyNBHFA is almost one million times less absorbing than PHOST. The natural extension of this observation was to introduce additional fluorination to the norbornane ring, however as the degree of fluorination increases so too does synthetic difficulty.

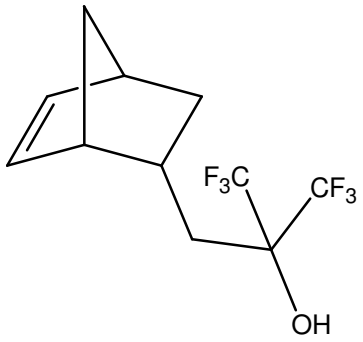

Figure 2.2 Structure of monomeric NBHFA

Many geminally substituted fluorinated materials such as those shown in Figure 2.3 were synthesized and showed promise according to gas phase measurements, however, they were often synthetically challenging and all geminally substituted norbornane monomers were inert to polymerization via transition metal catalysis. These materials led to attempts to alter the molecular composition in such a way that transition metal catalysis could be used or to circumvent the need for those catalysts.[13,14]

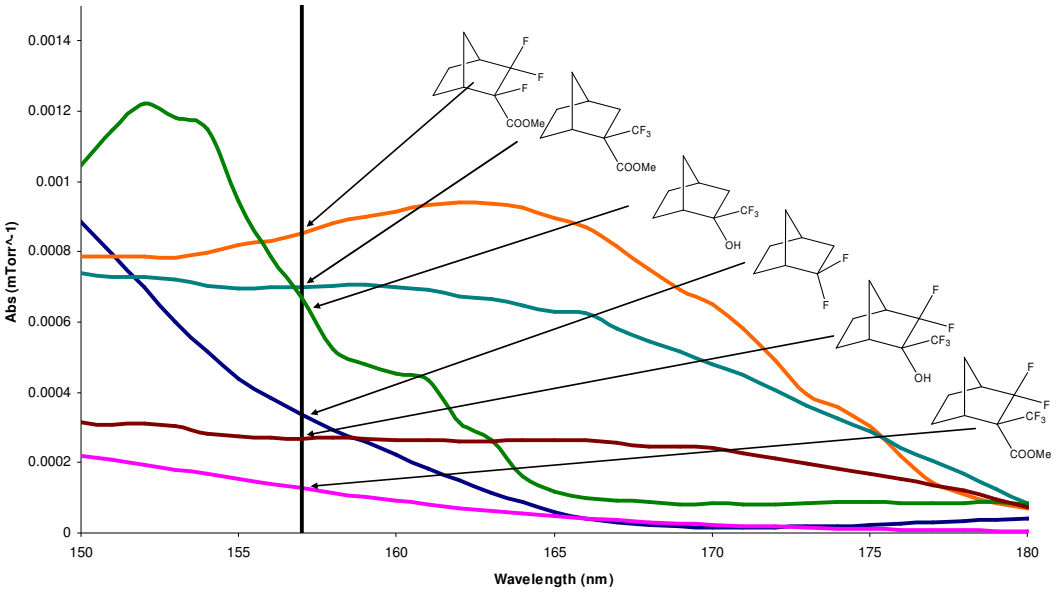

Figure 2.3 Various promising non-polymerizable geminally-substituted materials[18]

MONOMER REDESIGN TO ENABLE ALTERNATE POLYMERIZATION TECHNIQUES

The 2+2 reaction of quadricyclane with an olefin produces a tricyclononane (TCN) following hydrogenation. TCNs with geminal substitution on the 4-membered ring leave the bicyclo[2.2.1]heptane portion of the molecule vicinally substituted and thereby polymerizable. TCNs were found to follow the same trend of decreasing absorbance with increasing fluorination and were effectively imaged.[15] The corresponding oxetanes were found to be highly transparent when appropriately substituted and would ring open under acidic conditions to produce a solubility switch.[16]

a

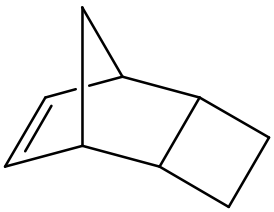

b

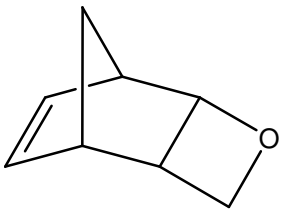

Figure 2.4 Example of unsubstituted a) TCN and b) oxetane

Ring Opening Metathesis Polymerization (ROMP) of norbornane monomers typically produces low glass transition temperature (T_g) polymers that are not useful for lithographic processing and lack sufficient etch resistance due to the destruction of the bridged system.[17] Dinorbornenes can be polymerized via ROMP while maintaining a cage system, however they too suffer from low T_gs as well as high absorbance. Polymers synthesized by ROMP were ultimately deemed not appropriate for 157 nm applications.[18]

VICINAL DIOLS AS A USEFUL TRANSPARENT FUNCTIONALITY

It has been shown that appropriately substituted dihydroxylated norbornanes maintain a low absorbance at 157 nm (Figure 2.5). This observation coupled with the knowledge that carbonate protecting groups were surprisingly transparent led to attempts to produce polycarbonates.[18] Dihydroxylation of norbornene occurs nearly exclusively on the *exo* face and the proximity of the vicinal hydroxyl groups led to the formation of the stable five-membered, carbonate ring upon attempts to form polycarbonates. Seeking to overcome this limitation, Grayson *et al.* attempted to produce a norbornane compound with a hydroxyl group on each the *endo* and the *exo* face.[19] This seemingly simple proposal turned out to be anything but simple, leading to a multi-year undertaking that ultimately produced a polycarbonate albeit via a tedious synthetic route.

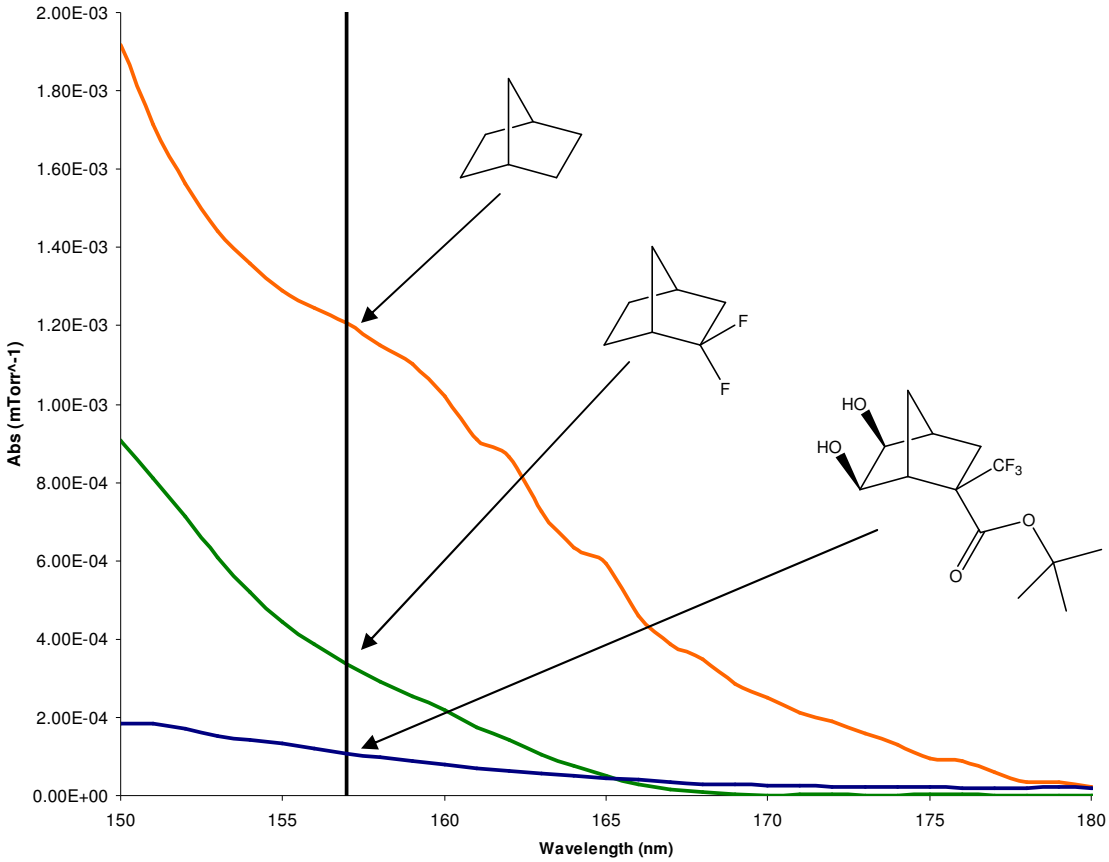

Figure 2.5 Example of a dihydroxylated highly transparent material[18]

During this work it became apparent that accepting the nature of the dihydroxyl group formation would be easier than fighting to change its stereochemistry. Turning again toward the knowledge of protecting groups previously used in photolithography, acetals appeared to be a logical target. The convenient vicinal placement of two hydroxyl groups, it was postulated, would make it straightforward to form 5-membered rings that would constitute the linkages of a polymer backbone.

TARGETING NORBORNANE-BASED POLYACETALS

A proof of concept was desired and as such a modular design approach was taken toward the construction of the first norbornane-based polyacetal. The requirements were:

1. Norbornane system.
2. An attached vicinal diol.
3. A pendant ketone or aldehyde.

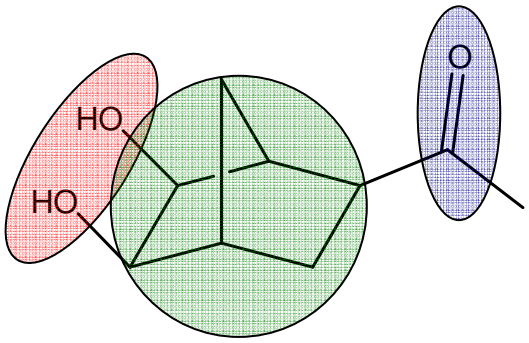

2 **1** **3**

Figure 2.6 Modular design of a norbornane-based polyacetal

Retrosynthetic analysis allowed for the facile construction of norbornane based keto-diol, **2.1**, in two steps from commercially available materials (Figure 2.7).

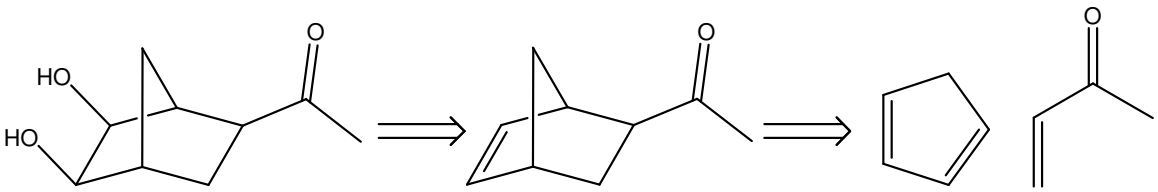

2.1 **2.2**

Figure 2.7 Retrosynthetic analysis of model acetal monomer

Freshly cracked cyclopentadiene (CPD) and methyl vinyl ketone underwent a Diels-Alder reaction to form a norbornene ring while installing the necessary ketone functionality. The double bond of **2.2** was subsequently dihydroxylated to form the model compound **2.1**. The highly viscous material was subsequently polymerized (Figure 2.8) utilizing an acidic catalyst in aromatic solvents to drive the forward reaction through azeotropic removal of water.

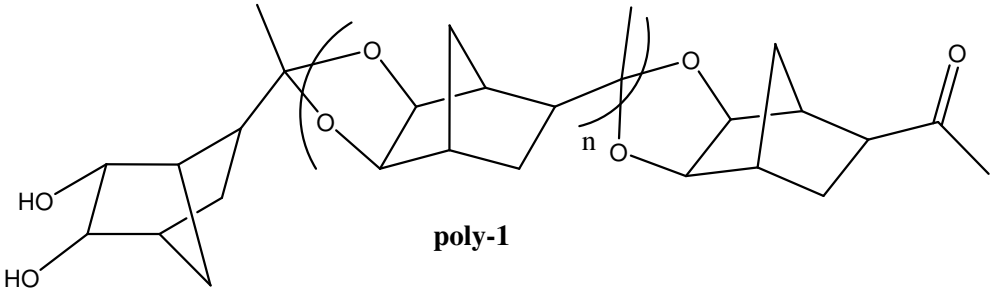

poly-1

Figure 2.8 Structure of model polymer

The polymerization produced a relatively low molecular weight material. End group analysis performed by ^{1}H NMR (Figure 2.9) indicated a number average molecular weight (M_n) of ~1200 Da. Analysis by Size Exclusion Chromatography (SEC) indicated a slightly higher M_n (~3700 Da) with PDI of 1.57. The material demonstrated robust thermal stability exhibiting the onset of decomposition at 320 ^{o}C as determined by Thermal Gravimetric Analysis (TGA). No T_g was observed using Differential Scanning Calorimetry (DSC) up to the decomposition temperature. This likely owes to the fact that the polymer backbone is comprised of a fairly rigid three-ring system with only a single methyl group pendant to the polymer backbone as well as the low MW. The most encouraging piece of data collected was that the A_{157} was low (3.50 μm^{-1}). This number is well above the targeted 0.4-0.7 μm^{-1} but is perhaps better appreciated when compared to polynorbornene (A_{157} = 6.10 μm^{-1}) as nearly 1000 times more light is transmitted at 157 nm.

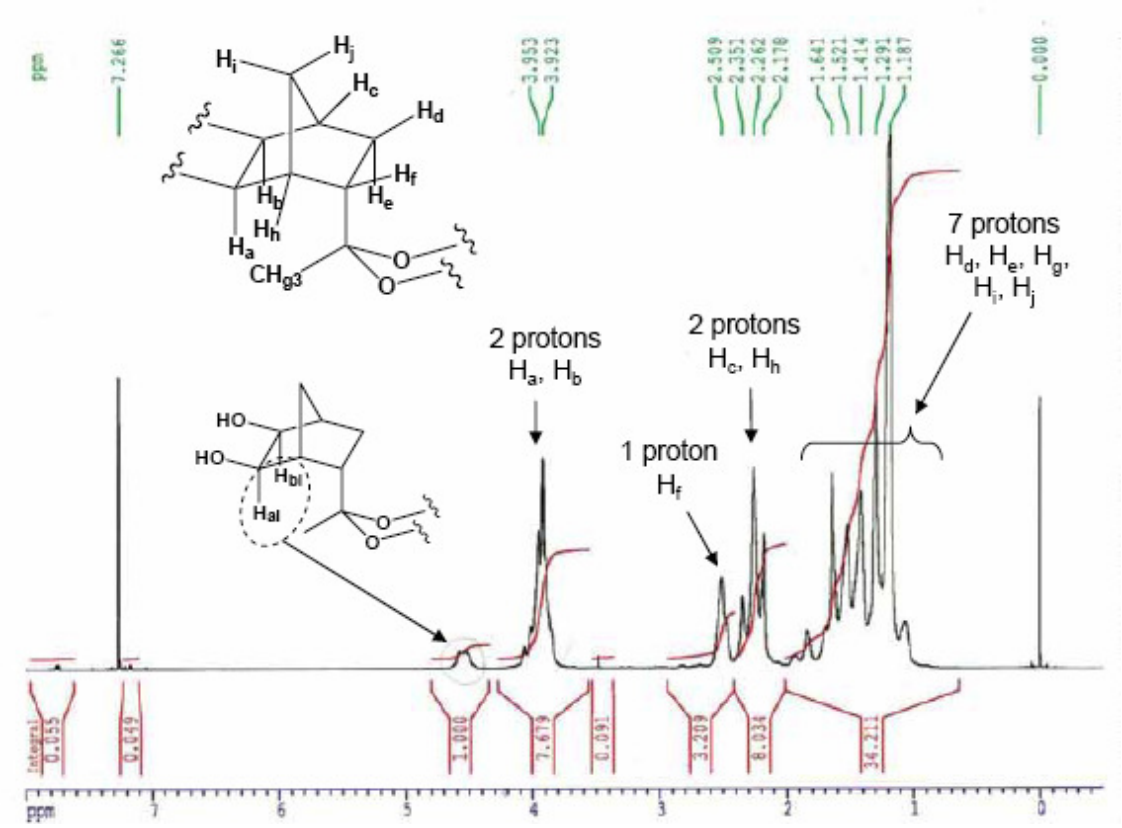

Figure 2.9 ^{1}H NMR analysis of poly-1 showing resolution of protons geminal to terminal hydroxyl groups from those geminal to the internal acetals

IMAGABLE POLYACETALS

Buoyed by these results, the next step was designing a material that could function as a photoresist. The model polyacetal incorporates two of the three required design elements. The polymerizable backbone is accounted for by the incorporation of vicinal diol and pendant ketone in the same molecule while etch resistance is provided by the alicyclic norbornane. The remaining functionality to be integrated is an acidic solubility-switching unit, therefore introduction of the HFIPA functionality was targeted. Retrosynthetic analysis of a new target molecule led to a viable synthetic route (Figure 2.10).

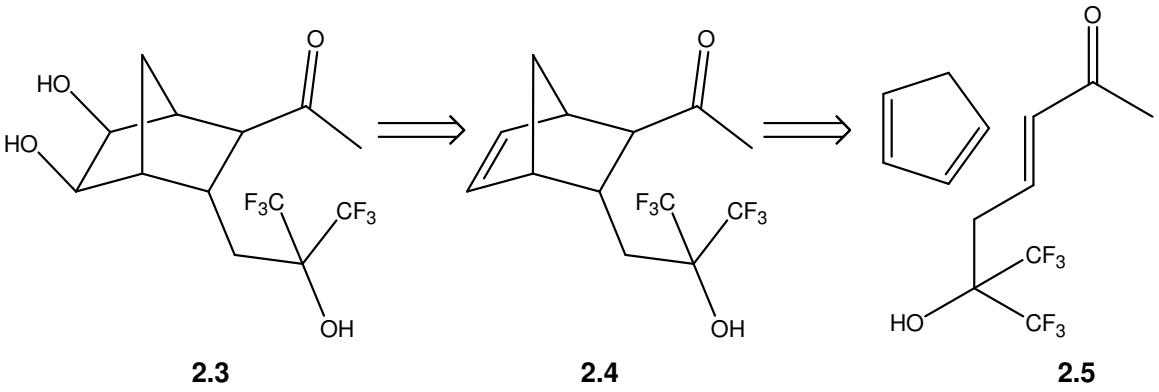

Figure 2.10 Retrosynthetic analysis of HFIPA functionalized acetal monomer

Fortunately, 7,7,7-trifluoro-6-hydroxy-6-trifluoromethyl-hept-3-en-2-one, **2.5**, has been previously reported.[20] Following a literature procedure, 4-penten-2-ol was formed through the zinc mediated allylation of acetaldehyde.[21] The hydroxyl group was subsequently benzoyl protected prior to the 'ene' reaction of the terminal olefin and hexafluoroacetone in a sealed Parr reaction vessel heated to 170 ^{o}C. The hydroxyl group was deprotected and then oxidized to the desired conjugated methyl ketone.

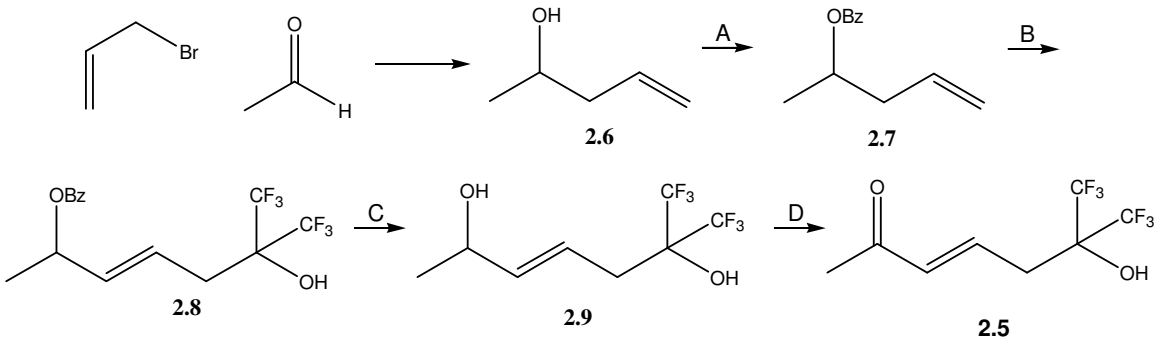

Figure 2.11 Synthetic route to HFIPA functionalized dienophile

Diels-Alder reaction of **2.5** with CPD and subsequent dihydroxylation produced the desired monomer as a highly viscous light yellow liquid in 4% overall yield with respect to acetaldehyde. The polymer, **poly-2**, was produced and analyzed in the same manner as the model compound. **Poly-2** also exhibits excellent thermal stability and a

relatively low M_n (~3625 Da) (Figure 2.12). The much lower peak height for **poly-2** can be attributed to both a less concentrated sample and to a decreased RI due to the incorporation of fluorine.[22] The material demonstrated an $A_{157\ nm}$ = of 2.2 μm^{-1}.

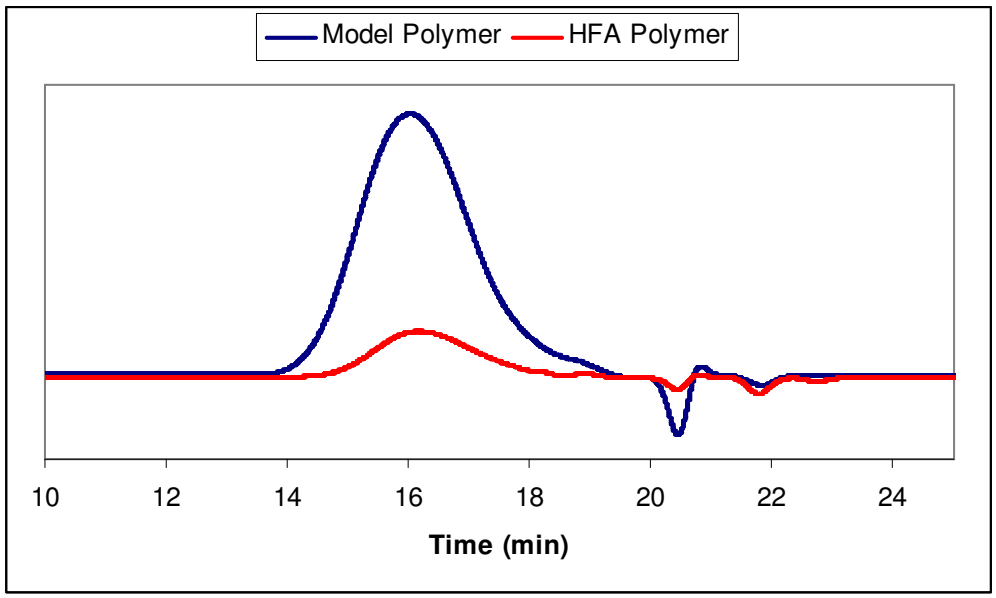

Figure 2.12 Comparable retention times for SEC traces of model and HFIPA containing polymers

With this material in hand, it was desirable to perform an imaging demonstration. To do so the acidic HFIPA functionality was protected post polymerization with tert-butyloxycarbonyl (*t*-BOC) through reaction of **poly-2** with di-*tert*-butyl carbonate and catalytic DMAP.

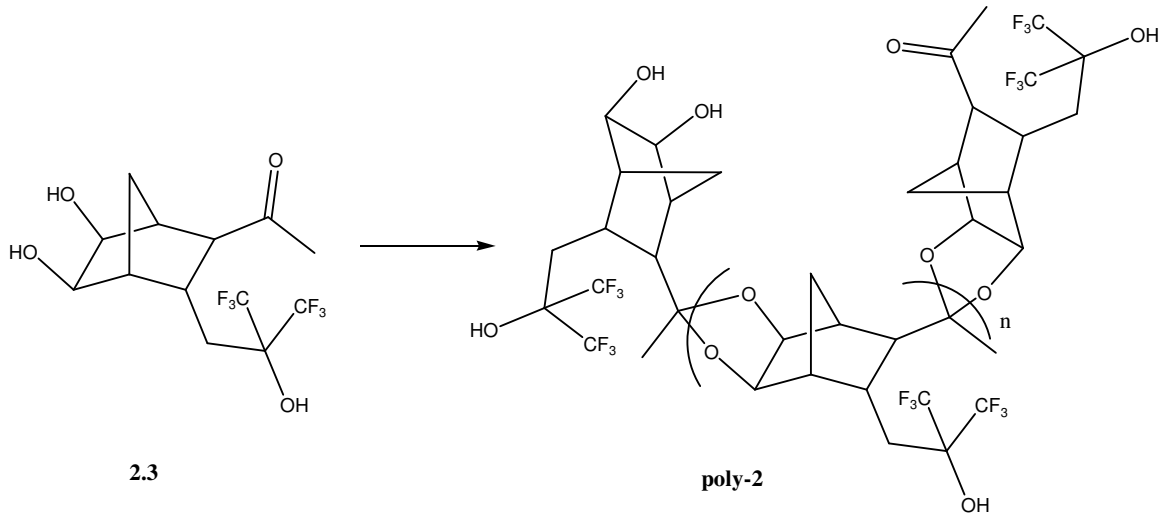

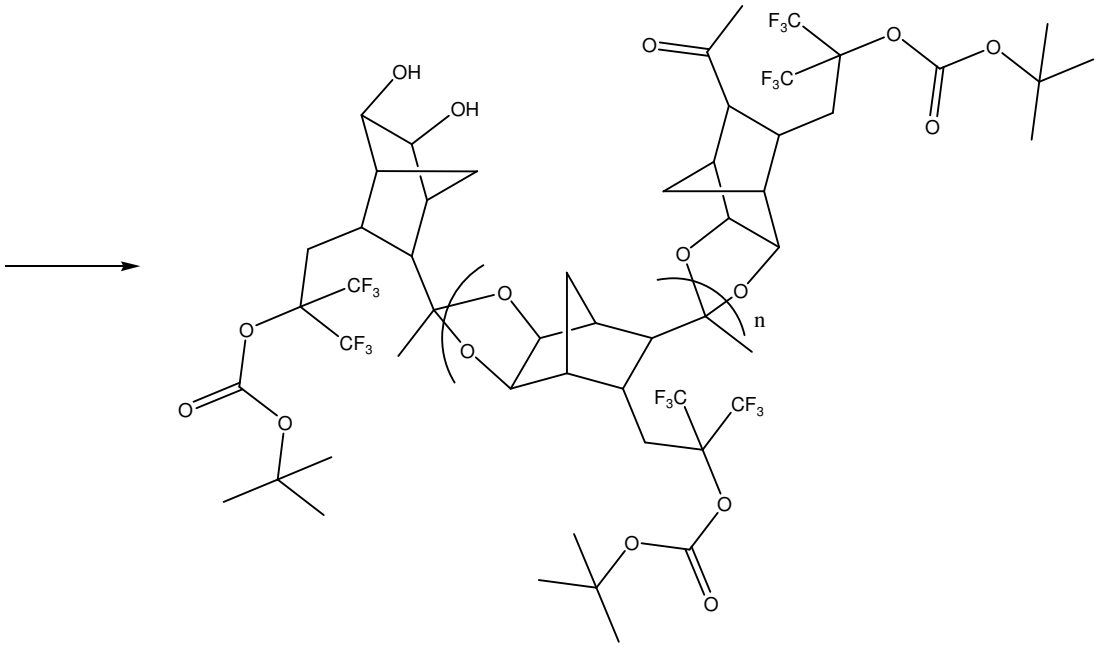

Figure 2.13 Formation and protection of acidic functionalized polyacetal

The protected polyacetal **poly-2a** showed thermally stability to 140 ^{o}C at which a mass loss corresponding to loss of the *t*-butyl carbonate was observed. The remaining polymer was stable to 270 ^{o}C. **Poly-2a** was formulated as a 10 wt% solution in PGMEA containing 5 wt% triphenyl sulfonium nanoflate for a PAG. After coating and exposure,

the film was developed with aqueous basic developer and images were observed on the wafer (Figure 2.14). The quality of the spin-coated films was poor as the polymer is brittle.

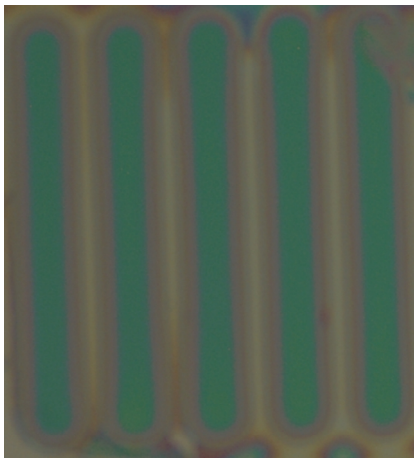

Figure 2.14 Image in polyacetal film produced via contact printing

Efforts were made towards increasing the molecular weight of the polymer. Using the more readily available model monomer, variations in catalyst type and amount, solvent and reaction time were examined through a series of experiments (Table 2-1). Additionally, the ratio of *endo*:*exo* material was varied through a range of ~10:1 to ~1:1. Unfortunately, no significant change in molecular weight was observed.

Table 2-1 Sample of conditions used in attempt to control MW

Time (h)	Concentration (g/mL)	Solvent	Catalyst	Catalyst Loading (mol %)
0.5-168	0.25	Benzene	*p*-TSA	1
12	0.01- 1.00	Benzene	*p*-TSA	1
12	0.25	Chlorobenzene	*p*-TSA	1
12	0.25	Toluene	*p*-TSA	1
12	0.25	Xylenes	*p*-TSA	1
12	0.25	Benzene	Amberlyst	1
12	0.25	Benzene	Dil. HCl	1
12	0.25	Benzene	*p*-TSA	0.25-10

TARGETING HIGHER MOLECULAR WEIGHT POLYACETALS

Increasing the MW of a step-growth polymer requires driving the reaction further towards completion. It was postulated that increasing the tendency of the reaction to proceed towards acetal formation would aid in the formation of higher MW polymer. Equilibrium constants (K_{eq}) heavily favor the formation of acetals or hydrates of trifluoromethyl ketones relative to their methyl ketone analogues often by orders of magnitude.[23] Thus, a trifluoromethyl ketone was targeted in hope that the equilibrium would favor the formation of high polymer with the likely benefit of also decreasing polymer absorbance. Retrosynthetic analysis led to the conclusion that acquisition of trifluoromethyl vinyl ketone would enable the synthesis of the trifluoromethyl analogue to the model compound (Figure 2.15).

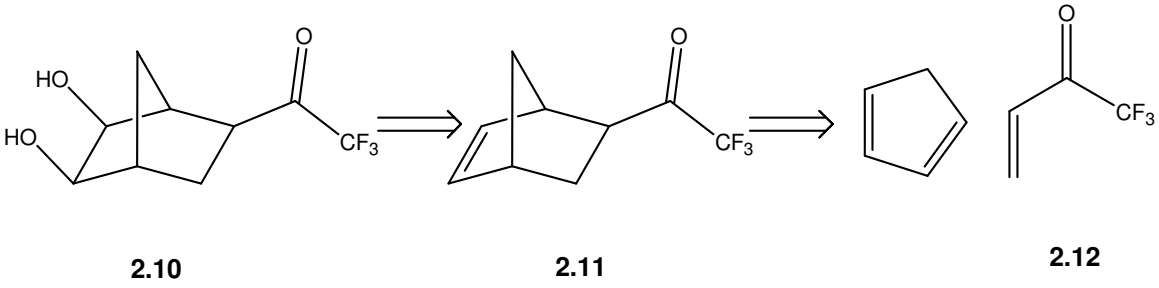

2.10 **2.11** **2.12**

Figure 2.15 Retrosynthetic analysis of trifluoromethyl model monomer

Unfortunately, trifluoromethyl vinyl ketone **2.12** is a far more difficult synthetic challenge than previously imagined. In spite of the valiant efforts by many, it was only produced in very small quantities and was never isolated from solvent. It was therefore necessary to revisit the design of a model trifluoromethyl compound. A new retrosynthetic analysis of **2.11** led to another synthetic possibility (Figure 2.16).

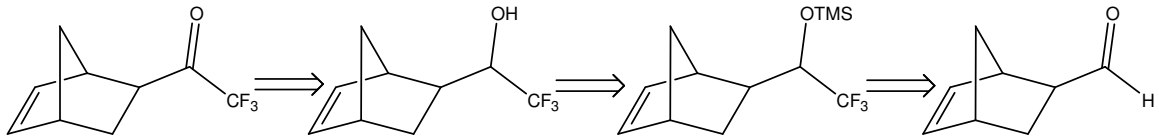

2.11 **2.13** **2.14** **2.15**

Figure 2.16 Retrosynthetic analysis of trifluoromethyl ketone

The construction of **2.11** begins with the Diels-Alder reaction of freshly cracked CPD and acrolein followed by nucleophilic addition to the aldehyde by Ruppert's reagent (trifluoromethyl trimethyl silane). Deprotection of the TMS ether led to trifluoromethyl carbinol **2.13**. Dess-Martin periodinane was utilized to oxidize the alcohol to the ketone. Consumption of the hydroxyl group and production of the trifluoromethyl ketone was observable spectroscopically. Isolation of the compound proved to be unexpectedly challenging as the maximum yield obtained was <2%. Analysis of organic solvent removed either by distillation at ambient pressure or in vacuo showed significant amounts

of the product as analyzed by gas chromatography. This behavior has been observed several times in the search for 157 nm materials. A number of low molecular weight compounds with high fluorine content display an unexplained high affinity for solvents. Azeotropic behavior has not been observed and when these compounds can be isolated most demonstrate boiling points significantly greater than that of the solvent yet they cannot be separated from the solvent even with a six foot, fully instrumented column.[24]

Unfortunately, during this time the pursuit of 157 nm lithography worldwide was collectively abandoned.[25] This meant the decommissioning of 157 nm imaging tools and the loss of a great deal of work performed around the world. Fortunately all was not lost, as many materials produced during this time period have found applicability in 193 nm dry and immersion lithography as well as other emerging technologies. The decision was made to continue investigating these new polymer materials because of their unusual thermal stability and ready solubility in common organic solvents.

It was still desired to compare a trifluoromethyl ketone to its methyl ketone analogue so a new target **2.16** was designed (Figure 2.17).

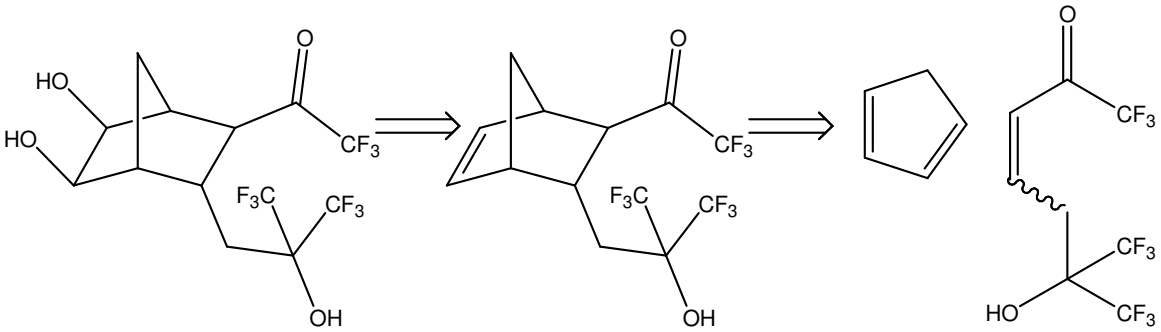

2.16 **2.17** **2.18**

Figure 2.17 Retrosynthetic construction of HFIPA functionalized trifluoromethyl ketone monomer

Following the same analysis that led to compound **2.5**, compound **2.18** was envisioned as a viable target. Trifluoroacetaldehyde methyl hemiacetal was allylated

according to a literature procedure[26] to form 1,1,1-trifluoro-pent-4-en-2-ol, **2.19**. Subsequently the same procedure found in Figure 2.11 was followed through the synthesis of compound **2.22** with the exception of the switch to the Dess-Martin periodinane as an oxidizing reagent to produce **2.18**, which was obtained in 1.3% yield from trifluoroacetaldehyde methyl hemiacetal.

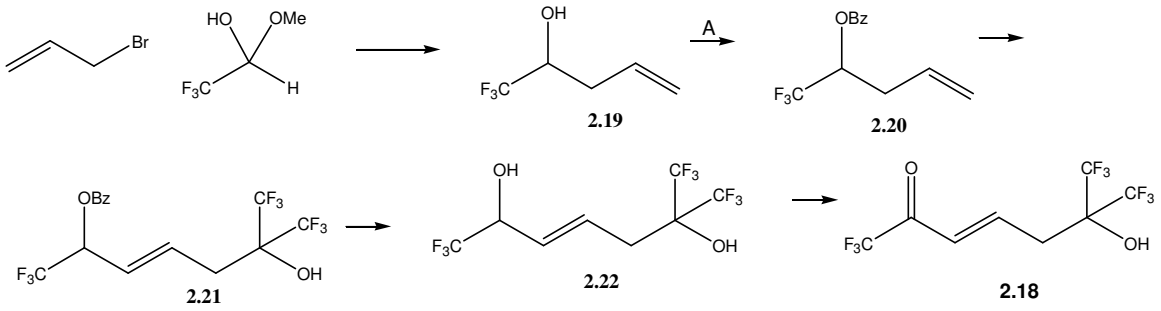

Figure 2.18 Synthesis of conjugated trifluoromethyl ketone dienophile

Diels-Alder reaction with CPD successfully produced **2.17,** and dihydroxylation of the olefin was likewise successful. However during dihydroxylation, hydration of the trifluoromethyl ketone occurred as well producing **2.23** (Figure 2.19). Repeated efforts to reverse the formation of the hydrate were unsuccessful yielding only starting material or decomposed product.

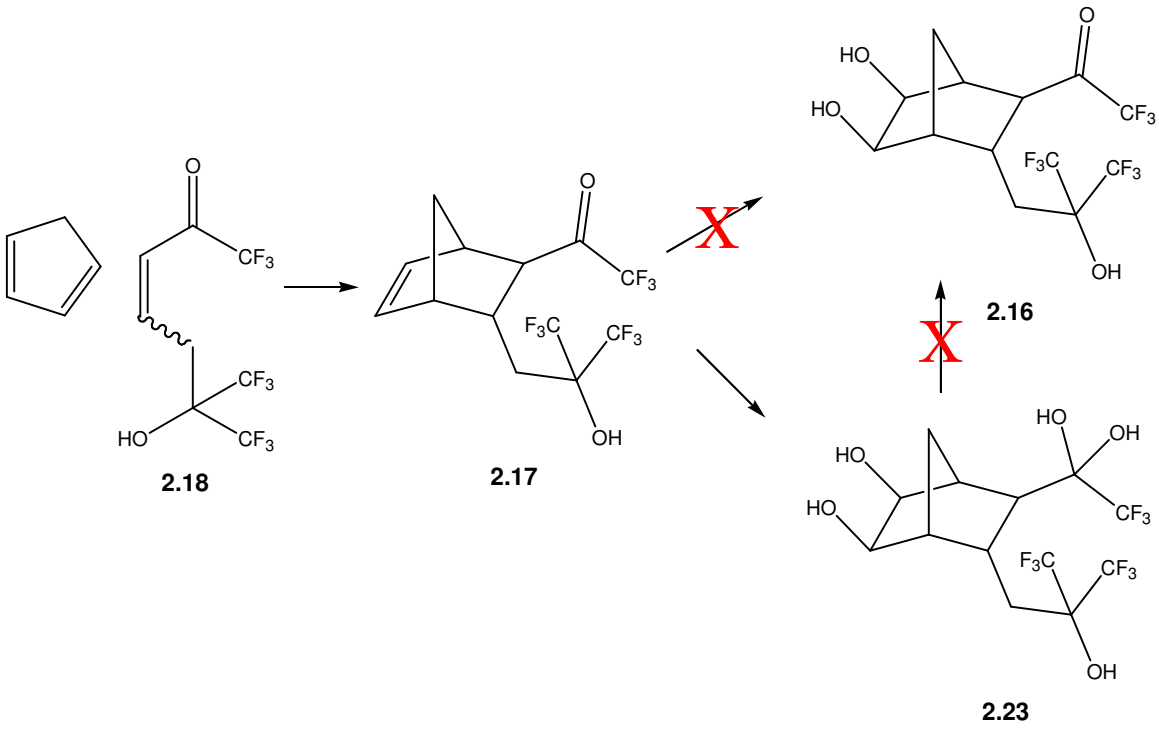

Figure 2.19 Attempted synthesis of HFIPA functionalized monomer and actual product

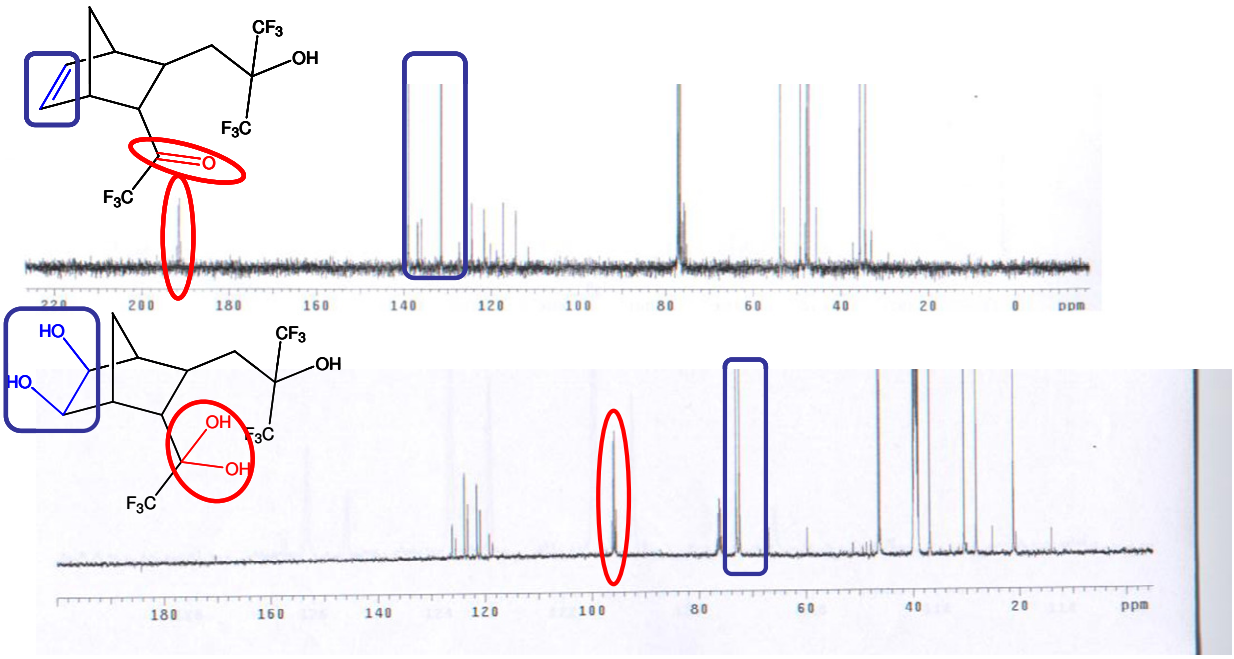

Figure 2.20 ^{13}C spectra illustrating oxidation of olefin and hydration of ketone

Due to the observation that the materials in this route were far less volatile than the ones in Figure 2.15 and Figure 2.16, a new route to an old target, **2.10**, was examined (Figure 2.21). By dihydroxylating and protecting the diol early in the reaction series, it was possible to provide the material with additional ballast that resulted in a more easily isolated compound. Deprotection of the TMS ether followed by oxidation gave an easily isolated compound. Deprotection of the acetal protecting group provided the trifluoromethyl analogue, **2.10**, of the model compound, **2.1**. Counter to expectations this compound did not polymerize when subjected to any of the previously tested conditions. It was postulated that the steric bulk of the material may be at fault for the inability to polymerize and that moving the ketone farther away from the bulky norbornane ring might overcome this issue.

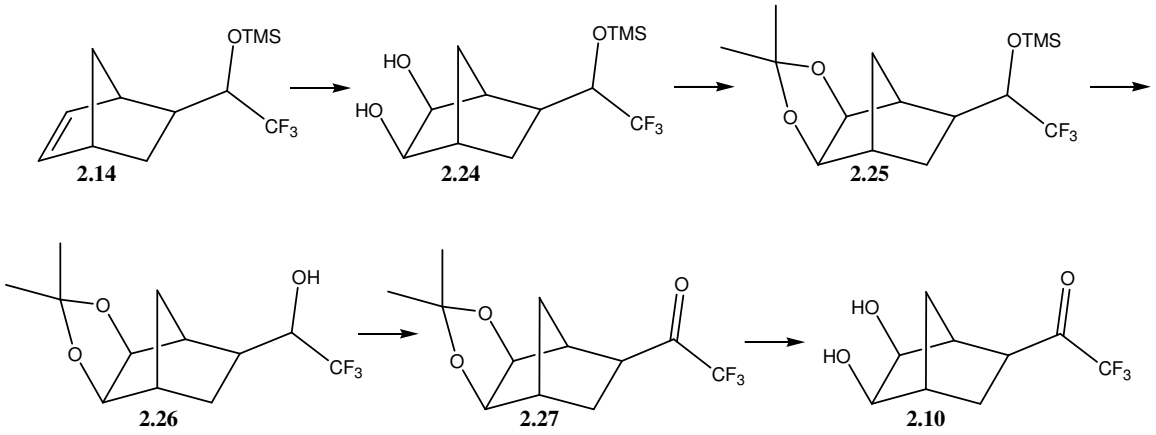

Figure 2.21 Amended route to trifluoromethyl ketone monomer

TARGETING EXTENDED CHAIN POLYACETALS

A single carbon spacer between the ketone and norbornane ring system was targeted. Retro-Diels-Alder analysis leads to a compound that is a much poorer dienophile due to a lack of conjugation with the ketone. Bromomethyl norbornene **2.28** was identified as a compound of interest as it was believed that both methylene-spaced

methyl ketone and trifluoromethyl ketone could be accessed from this compound. Compound **2.28** was originally synthesized in a three step procedure reducing **2.15** to the alcohol followed by tosylation and bromination; however, a more direct route to the material was desired. A variety of reaction conditions were tested in a pressure vessel, but all yielded little to no product. During this time Schrock *et al.* published a direct synthetic route to **2.28**.[27] The key to increased yield was to not crack dicyclopentadiene (DCPD) prior to running the reaction and to run the reaction neat. Grignard formation from **2.28** and reaction with acetaldehyde followed by Jones oxidation and dihydroxylation formed the model monomer with a single methylene spacer **2.31**.

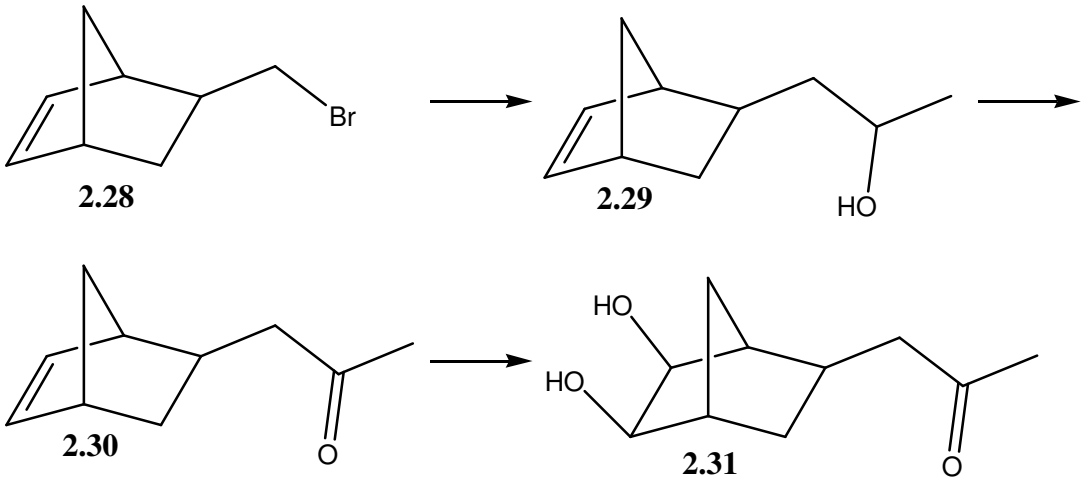

Figure 2.22 Synthetic route to methylene spaced model monomer

Polymerization successfully produced **poly-3** (Figure 2.22) that had similar properties to the model **poly-1**. Analysis of **poly-3**, showed a molecular weight of ~7500 as analyzed by SEC.

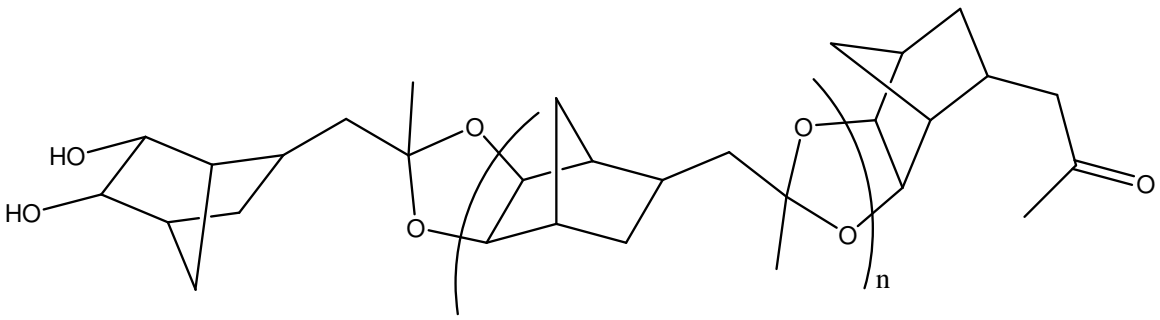

Figure 2.23 Structure of methylene spaced poly(**2.31**)

The next synthetic target was the trifluoromethyl ketone analogue of **2.31**. The reaction of a Grignard reagent with trifluoroacetic acid is a poor yielding reaction as at least half of the starting material is sacrificed in a simple acid-base reaction. It does, however, provide a direct route to trifluoromethyl ketones from an alkyl halide. Using this method, compound **2.32** was synthesized. This compound demonstrated some affinity for solvent, further decreasing yield, but the methylene spacer was enough alteration to isolate the material. Dihydroxylation of the material gave a potential polyacetal monomer bearing trifluoromethyl substituent (Figure 2.24).

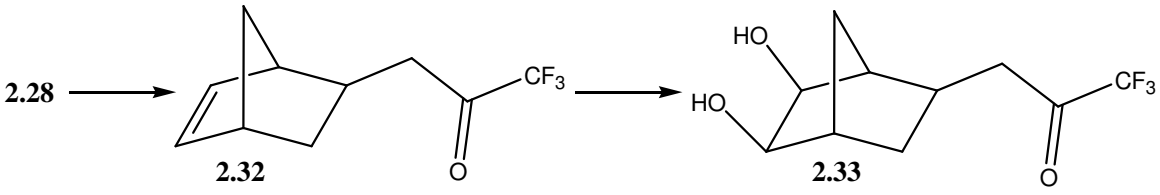

Figure 2.24 Synthetic route to methylene-spaced trifluoromethyl keto-diol

Polymerization was problematic with this material as well. SEC revealed a bimodal distribution. Formation of higher molecular weight material was observed as was a peak with the same retention volume as the monomer.

NMR Observation of Acid Catalyzed Equilibrium

NMR analysis was utilized to investigate this phenomenon. The most well-resolved portion of the ^{1}H-NMR spectra is a doublet of doublets of doublets (ddd) near 0.5 ppm corresponding to a single bridge proton. This region of the spectra of **2.31** and **2.33** was compared. A single ddd was observed for **2.31** (Figure A.5) whereas two smaller sets of ddd were clearly observable for **2.33** (Figure A.10). It is believed this is indicative of higher MW material, as discussed herein. Desiring to observe a shift or lack thereof in the equilibrium between monomer and higher MW products, a second sample of each material was prepared containing two drops of a 7.5 wt% solution of *p*-TSA in DMSO-d_6. This same procedure was performed on the model compound **2.1** and no change was observed in the ^{1}H NMR spectrum (Figures A.1-A.4). Unexpectedly, the acidified version of **2.31** clearly showed the emergence of additional peaks around the ddd indicating the methyl spacer may enable an equilibrium shift. As predicted, **2.33** demonstrated an increase in intensity of the other ddds as well as the appearance of another set of ddd.

Measuring T_1

T_1 relaxation times for all four samples were measured (Figure A.16-A.19). Typical small molecule T_1 relaxation times are ~1 s while higher MW materials such as oligomers and polymers typically possess a shorter T_1.[28] It was noted the non-acidified **2.31** sample demonstrated a shorter T_1 (~0.5 s) than most small molecules. This is likely due to the material being well-ordered in solution due to the availability of both hydrogen-bond donor and acceptor sites. As expected the emerging ddd in the acidified sample showed shorter relaxation times (~0.25 s).

The T_1 values of **2.33** presented a further unexpected result. The dominant peaks in the non-acidified sample demonstrated the smallest T_1 value (~0.3 s). These peaks,

which decreased in intensity relative to the others upon addition of acid, had been postulated to correlate to the monomeric species.

Emergence of Acetal Carbon Signals

To further confirm the likelihood of an equilibrium shift, ^{13}C NMR were collected. Many new carbon signals emerged in the acidified sample of **2.31** including most notably a series of signals near 109 ppm (Figure A.9). This is within the region where an acetal carbon would be likely to appear strongly suggesting that higher MW material is being generated.

Observing the ^{13}C spectra for fluorinated materials is complicated by signal splitting. In the case of the acidified **2.33** sample, the ketone was not observed, likely due to low concentration, however peaks did emerge near 93 ppm (Figure A.15) and were attributed to an increase in the concentration of acetal carbons in the sample.

IODINE CATALYZED POLYMERIZATIONS

Iodine is well known as a participant in polymerizations, namely in reverse iodine transfer radical polymerization (RITP)[29] and in living cationic polymerization.[30] Iodine has been utilized for both the formation of acetals[31] as well as deprotection.[32] However, iodine has never been reported in the literature as the catalyst for a step-growth polymerization and this is the first example of iodine as a catalyst in a step-growth polymerization. The polymer produced using **2.1** possessed the same MW distribution and same mechanical properties as that of the acid catalyzed polymerizations. Iodine successfully catalyzed the polymerization of **poly-2** and AA-BB polymers to be discussed further in this document.

EXTENDING THE UTILITY OF NORBORNANE BASED POLYACETALS

During the search for these materials it was desirable to determine if similar materials could be produced with an eye towards other potential applications of this chemistry. Sulfur-containing polymers have been of interest to photolithographers for 157 nm materials due to high transparency and for immersion lithography applications. It is not a difficult leap to imagine the production of polythioacetals similar to the polyacetals reported. To prove this concept, a model polythioacetal monomer was designed and successfully synthesized (Figure 2.25). Sulfuration of the double bond of a norbornene compound results in a mixture of both the 5- and 7-membered ring structure.[33] The 7-membered ring, with heat and time decomposes to the 5-membered ring, however for this route, it is not necessary to isolate the single product. It is however necessary to protect the ketone from the harsh reduction conditions necessary to form the dithiol. Aqueous removal of the ethylene glycol acetal protecting group produces **2.37,** a dithiol model compound.

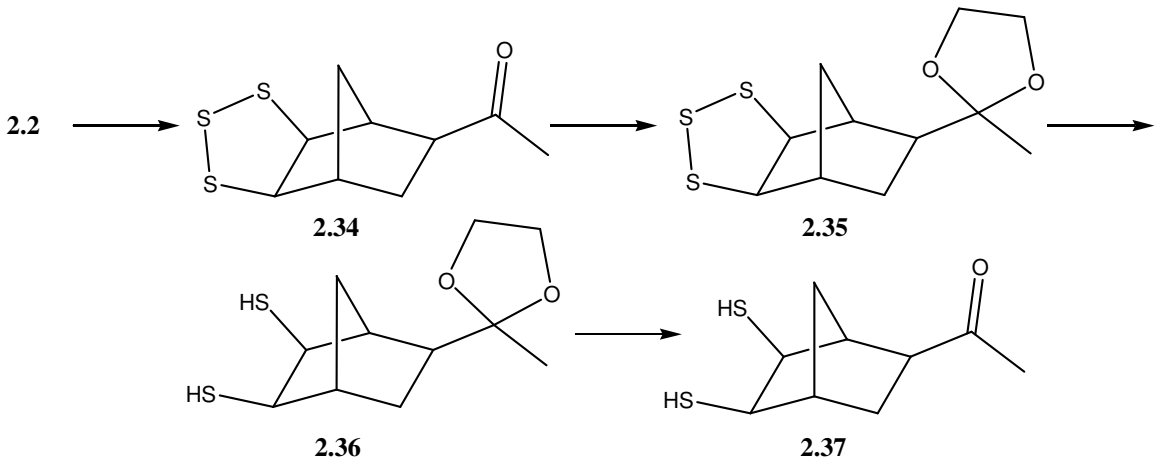

Figure 2.25 Synthetic route to model polythioacetal

Polymerization of this compound was successful. The resulting polymer has properties similar to the model polyacetal. The molecular weight is approximately the same however its thermal stability is slightly decreased as it decomposes at 260 ^{o}C.

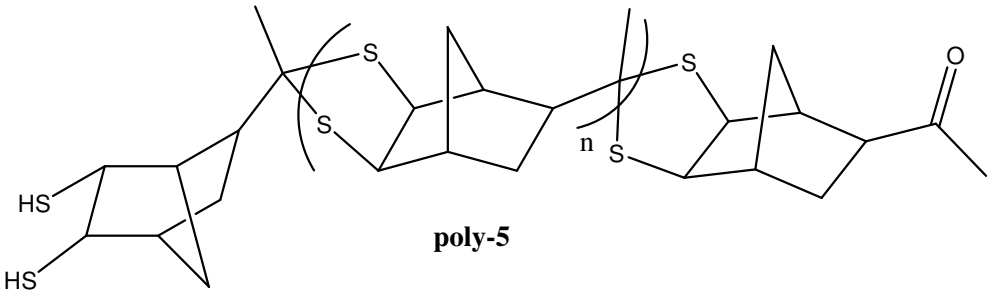

Figure 2.26 Structure of norbornane based polythioacetal

While ring opening polymers tend to have replaced many commercially produced step-growth polymers, there is still utility for materials produced from an AA-BB step-growth polymerization. Looking to use the same basic structure as the AB polymers, a norbornene based tetraol was targeted. Attempts to directly synthesize the tetraol resulted in difficult work ups and very low yields.[34] Alternately, using an excess of bicyclo[2.2.1]hepta-2,5-diene a single olefin can be dihydroxylated and isolated.

Protection of the diol as the dimethyl acetal followed by dihydroxylation of the remaining olefin results in **2.40** which serves as a 'masked' tetraol. Sublimation of the product twice produces a solid material in 24% yield.

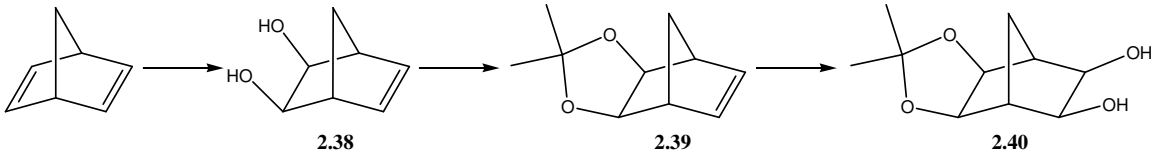

2.38 **2.39** **2.40**

Figure 2.27 Route to a 'masked' tetraol

Combining equimolar amounts of the 'masked' tetraol, with commercially available dialdehydes and diketones, results in AA-BB polyacetals (Figure 2.27). This is accomplished with an acid catalyst or iodine through a two stage heating process.

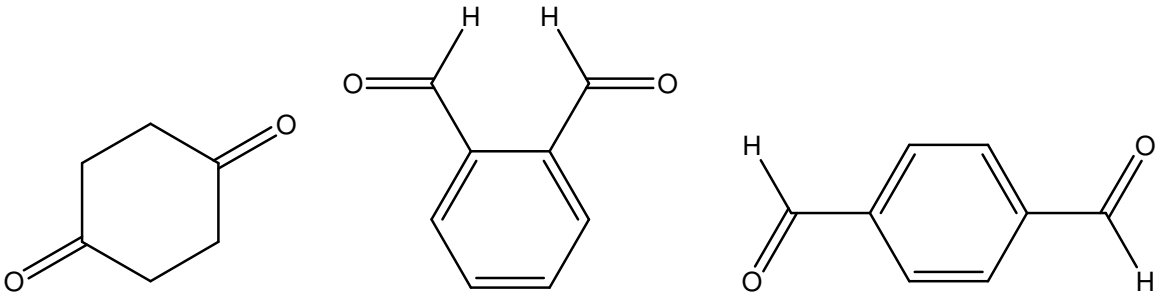

Figure 2.28 Example of BB type monomers used for polymerization with **2.40**

SUMMARY

A new class of step-growth polymeric materials based upon the formation of an acetal backbone has been developed. These materials demonstrated high thermal stability and are soluble in common organic solvents. One such polyacetal was functionalized with a protectable acidic functionality that allowed for the first imaging demonstration with such a system. Polyacetal materials have been polymerized in both AB and AA-BB fashion. The first reported step-growth polymerization catalyzed by iodine has been presented. A polythioacetal was also produced. All materials showed high thermal stability and good solubility in organic solvents.

EXPERIMENTAL METHODS

Solvents and reagents.

Diethyl ether, tetrahydrofuran (THF) and dimethyl formamide (DMF) were obtained from a dry solvent system. Pyridine and triethylamine were dried over potassium hydroxide. All other solvents (Fisher) were reagent grade (99.9%) and used as received. All reagents were purchased from either Aldrich or Acros and used as received unless otherwise specified.

General.

All reactions were performed under a dry nitrogen atmosphere unless otherwise noted. Thin-layer chromatography was performed on Whatman AL SIL G/UV F_{254} plates. Silica used for flash chromatographic separation was Sorbent Technologies 60 Å (230-450 mesh).

Analysis.

^{1}H, ^{13}C and ^{19}F NMR spectra were acquired at room temperature on a Varian Unity Plus 300 or 400 spectrometer at 300 or 400 MHz. All NMR data are reported in parts per million and referenced to solvent ^{1}H: $CDCl_3$ = 7.24 ppm or DMSO-d6 = 2.49 ppm, ^{13}C $CDCl_3$ = 77.0 ppm or DMSO-d6 = 39.5 ppm. Splitting patterns are designated as follows: s, singlet; d, doublet; t, triplet; q, quartet; p, pentet; sex, sextet; sept, septet; or as more complex combinations eg. ddd, doublet of doublets of doublets or otherwise as m, multiplet. Low-resolution mass spectra (LRMS) were obtained on a Hewlett-Packard 5971A GC-MS spectrometer equipped with a DB-1 (15 m x 0.25 mm, 1 mm film thickness) capillary column; high-resolution mass spectra (HRMS) were obtained on a VG ZAB2-E mass spectrometer. Thermo-gravimetric analysis was performed on a TA Instruments TGA Q-500. Differential scanning calorimetry was performed on a TA Instruments DSC Q100. Infrared spectra were recorded on a Nicolet Magna-IR 550

spectrometer. Molecular weights (M_w) and polydispersity indices (PDI) were measured from THF solutions using an Agilent 1100 Series GPC equipped with a set of two Agilent PLgel 5 mm crosslinked polystyrene columns (10^4 Å and 100 Å) and are reported relative to polystyrene standards. Thin layer chromatography was visualised using either 254nm UV light, ethanolic phosphomolybdic acid or permanganate.

General AA-BB Polymerization

AA-BB polymers were polymerized in benzene in the presence of a catalytic amount of *p*-TSA. In a two stage reaction, **2.40** and commercially available diketone or dialdehyde (1 eq) were stirred in refluxing benzene with 10 % H_2O. After refluxing 12 h, the reaction was equipped with a Dean-Stark trap and reflux condenser. The reaction was heated to vigorous reflux for an additional 12 h. After cooling to RT, the reaction was concentrated and redissolved in DCM. The polymers were precipitated into cold MeOH or hexanes.

1-(5,6-Dihydroxy-bicyclo[2.2.1]hept-2-yl)-ethanone (2.1): NMO (1.97 g, 16.82 mmol) was dissolved in a 9:1 mixture of THF:H_2O. To this was added compound **2.2** (2.01 g, 14.76 mmol). To this stirred solution, under N_2, was added via syringe OsO_4 (0.08 eq. 2.5 wt% solution in 2-methyl-2-propanol). The resultant dark brown solution was refluxed overnight. Solvent was removed by rotary evaporation. The isolated viscous brown liquid was purified by distillation (153 ^oC, 0.9 torr) to yield a yellow tinged, highly viscous liquid (1.89 g, 11.11 mmol, 75%). ^1H NMR ($CDCl_3$) δ= 3.790 (br s, 4H), 3.694 (d, *J*= 5.282 Hz, 1H), 3.658 (d, *J*= 5.869 Hz, 1H), 3.623 (d, *J*= 5.478 Hz, 1H), 3.496 (d, *J*= 5.869 Hz, 1H), 2.761 (dt, J_1= 10.955 Hz, J_2= 4.891 Hz, 1H), 2.468 (br dd, J_1= 4.304 Hz, J_2= 1.369 Hz, 1H) 2.304 (br s, 1H), 2.28-2.20 (m, 1H), 2.138 (s, 3H), 2.117 (s, 3H), 1.864 (dq, J_1= 10.368 Hz, J_2= 1.826 Hz, 1H), 1.797 (dt J_1= 12.911 Hz, J_2= 4.891 Hz,

1H), 1.605 (ddd, J_1= 10.760 Hz, J_2= 2.152 Hz, J_3= 1.370, 1H), 1.543 (ddd, J_1= 13.107 Hz, J_2= 5.282 Hz, J_3= 2.152, 1H), 1.447 (ddd, J_1= 13.302 Hz, J_2= 10.955 Hz, J_3= 4.891, 1H), 1.247 (dp, J_1= 10.564 Hz, J_2= 1.565 Hz, 1H), 1.140 (ddd, J_1= 12.911 Hz, J_2= 8.998 Hz, J_3= 2.347, 1H), 1.047 (dp, J_1= 10.759 Hz, J_2= 1.565 Hz, 1H). ^{13}C NMR ($CDCl_3$): δ= (*exo* and *endo*) 209.757, 209.058, 73.972, 73.778, 73.749, 70.140, 51.331, 50.014, 46.249, 46.167, 43.742, 42.589, 33.809, 29.598, 29.315, 28.720, 27.083, 25.409. FTIR (cm^{-1})= 3392.48, 2964.15, 1700.23. HRMS (CI^+): calc. 137.0966 found 137.0966.

1-Bicyclo[2.2.1]hept-5-en-2-yl-ethanone (2.2): Freshly cracked CPD (13.15 g, 199 mmol) in 100 mL DCM was stirred at 0 ^oC and methyl vinyl ketone (9.56 g, 136 mmol) was added drop-wise over 1 hour. The reaction was concentrated to yield a colorless liquid containing 6.7 % DCPD as determined by GC (19.61 g, ~143 mmol, 98 %, ~4:1 endo:exo; ~50:50 upon base catalyzed isomerization with sodium ethoxide in ethanol). The material was used without further purification. ^{1}H NMR ($CDCl_3$) δ= (*endo*) 6.13 (m, 1H), 5.84 (m, 1H), 3.24 (m, 1H), 3.01 (m, 1H), 2.89 (m, 1H), 2.12 (s, 3H), 1.74 (m, 1H), 1.50 (m, 1H), 1.46 (m, 1H), 1.34 (m, 1H). ^{13}C NMR ($CDCl_3$): δ= (*exo* and *endo*) 209.91, 208.19, 137.73, 137.32, 135.37, 130.84, 53.20, 51.85, 51.16, 49.52, 45.40, 44.95, 42.25, 41.24, 29.35, 28.72, 28.58, 26.95. FTIR (cm^{-1})= 3059.76, 2968.25, 2870.25, 1700.95. HRMS (CI^+): calc. (for loss of H_2O) 153.0916 found 153.0916.

Poly-1-(5,6-Dihydroxy-bicyclo[2.2.1]hept-2-yl)-ethanone (poly-1). In a flask equipped with reflux condenser and Dean-Stark trap, **2.1** was stirred in benzene with *p*-toluenesulfonic acid (0.01 eq) at vigorous reflux for 48 h. Solvent was removed by rotary evaporation. The flaky off-white product was redissolved in a small volume of methylene chloride and precipitated from cold methanol. The product was filtered on a coarse fritted funnel and dried in vacuo. M_n = 3600 Da. ^{1}H NMR ($CDCl_3$) δ= 4.45-4.65

(m, 2H, terminal), 3.82-4.05 (m, 2H, interior), 2.42-2.58 (m, 1H), 2.10-2.35 (m, 2H), 1.00-1.70 (m, 7H).

1-[5,6-Dihydroxy-3-(3,3,3-trifluoro-2-hydroxy-2-trifluoromethyl-propyl)-bicyclo[2.2.1]hept-2-yl]-ethanone (**2.3**): NMO (1.32 g, 11.2 mmol) was dissolved in a 9:1 mixture of THF and water. To this solution was added **2.4** (3.09 g, 9.77 mmol). The system was stirred under N_2 and 0.1 mL of a 2.5 wt% solution of OsO_4 was injected. The reaction was stirred at rt for 48 h. The reaction was concentrated in vacuo and redissolved in ethyl acetate and passed through a 1" silica gel plug to yield a highly viscous golden brown material ^{1}H NMR (DMSO): δ= (2.02 g, 5.77 mmol, 59.1%). 7.742 (br s, 1H minor), 7.704 (br s, 1H major), 4.652 (br d, *J*= 4.988 Hz, 1H minor), 4.619 (br d, *J*= 5.282 Hz, 1H minor), 4.594 (br d, *J*= 4.255 Hz, 2H major), 3.832 (t, *J*= 4.842 Hz, 1H minor), 3.631 (t, *J*= 4.842 Hz, 1H minor), 3.395 (t, *J*= 4.842 Hz, 1H major), 3.276 (t, *J*= 4.842 Hz, 1H major), 2.508 (t, *J*= 4.842 Hz, 1H major), 2.419 (m, 1H minor), 2.326 (br d, *J*= 3.081 Hz, 1H major), 2.086 (s, 3H minor), 2.075 (s, 3H major), 2.07-2.04 (br m, 2H major, 2H minor), 2.006 (br s, 1H minor), 1.95-1.85 (m, 1H major), 1.82-1.66 (m, 2H major, 2H minor), 1.537 (br d, *J*= 9.39 Hz, 1H minor), 1.303 (br d, *J*= 10.417 Hz, 1H major), 1.039 (br d, *J*= 10.124 Hz, 1H minor). ^{13}C NMR (DMSO): δ= 207.903, 207.553, 123.634 (q, *J*= 288.72 Hz), 123.586 (q, *J*= 287.97 Hz), 75.957 (sep, *J*= 27.68 Hz), 73.375, 72.974, 68.934, 68.026, 59.648, 57.252, 49.373, 48.079, 47.863, 46.338, 34.969, 32.781, 32.052, 30.996, 30.787, 30.378, 29.642. ^{19}F NMR (DMSO): δ= -74.866 (q, *J*= 9.67 Hz), -75.170 (q, *J*= 9.67 Hz), -75.633 (q, *J*= 9.67 Hz), -76.092 (q, *J*= 9.80 Hz). FTIR (cm^{-1})= 3339.59, 3054.94, 2985.27, 1700.40, 1264.93. HRMS (CI^+): calc. 351.1031 found 351.1034.

1-[3-(3,3,3-Trifluoro-2-hydroxy-2-trifluoromethyl-propyl)-bicyclo[2.2.1]hept-5-en-2-yl]-ethanone (**2.4**): **2.5** (5.26 g, 21.03 mmol) was combined with approximately 30 mL ether and freshly cracked CPD (1.53 g, 23.13 mmol). The mixture was sealed in a Parr reaction vessel and heated to 120 ^{o}C for 3 h then cooled to rt and an additional 1.1 eq freshly cracked CPD was added. The reaction vessel was resealed and heated to 120 ^{o}C for 3 h. The reaction was cooled to rt and concentrated in vacuo. The product was purified via flash chromatography using first hexane as eluent and then DCM to collect the light yellowish solid product (3.09 g, 9.77 mmol, 46.5%). MP= 101-103 ^{o}C. ^{1}H NMR ($CDCl_3$): δ= 6.24 (dd, J_1= 3.2 Hz, J_2= 5.7 Hz, 1H), 6.09 (dd, J_1= 2.9 Hz, J_2= 5.7 Hz, 1H), 5.10 (s, 1H), 3.00 (d, J= 1.4 Hz, 1H), 2.83 (s, 1H), 2.61 (sex, J= 4.0 Hz, 1H), 2.20 (s, 3H), 2.00 (dd, J_1= 1.55 Hz, J_2= 4.65 Hz, 1H), 1.96 (dd, J_1= 3.7 Hz, J_2= 15.4 Hz, 1H), 1.56 (ddd, J_1= 1.13 Hz, J_2= 9.45 Hz, J_3= 15.37 Hz, 1H), 1.41(dq, J_1= 1.77 Hz J_2= 8.8 Hz, 1H), 1.35 (d, J= 8.8 Hz, 1H). ^{13}C NMR ($CDCl_3$): δ= 213.775, 139.379, 132.646, 123.513 (q, J= 287.225 Hz), 123.156 (q, J= 287.225 Hz), 75.817 (sept, J= 28.423 Hz), 61.985, 49.828, 46.949, 45.974, 35.878, 35.825, 28.474 ^{19}F NMR ($CDCl_3$): δ= -77.267 (q, J= 9.9 Hz), -77.346 (q, J= 9.9 Hz), -78.582 (q, J= 9.9 Hz), -78.933(q, J= 9.9 Hz). FTIR (cm^{-1})= 3238.10, 2967.55, 1693.37, 1266.56, 1142.99. HRMS (CI^{+}): calc. 317.0976 found 317.0979.

7,7,7-Trifluoro-6-hydroxy-6-trifluoromethyl-hept-3-en-2-one (**2.5**): **2.9** (6.96 g, 27.60 mmol) was stirred in acetone cooled in an ice bath. To this was added freshly prepared Jones Reagent. Addition continued drop-wise until a red color persisted. A small amount of IPA was added until a green color persisted. The reaction was then decanted from solids. An equal volume of water was added and extracted with 3 x 100 mL DCM. The combined organics were washed with brine, dried over $MgSO_4$ and dried in vacuo.

The yellowish liquid was distilled to yield the product as a colorless liquid (71 ^{o}C, 0.79 torr, 5.26 g, 21.03 mmol, 76.2%). ^{1}H NMR ($CDCl_3$): δ= 6.87 (dt, J_1= 15.1 Hz , J_2= 7.1 Hz, 1H), 6.15 (d, *J*= 16.0 Hz, 1H), 5.9 (br s, 1H), 2.83 (d, *J*= 7.5 Hz, 2H), 2.22 (s, 3H). ^{13}C NMR ($CDCl_3$): 200.71, 139.57, 134.55, 122.91 (q, *J*= 288.1 Hz), 75.75 (q, *J*= 29.0 Hz), 33.52, 26.32. ^{19}F NMR ($CDCl_3$): δ= -77.27. FTIR (cm^{-1})=3265.95, 3055.09, 2361.24, 1661.71, 1265.68. HRMS (CI^+): calc. 251.0507 found 251.0511.

4-Penten-2-ol (**2.6**)[21]: To a stirred solution of acetaldehyde (5.70 g, 129.4 mmol) and allyl bromide (46.40 g, 383.5 mmol) in sat. aq. ammonium chloride (500 mL) and THF (100 mL at 0 ^{o}C was added zinc dust (47.6 g, 727.8 mmol). After 1 h, the reaction mixture was filtered and extracted with DCM 3 x 100 mL. Combined organics were washed with brine, dried over $MgSO_4$, filtered and concentrated to yield a light yellow liquid (5.78 g, 67.1 mmol, 51.8%). ^{1}H NMR ($CDCl_3$): δ= 5.80-5.70 (m, 1H), 5.08-5.05 (m, 1H), 5.027 (t, *J*= 1.173 Hz, 1H), 3.772 (sex, *J*= 6.260 Hz, 1H), 2.285 (br s, 1H), 2.22-2.07 (m, 2H), 1.126 (d, *J*= 6.260 Hz, 3H). ^{13}C NMR ($CDCl_3$): δ= 134.752, 117.698, 66.822, 43.548, 22.552. FTIR (cm^{-1})= 3361.96, 3078.13, 2972.83, 2930.04. HRMS (CI^+): calc. 85.0653 found 85.0652.

Benzoic acid 1-methyl-but-3-enyl ester (**2.7**): In a 1L RB flask **2.6** (24.28 g, 281.90 mmol) was stirred at 0 ^{o}C in 400 mL DCM with 50 mL TEA. Benzoyl chloride (45.40 g, 322.97 mmol) in 100 mL DCM was added dropwise. The solution slowly changed from colorless to orange with a small amount of gas evolution noted. After warming to room temperature, the reaction was twice vacuum filtered. The salts were washed with DCM to whiteness. The filtrate was collected and washed 3 x 150 mL H_2O, 1 x 150 mL brine, dried over $MgSO_4$, filtered and concentrated in vacuo. The product was isolated as a colorless liquid via distillation (60 ^{o}C, 0.33 torr, 43.44 g, 228.36 mmol, 81.0%). ^{1}H NMR

($CDCl_3$): δ= 8.02 (m, 2H), 7.49 (m, 1H), 7.38 (m, 2H), 5.81 (m, 1H), 5.20 (s, *J*= 6.2 Hz, 1H), 5.08 (m, 2H), 2.42 (m, 2H), 1.32 (d, *J*= 6.2 Hz, 3H). ^{13}C NMR ($CDCl_3$): δ=165.79, 133.42, 132.56, 130.56, 129.32, 128.09, 117.67, 70.49, 40.17, 19.35. FTIR (cm^{-1})= 3074.67, 2978.94, 2934.29, 1718.78, 1273.80. HRMS (EI^+): calc. 190.0994 found 190.0996.

Benzoic acid 6,6,6-trifluoro-5-hydroxy-1-methyl-5-trifluoromethyl-hex-2-enyl ester (**2.8**): **2.7** (14.0 g, 73.4 mmol) was combined with dry toluene in a Parr reaction vessel. The mixture was sealed with parafilm and cooled to -78 ^oC. Hexafluoroacetone was condensed in a cold finger condenser attached to a jacketed addition funnel. The parafilm was removed from the reaction vessel and the hexafluoroacetone added rapidly. The reaction vessel was sealed and allowed to warm to RT. After warming the reaction vessel was then heated to 150 ^oC for 48 h. After cooling to RT the reaction vessel was vented and opened. The orange colored contents were concentrated in vacuo and a colorless liquid (23.6 g, 66.2 mmol, 90.2%) was isolated via column chromatography using 2:1 hexanes:DCM as eluent. ^1H NMR ($CDCl_3$): δ= 8.04 (d, *J*= 7.18 Hz, 2H), 7.56 (m, 1H), 7.43 (m, 2H), 5.7-5.8 (m, 2H), 5.55 (m, 1H), 4.4 (br s, 1H), 2.75 (d, *J*= 5.10 Hz, 2H), 1.47 (d, *J*= 6.60 Hz, 3H). ^{13}C NMR ($CDCl_3$): δ= 166.46, 137.25, 133.17, 130.05, 129.57, 128.37, 122.08, 71.35, 33.35, 20.02. ^{19}F NMR ($CDCl_3$): δ= -76.884, -77.872. FTIR (cm^{-1})= 3395.06, 3066.15, 2984.84, 2937.43, 1698.86, 1283.62. HRMS (CI^+): calc. 357.0925 found 357.0927.

7,7,7-Trifluoro-6-trifluoromethyl-hept-3-ene-2,6-diol (**2.9**): **2.8** (21.42 g, 60.12 mmol) was stirred in 300 mL water containing 4 eq NaOH. The reaction was stirred at reflux until complete dissolution was observed. Upon cooling to room temperature the reaction mixture was extracted 3 x 150 mL DCM. The aqueous layer was acidified and extracted

3 x 150 mL DCM. These extracts were not combined with the previous. The second combined extracts were washed with 2 x 150 mL sat. $NaHCO_3$. After drying over $MgSO_4$ the product was concentrated to yield a gold liquid. This was distilled (54.5 ^oC, 0.7 torr, lit. 90-100 ^oC, 20 torr) to yield a colorless liquid (7.54 g, 29.90 mmol, 49.7%). ^1H NMR ($CDCl_3$): δ= 5.65 (m, 2H), 5.27 (s br, 1H), 4.26 (p, *J*= 6.2 Hz, 1H), 3.47 (s br, 1H), 2.62 (m, 2H), 1.22 (d, *J*= 6.4 Hz, 3H). ^{13}C NMR ($CDCl_3$): δ= 140.52, 123.14 (q, *J*= 286 Hz), 120.82, 75.65 (q, *J*= 28.7 Hz), 68.76, 33.42, 22.26. ^{19}F NMR ($CDCl_3$): δ= -76.92, -77.51. FTIR (cm^{-1})= 3332.38, 2980.04, 1216.76, 1150.02. HRMS (CI^+): calc. 253.0663 found 253.0660.

Poly (1-[5,6-Dihydroxy-3-(3,3,3-trifluoro-2-hydroxy-2-trifluoromethyl-propyl)-bicyclo[2.2.1]hept-2-yl]-ethanone) (**poly-2**): In a 50mL RBF, **6** (1.82 g, 5.20 mmol) was dissolved in 25 mL benzene. To this was added a catalytic amount of *p*-TSA. The flask was equipped with a Dean-Stark trap and reflux condenser. The polymerization was heated to vigorous reflux for 12 h. Water was observed to be collecting in the Dean-Stark trap. The polymerization was cooled to RT and concentrated. The solid product was dissolved in a small amount of DCM and precipitated from cold hexanes. The white powdery solid (0.79 g) was recovered by filtering through a medium fritted funnel. M_n = 3625 Da. FTIR (cm^{-1})= 3393.49, 2979.70, 1707.57, 1212.29.

Poly (Carbonic acid 1-(3-acetyl-5,6-dihydroxy-bicyclo[2.2.1]hept-2-ylmethyl)-2,2,2-trifluoro-1-trifluoromethyl-ethyl ester *tert*-butyl ester) (**poly-2a**): To a 50 mL RBF with 25 mL dry THF was added **poly-2** (0.156 g) and di-*tert*-butyl dicarbonate (0.147 g, 0.67 mmol). The solution was stirred at RT for 5 min then 4-(*N*,*N*-dimethylamino)pyridine (DMAP) (0.01 g, 0.07 mmol) was added. The solution turned off color and a small amount of gas evolution was noted. The solution was stirred at RT

overnight under N_2. The solvent was removed in vacuo and the product dissolved in ether. The ethereal layer was washed with 2% HCl, sat $NaHCO_3$ and brine. After drying over $MgSO_4$, the product was isolated as a white powder (0.15 g). The disappearance of the hydroxyl group was observed using FTIR.

Imaging of poly-2a: A formulation of 10 wt% polymer and 5 wt% TPS Nanoflate in PGMEA was spin coated on a 4" wafer and subjected to a post apply bake (PAB) at 110 ^{o}C for 60 s. Using contact printing the film was exposed to 365 nm wavelength light for 30 s. A post exposure bake (PEB) (110 ^{o}C, 90 s) was performed and the wafer was developed for 30 s in 0.26 N TMAH.

1-(5,6-Dihydroxy-bicyclo[2.2.1]hept-2-yl)-2,2,2-trifluoro-ethanone (**2.10**): In a 250 mL RBF, 6 (3.69 g, 13.96 mmol) was stirred in a 9:1 mixture of vigorously refluxing *n*-butanol:water (100 mL) with Amberlyst® 15 ion-exchange resin overnight. After cooling to RT the reaction mixture was diluted with 50 mL H_2O extracted 3 x 75 mL ethyl acetate. The combined organics were washed with sat. aq. $NaHCO_3$, water and brine, dried over $MgSO_4$, filtered and concentrated to yield a light golden viscous liquid. This liquid was further purified via column chromatography (eluent 3:1 hexanes:EA) to yield a viscous golden liquid (1.54 g, 6.87 mmol, 49.2%). ^{1}H NMR ($CDCl_3$): δ=3.955 (br s, 2H *endo*, 2H *exo*), 3.711 (dd, J_1= 6.02 Hz, J_2= 1.40 Hz, 1H *endo*), 3.668 (dd, J_1= 6.02 Hz, J_2= 1.47 Hz, 1H *endo*), 3.652 (dd, J_1= 5.99 Hz, J_2= 1.36 Hz, 1H *exo*), 3.533 (dd, J_1= 5.94 Hz, J_2= 1.62 Hz, 1H *exo*), 3.126 (dt, J_1= 10.30 Hz, J_2= 5.03 Hz, 1H *exo*), 2.614 (dd, J_1= 8.80 Hz, J_2= 5.50 Hz, 1H *endo*), 2.540 (br d, J=3.52 Hz, 1H *exo*), 2.374 (s, 1H *endo*), 2.174 (m, 1H *endo*, 1H *exo*), 1.914 (dq, J_1= 10.71 Hz, J_2= 1.76 Hz, 1H *exo*), 1.847 (dd, J_1= 13.20 Hz, J_2= 5.14 Hz, 1H *endo*), 1.653 (m, 1H *endo*, 1H *exo*), 1.562 (ddd, J_1= 13.39 Hz, J_2= 5.40 Hz, J_3= 2.28 Hz, 1H *exo*), 1.294 (m, 1H *endo*, 1H *exo*), 1.148 (dp, J_1=

11.12 Hz, J_2= 1.54 Hz, 1H *endo*). ^{13}C NMR ($CDCl_3$): δ=192.516 (q, *J*= 34.2 Hz), 192.136 (q, *J*= 33.7 Hz), 115.686 (q, *J*= 293.0 Hz), 115.568 (q, *J*= 292.7 Hz), 73.673, 73.652, 73.323, 69.769, 46.209, 46.177, 45.232, 43.778, 43.343, 42.416, 34.087, 29.188, 27.282, 25.971. ^{19}F NMR ($CDCl_3$): δ= -77.061 (s, 3F, *endo*), -77.974 (s, 3F, *exo*). FTIR (cm^{-1})= 3348.25, 2963.20, 1752.27, 1206.96, 1139.17, 1058.38. HRMS (CI^+): calc. 225.0739 found 225.0744.

(1-(bicyclo[2.2.1]hept-5-en-2-yl)-2,2,2-trifluoroethoxy)trimethylsilane (**2.14**): In a 250 mL RBF, 2.15 (7.9 g, 64.7 mmol) was dissolved in 100 mL DCM. This was cooled in an ice bath and a small amount of TBAF (1 M in THF) was added. Ruppert's reagent (9.2 g, 64.7 mmol) in 10 mL DCM was injected dropwise over 15 min with stirring under nitrogen. The mixture was stirred for 3 h then washed with 100 mL water. The extract was washed with brine, dried over $MgSO_4$, filtered and concentrated to yield a colorless liquid (10.3 g, 38.9 mmol, 60%). ^{1}H NMR ($CDCl_3$): δ=6.221 (dd, J_1= 5.72 Hz, J_2= 3.08 Hz, 1H *endo*), 6.180 (dd, J_1= 5.76 Hz, J_2= 3.05 Hz, 1H *endo*), 6.119 (dd, J_1= 5.65 Hz, J_2= 3.16 Hz, 1H *exo*), 6.088 (m, 2H *exo*), 6.071 (dd, J_1= 5.65 Hz, J_2= 3.94 Hz, 1H *exo*), 5.924 (dd, J_1= 5.72 Hz, J_2= 3.12 Hz, 1H *endo*), 5.909 (dd, J_1= 5.76 Hz, J_2= 2.90 Hz, 1H *endo*), 3.985 (dq, J_1= 6.97 Hz, J_2= 4.88 Hz, 1H *exo*), 3.761 (dq, J_1= 9.17 Hz, J_2= 6.17 Hz, 1H *exo*), 3.327 (m, 2H *endo*), 3.025 (m, 1H), 2.933 (m, 1H *exo*), 2.908 (m, 1H *endo*), 2.860 (m, 1H *exo*), 2.829 (m, 1H *exo*), 2.814 (m, 1H *endo*), 2.784 (br s, 1H *endo*), 2.640 (br s, 1H *exo*), 2.391 (m, 2H *endo*), 1.917 (ddd, J_1= 12.11 Hz, J_2= 9.17 Hz, J_3= 3.82 Hz, 1H *endo*), 1.793 (ddd, J_1= 12.21 Hz, J_2= 9.10 Hz, J_3= 3.86 Hz, 1H *endo*), 1.688 (m, 1H *endo*), 1.497-1.255 (m, 1H *endo*, 9H *exo*), 1.415 (dq, J_1= 8.35 Hz, J_2= 2.04 Hz, 1H, *endo*), 1.215 (m, 1H *endo*), 1.183 (m, 1H *exo*), 0.833 (m, 2H *endo*), 0.171 (s, 9H *exo*), 0.158 (s, 9H *endo*), 0.151 (s, 9H *exo*), 0.090 (s, 9H *endo*). ^{13}C NMR ($CDCl_3$):

δ=138.903, 137.987, 137.390, 137.329, 136.786, 136.362, 132.620, 131.498, 125.758 (q, *J*=283.4 Hz), 125.620 (q, *J*=283.6 Hz), 125.296 (q, *J*=283.4 Hz), 75.138 (q, *J*=29.9 Hz), 75.114 (q, *J*=28.8 Hz), 74.957 (q, *J*=28.9 Hz), 73.958 (q, *J*=29.4 Hz), 49.741, 48.439, 45.846, 45.602, 44.907, 44.444, 44.092, 43.237, 42.693, 42.215, 41.631, 41.537, 40.912, 40.404, 39.863, 39.424, 30.178, 29.668, 28.576, 27.230, 0.080, -0.052, -0.108. ^{19}F NMR ($CDCl_3$): -76.465 (d, *J*=6.63 Hz, 3F *exo*), -76.572 (d, *J*=7.46 Hz, 3F *exo*), -76.640 (d, *J*=5.81 Hz, 3F *endo*), -77.175 (d, *J*=6.63 Hz, 3F *endo*). FTIR (cm^{-1}) = 3063.4, 2877.4, 1497.8, 1381.1, 1254.4, 1125.7. HRMS (CI^+): calc. (for loss of TMS) 191.0684 found 191.0684.

Bicyclo[2.2.1]hept-5-ene-2-carbaldehyde (2.15): To freshly cracked CPD in DCM at 0 ^oC was added acrolein (1 eq.) drop-wise. After 1 h, the reaction mixture was concentrated and the title compound was used in further reactions without further isolation from residual DCPD.

2,2,2-Trifluoro-1-[3-(3,3,3-trifluoro-2-hydroxy-2-trifluoromethyl-propyl)-bicyclo[2.2.1]hept-5-en-2-yl]-ethanone (2.17): Freshly cracked CPD (2.00 g, 30.26 mmol) was combined with **2.18** (5.27 g, 17.33 mmol) in a Parr 250 ml reaction vessel in 100 ml toluene. The reaction vessel was sealed and heated overnight at 120 ˚C. The reaction was cooled to RT and concentrated to yield a golden yellow liquid. This product was eluted from a 1" silica gel plug with DCM to yield a light yellow solid (5.79 g, 15.64 mmol, 90.2%). Mp= 101-103 ^oC. ^{1}H NMR ($CDCl_3$): δ= 6.326 (dd, J_1= 5.65 Hz, J_2= 3.23 Hz, 1H major), 6.306 (dd, J_1= 5.62 Hz, J_2= 3.20 Hz, 1H minor), 6.203 (dd, J_1= 5.65 Hz, J_2= 2.94 Hz, 1H minor), 5.775 (dd, J_1= 5.69 Hz, J_2 = 2.76 Hz, 1H major), 3.339 (br s, 1H major), 3.307 (br s, 1H major C-OH), 3.221 (br s, 1H minor C-OH), 3.204 (t, *J*=3.85 Hz, 1H major), 3.025 (br s, 1H minor), 2.971 (br s, 1H minor), 2.894 (m, 1H minor), 2.736

(br s, 1H major), 2.504 (d, *J*= 4.47 Hz, 1H, minor), 2.265 (m, 1H major), 2.176 (m, 1H major), 2.022-1.963 (m, 1H major, 1H minor), 1.641-1.560 (m, 2H major, 2H minor), 1.419 (dd, J_1= 9.17 Hz, J_2= 1.55 Hz, 1H minor). ^{13}C NMR ($CDCl_3$): δ= 192.921 (q, *J*= 33.7 Hz), 191.624 (q, *J*= 33.8 Hz), 138.970, 136.825, 135.964, 131.450, 123.136 (q, *J*= 287.0 Hz), 123.098 (q, *J*= 287.3 Hz), 123.050 (q, *J*= 286.8 Hz), 123.012 (q, *J*= 286.7 Hz), 115.975 (q, *J*= 292.7 Hz), 115.851 (q, *J*= 292.6 Hz), 76.115 (sep, *J*= 29.0 Hz), 75.947 (sep, *J*= 29.1 Hz), 53.942, 53.048, 49.276, 48.186, 47.791, 47.278, 47.260, 45.576, 37.287, 35.737, 34.513, 33.128. ^{19}F NMR ($CDCl_3$): δ= -77.43 (q, *J*=10.0 Hz), -78.34, -78.77 (q, *J*=10.0 Hz). FTIR (cm^{-1}) = 3565.73, 3387.74, 2979.10, 1752.71, 1215.44, 1151.39, 911.67, 742.57. HRMS (CI^+): calc: 371.0694 found: 371.0697.

1,1,1,7,7,7-Hexafluoro-6-hydroxy-6-trifluoromethyl-hept-3-en-2-one (**2.18**): Dess-Martin periodinane (3.5 eq., 0.16 M) was stirred in dry DCM at RT. To this was added **2.22** (4.44 g, 14.5 mmol) and the reaction was heated to reflux under nitrogen until complete consumption of starting material. After cooling to RT an equal amount of ether was added then a 0.26 M solution of sodium thiosulfate (7 eq. relative to Dess-Martin) in sat. aq. $NaHCO_3$ was added. The layers were separated and the organic layer was washed with brine, dried over $MgSO_4$, and concentrated. The product was distilled (57 ^{o}C, 2.25 torr) to yield a colorless liquid (1.4 g, 4.6 mmol, 31.8%). ^{1}H NMR ($CDCl_3$): δ= 7.23 (dt, J_1= 15.8 Hz, J_2= 7.4 Hz, 1H), 6.47 (d, *J*= 15.8 Hz, 1H), 3.82 (br s, 1H), 2.88 (d, *J*= 7.4 Hz, 2H). ^{13}C NMR ($CDCl_3$): δ=179.74 (q, *J*= 35.9 Hz), 145.26, 125.37, 122.61 (q, *J*= 288.0 Hz), 115.97 (q, *J*= 290.2 Hz), 75.94 (sep, *J*= 29.2 Hz), 33.47. ^{19}F NMR ($CDCl_3$): δ=-77.6 (s, 6F), -78.3 (s, 3F). FTIR (cm^{-1})= 3566.61, 3462.04, 1734.83, 1636.89, 1222.00, 1156.18. HRMS (CI^+): calc. 305.0224 found 305.0222.

1,1,1-Trifluoro-pent-4-en-2-ol (**2.19**): In a 250 mL 3-neck RBF, indium powder (8.8 g, 76.7 mmol) was suspended in H_2O. To this was added allyl bromide (13.99 g, 115.6 mmol). The mixture was stirred for 10 min. Trifluoromethylacetaldehyde ethyl hemiacetal (5.03 g, 38.7 mmol) was added and the gray reaction was stirred overnight under nitrogen. The reaction mixture turned white. The reaction mixture was decanted from solids and the solids washed with ether. The reaction mixture was extracted 3 x 50 mL ether and the combined organics were washed with water then brine, dried over $MgSO_4$ and concentrated to yield a colorless liquid (2.65 g, 18.9 mmol, 49%). ^{1}H NMR ($CDCl_3$): δ= 5.79 (m, 1H), 5.16 (m, 2H), 3.92 (m, 1H), 3.61 (s, 1H), 2.39 (m, 2H). ^{13}C NMR ($CDCl_3$): 131.95, 124.93 (q, *J*=282.0 Hz), 119.157, 69.60 (q, *J*=30.7 Hz), 34.26. ^{19}F NMR ($CDCl_3$): δ= -80.09 (d, *J*=7.5 Hz, 3F). FTIR (cm^{-1})= 3338.45, 2980.53, 2877.93. HRMS (CI^+): calc. 141.0527 found 141.0531.

Benzoic acid 1-trifluoromethyl-but-3-enyl ester (**2.20**): **2.19** (2.63 g, 18.8 mmol) was stirred in 40 mL dry DCM with 5 mL dry TEA at 0 ^{o}C. To this was slowly added via syringe and under nitrogen, benzoyl chloride (3.20 g, 22.8 mmol). The reaction was allowed to warm to RT overnight. The reaction mixture was filtered on a Buchner funnel and the salts were washed with DCM to whiteness. The eluent was washed with sat. aq. sodium bicarbonate, water and brine, dried with $MgSO_4$ and concentrated. Distillation produced a colorless liquid (47 ^{o}C, 0.6 torr, 2.69 g, 11.02 mmol, 58.7%). ^{1}H NMR ($CDCl_3$): δ= 8.13 (m, 2H), 7.63 (m, 1H), 7.49 (m, 2H), 5.83 (m, 1H), 5.68 (m, 1H), 5.24 (dq *J*= 17.1 Hz, *J*= 1.5 Hz, 1H), 5.17 (m, 1H), 2.70 (m, 2H). ^{13}C NMR ($CDCl_3$): δ= 164.75, 133.63, 130.60, 129.9, 128.71, 128.48, 123.79 (q, *J*= 281.0 Hz), 119.49, 69.45 (q, *J*= 32.04 Hz), 32.66. ^{19}F NMR ($CDCl_3$): δ= -77.11, (d, *J*= 6.5 Hz, 3F). FTIR (cm^{-1})= 3086.38, 1736.04, 1261.56, 1185.31. HRMS (CI^+): calc. 245.0789 found 245.0792.

Benzoic acid-6,6,6-trifluoro-5-hydroxy-1,5-bis-trifluoromethyl-hex-2-enyl ester (**2.21**): **2.20** (2.48 g, 10.2 mmol) was combined with dry toluene in a Parr reaction vessel. The mixture was sealed with parafilm and cooled to -78 ^{o}C. Excess hexafluoroacetone was condensed in a cold finger condenser attached to a jacketed addition funnel. The parafilm was removed and the hexafluoroacetone added rapidly. The reaction vessel was sealed and allowed to warm to room temperature. After warming to room temperature the reaction vessel was heated to 150 ^{o}C and held at that temperature for 48 h. After cooling to room temperature the reaction vessel was vented and opened. The orange colored contents were concentrated in vacuo. A colorless liquid was isolated via column chromatography using 2:1 hexanes:DCM as eluent (2.10 g, 5.1 mmol, 50%). ^{1}H NMR ($CDCl_3$): δ= 8.09 (d, *J*= 8.0 Hz, 2H), 7.62 (t, *J*= 7.6 Hz, 1H), 7.47 (t, *J*= 7.7 Hz, 2H), 6.25 (m, 1H), 5.87 (m, 2H), 4.34 (s, 1H), 2.83 (d, *J*= 7.2 Hz, 2H). ^{13}C NMR ($CDCl_3$): 165.35, 134.18, 130.78, 130.06, 128.69, 128.35, 125.11, 123.09 (q, *J*= 279.7 Hz), 122.96 (q, *J*= 287.9 Hz), 75.97 (sept, *J*= 29.2 Hz), 71.32 (q, *J*= 33.7 Hz), 33.42. ^{19}F NMR ($CDCl_3$): -77.21 (s, 6F), -77.32 (d, *J*= 6.6 Hz, 3F). FTIR (cm^{-1})= 3433.68, 3068.43, 2968.12, 1719.98, 1602.42. HRMS (CI^{+}): calc. 411.0643 found 411.0640.

1,1,1,7,7,7-Hexafluoro-6-trifluoromethyl-hept-3-ene-2,6-diol (**2.22**): **2.21** (8.44 g, 20.6 mmol) was stirred in 50 mL refluxing water containing 4 eq NaOH overnight. Upon cooling to room temperature the reaction mixture was acidified and extracted with 3 x 50 mL DCM. The combined extracts were washed with sat. aq. $NaHCO_3$, water and brine then dried over $MgSO_4$ and concentrated. The product was distilled (59 ^{o}C, 0.78 torr) to yield a colorless liquid (4.76 g, 15.6 mmol, 75.6%). ^{1}H NMR ($CDCl_3$): δ= 6.01 (m, 1H), 5.71 (dd, J_1= 15.6 Hz, J_2= 6.6 Hz, 1H), 4.42 (p, *J*= 6.6 Hz, 1H), 3.59 (br s, 1H), 3.11 (br

s, 1H) 2.72 (d, *J*= 7.2 Hz, 2H). ^{13}C NMR ($CDCl_3$): δ=128.80, 128.25, 124.00 (q, *J*= 281 Hz), 122.91 (q, *J*= 282 Hz), 75.89 (sep, *J*= 29.2 Hz), 71.44(q, *J*= 32.9 Hz), 33.34. ^{19}F NMR ($CDCl_3$): δ= -77.2 (q, *J*= 9.1 Hz, 3F), -77.6 (q, *J*= 9.1 Hz, 3F), -80.1 (d, *J*= 6.6 Hz, 3F). FTIR (cm^{-1})= 3601.40, 3404.79, 2935.45, 1209.44. HRMS (CI^+): calc. 306.0302 found 306.0305.

5-(2,2,2-Trifluoro-1,1-dihydroxy-ethyl)-6-(3,3,3-trifluoro-2-hydroxy-2-trifluoromethyl-propyl)-bicyclo[2.2.1]heptane-2,3-diol (2.23): NMO (0.46 g, 3.93 mmol) was dissolved in a 9:1 mixture of THF and water. To this solution was added **2.17** (1.25 g, 3.38 mmol). 0.1 mL of a 2.5 wt% solution of OsO_4 was injected. The reaction was stirred at gentle reflux for 48 h. The reaction was concentrated in vacuuo, redissolved in ethyl acetate and eluted from a 1" silica gel plug to yield a light yellow solid (0.60 g, 1.42 mmol, 42.0%). MP= 214-216 ^oC. ^1H NMR (500 MHz, DMSO): δ= 8.23 (d, *J*= 1.8 Hz, 1H), 4.73 (d, *J*= 4.8 Hz, 1H), 4.68 (d, *J*= 5.1Hz, 1H), 3.60 (t, *J*= 4.9 Hz, 1H), 3.52 (t, *J*= 4.9 Hz, 1H), 2.28 (dd, J_1= 14.5 Hz, J_2= 5.8 Hz, 1H), 2.06 (s, 1H), 1.99 (t, *J*= 11.5 Hz, 1H), 1.84 (s, 2H), 1.79 (m, 1H), 1.70 (d, *J*= 10.7 Hz, 1H), 1.58 (d, *J*= 10.6 Hz, 1H). ^{13}C NMR (DMSO): δ= 122.64 (q, *J*= 288.7 Hz), 122.03 (q, *J*= 286.9 Hz), 95.80 (q, *J*= 30.9 Hz), 76.19 (sep, *J*= 29.4 Hz), 73.03, 72.41, 46.51, 46.21, 36.91, 30.46, 28.18, 21.18. ^{19}F NMR (DMSO): δ= -73.74 (q, *J*= 10.4 Hz, 3F), -77.21 (q, *J*= 10.4 Hz, 3F), -83.201 (s, 3F). FTIR (cm^{-1})= 3415.99, 3258.84, 3018.64, 2971.49, 1203.81, 1056.50, 978.98, 902.51. HRMS (CI^+): calc. 405.0748 found 405.0746.

5-(2,2,2-trifluoro-1-(trimethylsilyloxy)ethyl)bicyclo[2.2.1]heptane-2,3-diol (**2.24**): 150 mL 9:1 THF: H_2O was used to dissolve NMO (5.24 g, 44.7 mmol) in a 250 mL RBF. Solvent-dissolved **2.14** (10.3 g, 38.9 mmol) was added to the reaction mixture. The reaction was stirred under N_2 and a syringe was used to add OsO_4 (0.008 eq.). The

reaction turned a light-yellow color upon addition and was equipped with a reflux condenser. The reaction was heated to gentle reflux overnight then concentrated. The brown liquid was diluted with approximately 100 mL ethyl acetate, washed with water, brine, dried over $MgSO_4$, filtered, and concentrated to yield a viscous light-brown/gold product (7.91 g, 35.0 mmol, 90%). ^{1}H NMR ($CDCl_3$): δ= 4.1-3.5 (m, 5H), 2.5-2.0 (m, 3H), 1.8-0.7 (m, 4H), 0.13-0.09 (s, 9H). ^{13}C NMR ($CDCl_3$): 74.478, 74.165, 73.592, 72.052, 71.762, 71.457, 69.433, 69.277, 67.863, 66.412, 55.066, 46.100, 45.937, 45.409, 43.496, 42.819, 38.988, 38.556, 33.340, 32.544, 29.687, 29.129, 28.512, 27.165, 25.454, -0.022, -0.134. ^{19}F NMR ($CDCl_3$): δ=-75.845 (d, *J*=5.961 Hz), -76.181 (d, *J*=6.759 Hz), -76.481 (d, *J*=5.961 Hz), -77.001 (d, *J*=6.358 Hz). FTIR (cm^{-1}) = 3371.9, 2961.2, 1393.9, 1255.6, 1133.5. HRMS (CI^+): calc 299.1288 found 299.1290.

[1-(4,4-Dimethyl-3,5-dioxa-tricyclo[5.2.1.0^{2,6}]dec-8-yl)-2,2,2-trifluoro-ethoxy]-trimethyl-silane (**2.25**): **2.24** (7.91 g, 35.0 mmol) was dissolved in 125 mL benzene in a 250 mL RBF. Excess 2,2-dimethoxypropane was added to the mixture with a catalytic amount of *p*-TSA. The reaction vessel was submerged in an oil bath up to the level of the solvent and heated open to the atmosphere to 58 ºC. The bath temperature was increased in steps of 2 ºC until the methanol-benzene azeotrope (58 ^{o}C) boiled from the reaction and the forward reaction was complete. The reaction was then concentrated and eluted through a one inch silica gel plug with hexanes. The eluent was concentrated to yield a light yellow liquid (8.28 g, 24.4 mmol, 83%). ^{1}H NMR ($CDCl_3$): δ= 4.4-3.7 (m, 3H), 2.4-2.0 (m, 3H), 1.8-1.5 (m, 2H), 1.41-1.38 (m, 3H), 1.25-1.21 (m, 3H), 1.15-1.03 (m, 1H), 0.90-0.70 (m, 1H), 0.16-0.12 (s, 9H). ^{13}C NMR ($CDCl_3$): 109.060, 108.391, 108.279, 82.059, 81.903, 81.784, 81.524, 77.737, 77.565, 72.052, 71.613, 71.308, 43.794, 43.251, 42.306, 40.431, 39.962, 37.953, 37.611, 36.346, 33.214, 32.351, 29.449, 26.317, 25.997,

25.528, 25.335, 24.159, 24.01, 23.839, 0.968, 0.082, -0.037. ^{19}F NMR ($CDCl_3$): -75.772 (d, *J*=5.563 Hz), -76.2172 (d, *J*=6.755 Hz), -76.6033 (d, *J*=6.358 Hz), -76.9941 (d, *J*=6.358 Hz). FTIR (cm^{-1}) = 2961.7, 1457.6, 1373.0, 1255.6, 1162.6, 1054.3. HRMS (CI^+): calc 305.0610 found 305.612.

1-(4,4-Dimethyl-3,5-dioxa-tricyclo[5.2.1.0^{2,6}]dec-8-yl)-2,2,2-trifluoro-ethanol (**2.26**): In a 500 mL RBF, **2.25** (7.48 g, 22.1 mmol) and 75 wt% TBAF in H_2O (6.64, 25.4 mmol) was stirred in 100 mL THF open to the atmosphere. Upon addition of TBAF, the reaction changed from a light yellow to a light orange color. After about one hour, the reaction was complete as observed by GC/MS. The reaction was concentrated, diluted with 75 mL ethyl acetate, washed with water, brine, dried over $MgSO_4$, filtered and concentrated to yield a powdery white solid (5.65 g, 21.2 mmol, 93%). MP= 91-93 ºC. ^{1}H NMR ($CDCl_3$): δ= 4.4-3.5 (m, 3H), 2.5-2.0 (m, 3H), 1.8-1.4 (m, 2H), 1.38 (s, 3H), 1.23 (s, 3H), 1.2-0.7 (m, 3H). ^{13}C NMR ($CDCl_3$): δ=125.44 (q, *J*= 283.111 Hz), 125.023 (q, *J*= 283.111 Hz), 109.246, 108.718, 108.525, 81.933, 81.851, 81.792, 81.695, 81.695, 81.658, 81.479, 77.759, 77.417, 71.967 (sex, *J*= 29.172 Hz), 70.325 (sex, *J*= 29.919 Hz), 43.355, 43.087, 41.748, 41.175, 40.208, 39.999, 39.739, 36.688, 35.885, 32.916, 31.815, 29.308, 28.861, 27.455, 26.503, 26.079, 25.439, 25.163, 25.119, 25.074, 23.854, 23.809. ^{19}F NMR ($CDCl_3$): δ= -76.684 (d, *J*= 5.961 Hz), -77.134 (d, *J*= 6.357 Hz), -77.9516 (d, *J*= 5.960 Hz), -78.3641 (d, *J*= 6.357 Hz). FTIR (cm^{-1}) = 3380.7, 2984.8, 1457.3, 1375.5. HRMS (CI^+): calc. 267.1208 found 267.1208.

1-(4,4-Dimethyl-3,5-dioxa-tricyclo[5.2.1.0^{2,6}]dec-8-yl)-2,2,2-trifluoro-ethanone (**2.27**): Dess-Martin periodinane (1.5 eq., 0.16 M) was stirred in DCM at RT. To this was added **2.26** (4.05 g, 16.71 mmol) and the reaction was heated to reflux under nitrogen until complete consumption of starting material as monitored by GC/MS. After cooling to RT

an equal amount of ether was added then a 0.26 M solution of sodium thiosulfate (7 eq. relative to Dess-Martin) in sat. aq. $NaHCO_3$ was added. The layers were separated and the organic layer was washed with brine, dried over $MgSO_4$, and concentrated to yield a light-yellow solid (4.08 g, 15.4 mmol, 93%). MP= 121-122 ^oC. ^1H NMR ($CDCl_3$): δ= 4.03 (br d, *J*= 5.36 Hz, 1H, *exo*), 3.98 (br d, *J*= 5.36 Hz, 1H, *exo*), 3.96 (br d, *J*= 5.14 Hz, 1H, *endo*), 3.80 (dd, J_1= 5.43 Hz, J_2= 1.24 Hz 1H, *endo*), 3.12 (m, 1H, *endo*), 2.67 (br s, 1H, *endo*), 2.50 (m, 2H, *exo*), 2.28 (m, 1H, *endo*), 2.28 (m, 1H, *exo*), 1.86 (m, 1H, *endo*), 1.86 (m, 1H, *exo*), 1.62 (m, 1H, *endo*), 1.62 (m, 1H, *exo*), 1.52 (ddd, J_1= 13.35 Hz, J_2= 5.21 Hz, J_3= 2.42 Hz, 1H, *endo*), 1.33 (s, 3H, *exo*), 1.32 (s, 3H, *endo*), 1.22 (dp, J_1= 10.53 Hz, J_2= 1.50 Hz, 1H, *endo*), 1.19 (s, 3H, *exo*), 1.17 (m, 1H, *exo*), 1.15 (s, 3H, *endo*), 1.08 (m, 1H, *exo*). ^{13}C NMR ($CDCl_3$): δ=192.16 (q, *J*= 34.4 Hz), 191.91 (q, *J*= 33.7 Hz), 115.71 (q, *J*= 293.0 Hz), 115.59 (q, *J*= 292.7 Hz), 109.48, 108.78, 81.43, 81.40, 81.26, 77.60, 44.33, 43.40, 43.25, 42.71, 40.43, 39.53, 33.91, 28.87, 25.87, 25.17, 25.13, 24.53, 23.85, 23.75. ^{19}F NMR ($CDCl_3$): δ-77.276, -78.126. FTIR (cm^{-1}) = 2973.5, 1751.3, 1375.3, 1212.1, 1058.0. HRMS (CI^+): calc. 265.1052 found 265.1057.

5-Bromomethyl-bicyclo[2.2.1]hept-2-ene (2.28): Prepared according to literature procedure.[27] In a Parr reaction vessel uncracked DCPD (119.82 g, 906.3 mmol) was combined neat with allyl bromide (175.00 g, 1446.6 mmol) and in the presence of hydroquinone. The vessel was sealed and heated to 170 ^oC overnight. After cooling to RT, the vessel was vented and the reaction mixture was distilled (35 ^oC, 5.0 torr, lit. 40 ^oC, 0.3 torr) to yield a mixture of DCPD and product (75.6 g total, ~80% product) and used without further purification.

1-Bicyclo[2.2.1]hept-5-en-2-yl-propan-2-ol (2.29): In a 1 L 3-neck RBF, magnesium was flame dried under vacuum. Upon cooling 200 mL dry THF was transfer to the

system via cannula and the flask was filled with nitrogen. **2.28** (17.02 g, ~90.9 mmol) containing residual DCPD and one drop of 1,2-dibromoethane was added slowly via syringe to the system maintaining a slight reflux. Upon complete addition the reaction was stirred an additional 2 h. The reaction mixture was cooled to 0 ^{o}C. To this was added excess acetaldehyde. After 30 min an additional portion of excess acetaldehyde was added. The reaction was quenched slowly with H_2O, slightly acidified and vacuum filtered. 150 mL H_2O was added and extracted 3x 150 mL EA. The combined organics were washed with brine, dried over $MgSO_4$, filtered and concentrated to yield a colorless liquid. Product isolated via column chromatography (eluent 3:1 Hex:EA, 7.55 g, 49.6 mmol, 54.6%). ^{1}H NMR ($CDCl_3$): δ= 6.5-6.2 (m, 2H), 4.6 (m, 1H), 3.9 (m, 1H), 3.1 (m, 2H), 2.2 (m, 1H), 1.7-1.3 (m, 7H), 0.8 (m, 1H). ^{13}C NMR (DMSO): δ= 136.476, 136.327, 132.555, 132.384, 65.154, 64.946, 49.157, 49.053, 45.460, 44.894, 44.433, 44.247, 42.015, 41.995, 34.842, 34.582, 32.179, 32.104, 24.069. FTIR (cm^{-1})= 3400.50, 3057.78, 2965.90, 2867.63, 1265.22. HRMS (CI^{+}): calc. (for loss of H_2O) 135.1174 found 135.1171.

1-Bicyclo[2.2.1]hept-5-en-2-yl-propan-2-one (2.30): **2.29** (7.55g, 49.6 mmol) was stirred in acetone (25 mL). To this was added Jones reagent slowly until a red color persisted. The reaction was quenched with IPA until a green color persisted. The reaction mixture was filtered and an equal volume of EA was added. This was washed with H_2O and brine, dried over $MgSO_4$, filtered and concentrated. The green tinted material was purified to a colorless liquid (4.14 g, 27.6 mmol, 55.6%) by column chromatography (hexanes). ^{1}H NMR ($CDCl_3$): δ= 5.985 (dd, J_1= 5.73 Hz, J_2= 2.93 Hz, 1H, endo), 5.934 (dd, J_1= 5.74 Hz, J_2= 2.93 Hz, 1H, exo), 5.862 (dd, J_1= 5.86 Hz, J_2= 2.93 Hz, 1H, exo), 5.743 (dd, J_1= 5.85 Hz, J_2= 2.92 Hz, 1H, endo), 2.631 (br s, 1H endo),

2.631 (br s, 1H exo), 2.601 (br s, 1H endo), 2.601 (br s, 1H exo), 2.39-2.32 (m, 2H exo) 2.327 (br s, 1H exo), 2.31-2.24 (m, 1H endo), 2.19-2.14 (m, 1H endo), 2.04-1.97 (m, 1H endo, 1H exo), 1.979 (s, 3H exo), 1.935 (s, 3H endo), 1.787 (ddd, J_1= 11.71 Hz, J_2= 9.02 Hz, J_3= 3.90 Hz, 1H, endo), 1.243 (dq, J_1= 8.17 Hz, J_2= 1.95 Hz, 1H, endo), 1.26-1.13 (m, 3H, exo), 1.104 (br d, J= 8.29 Hz, 1H, endo), 0.329 (ddd, J_1= 11.58 Hz, J_2= 4.27 Hz, J_3= 2.56 Hz, 1H, endo). ^{13}C NMR ($CDCl_3$): δ= 208.860, 208.537, 137.362, 136.051, 136.000, 131.773, 50.108, 49.258, 48.606, 45.998, 45.244, 44.746, 42.174, 41.713, 33.406, 33.369, 32.387, 31.926, 29.728, 29.677. FTIR (cm^{-1})= 3059.60, 2967.33, 2869.82, 1701.92. HRMS (CI^+): calc. 151.1123 found 151.112.

1-(5,6-Dihydroxy-bicyclo[2.2.1]hept-2-yl)-propan-2-one (2.31): **2.30** (3.41 g, 22.7 mmol), NMO (5.86 g, 50 wt% solution, 25.0 mmol) and a catalytic amount of OsO_4 were combined in 100 mL THF. The reaction was heated to gentle reflux overnight. The reaction was concentrated in vacuo and redissolved in ethyl acetate and eluted from a 1" silica gel plug to yield a highly viscous golden brown material (1.64 g, 8.91 mmol, 39.3%). ^1H NMR ($CDCl_3$): δ= 4.532 (d, J= 5.013 Hz, 1H), 4.511 (d, J= 5.013 Hz, 1H), 3.727 (m, 1H), 3.420 (m, 1H), 2.50-2.32 (m, 2H), 2.050 (s, 3H), 1.90-185 (m, 2H), 1.70-1.60 (m, 2H), 1.018 (dt, J_1= 9.781 Hz, J_2= 9.781 Hz, 1H), 0.419 (ddd, J_1= 12.655 Hz, J_2= 5.563 Hz, J_3= 2.201 Hz, 1H). ^{13}C NMR ($CDCl_3$): δ=208.171, 73.747, 68.405, 46.464, 45.058, 43.555, 33.057, 32.328, 31.740, 29.887. FTIR (cm^{-1})= 3446.40, 2958.67, 1699.82. HRMS (CI^+): calc. 185.1178 found 185.1180.

3-Bicyclo[2.2.1]hept-5-en-2-yl-1,1,1-trifluoro-propan-2-one (2.32): In a 500 mL 3-neck RBF, magnesium (2.04 g, 83.92 mmol) was flame dried under vacuum. Upon cooling 100 mL of dry THF was transferred to the system via cannula and the flask was filled with nitrogen. **2.28** (17.0 g, ~187.09 mmol) containing residual DCPD and one

drop of 1,2-dibromoethane was added slowly via syringe to the system maintaining a slight reflux. Upon complete addition the reaction was stirred an additional two hours. To this was slowly added trifluoroacetic acid (3.78 g, 33.15 mmol). The reaction was quenched slowly with H_2O, slightly acidified and vacuum filtered. 150 mL H_2O was added and extracted 3x 150 mL EA. The combined organics were washed with brine, dried over $MgSO_4$, filtered and concentrated to yield a colorless liquid. Product isolated via column chromatography using hexanes as eluent. Due to volatility, the material (3.23 g) was not fully dried before use in the next step. ^{1}H NMR ($CDCl_3$): δ= 6.153 (dd, J_1= 5.80 Hz, J_2= 3.05 Hz, 1H), 5.871 (dd, J_1= 5.74 Hz, J_2= 2.93 Hz, 1H), 2.799 (br s, 1H), 2.754 (br s, 1H), 2.60-2.52 (m, 1H), 2.50-2.43 (m, 1H), 2.43-2.37 (m, 1H), 1.973 (ddd, J_1= 11.78 Hz, J_2= 8.76 Hz, J_3= 3.82 Hz, 1H), 1.409 (dq, J_1= 8.30 Hz, J_2= 1.92 Hz, 1H), 1.25 (m, 1H), 0.472 (ddd, J_1= 11.79 Hz, J_2= 4.10 Hz, J_3= 2.67 Hz, 1H). ^{13}C NMR ($CDCl_3$): δ= 191.279 (q, *J*= 34.522 Hz), 138.282, 131.522, 115.451 (q, *J*= 292.287 Hz), 49.454, 45.260, 42.459, 41.455, 32.549, 32.062. ^{19}F NMR ($CDCl_3$): δ= -79.799 (br s, 3F, *exo*), -79.898 (br s, 3F, *endo*). FTIR (cm^{-1})= 3061.89, 2969.01, 2873.11, 1762.65. HRMS (CI^+): calc. 205.0840 found 205.0838.

3-(5,6-Dihydroxy-bicyclo[2.2.1]hept-2-yl)-1,1,1-trifluoro-propan-2-one (**2.33**): **2.32** (1.61 g, 7.89 mmol), NMO (2.12 g 50 wt% solution in H_2O, 9.07 mmol) and a 0.1 mL 2.5 wt% solution OsO_4 in 2-methyl-2-propanol were combined in 100 mL THF. The reaction was heated to gentle reflux overnight. The reaction was concentrated in vacuo and redissolved in ethyl acetate and eluted from a 1" silica gel plug to yield a highly viscous golden brown material (0.49 g, 2.06 mmol, 26.1%). ^{1}H NMR (DMSO): δ= 4.497 (dd, J_1= 10.09 Hz, J_2= 5.02 Hz, 2H), 3.739 (t, *J*= 4.95 Hz, 1H), 3.420 (t, *J*= 4.99 Hz, 1H), 2.04-1.86 (m, 3H), 1.72-1.62 (m, 3H), 1.510 (dd, *J*= 13.97 Hz J_2= 8.55 Hz, 1H), 1.00-

0.97 (m, 1H), 0.597 (ddd, J_1= 12.95 Hz, J_2= 5.61 Hz, J_3= 2.13 Hz, 1H). ^{13}C NMR (DMSO): δ= 190.773 (q, *J*= 5.155 Hz), 115.299 (q, *J*= 292.211 Hz), 74.441, 73.756, 73.429, 69.232, 47.469, 46.257, 43.437, 43.057, 42.336, 38.169, 33.028, 32.522, 31.644, 31.473, 31.101, 28.846. ^{19}F NMR (DMSO): δ= -79.417 (s, 3F, *endo*), -79.556 (s, 3F, *exo*). FTIR (cm^{-1})= 3045.61, 2961.04, 1761.76, 1179.50. HRMS (CI^+): calc. 239.0895 found 239.0899.

1-(3,4,5-Trithia-tricyclo[5.2.1.0^{2,6}]dec-8-yl)-ethanone (2.34): In a 500 mL RBF equipped with a reflux condenser and N_2 inlet, 250 mL DMF, 50 mL 2 M NH_3 in EtOH, sublimed sulfur (30.0 g, 0.936 atom mol) and **2.2** (42.0 g, 308.39 mmol) were combined and heated to 110 ^{o}C overnight. After cooling to RT the reaction mixture was poured over ice and extracted 3 x 200 mL DCM. The combined organics were washed with water and brine, dried over $MgSO_4$, filtered, concentrated to yield a black sludge. A highly viscous orange liquid (45.73 g, 196.78 mmol, 63.8%) was isolated via Kugelrohr distillation. ^{1}H NMR ($CDCl_3$) (multiple isomers): δ= [4.002 (dq, J_1= 7.04 Hz, J_2= 0.88 Hz), 3.921 (dq, J_1= 7.04 Hz, J_2= 1.76 Hz), 3.874 (dd, J_1= 7.04 Hz, J_2= 1.57 Hz), 3.745 (dd, J_1= 7.04 Hz, J_2= 1.57 Hz), 3.648 (dq, J_1= 7.04 Hz, J_2= 1.57 Hz), 3.593 (br d, *J*= 7.04 Hz), 3.452 (dd, J_1= 7.04 Hz, J_2= 1.57 Hz) 2H], 3.00-2.35 (m, 3H), 2.14-2.08 (m, 3H), 2.06-1.95 (m, 1H), 1.95-1.00 (m, 3H). ^{13}C NMR ($CDCl_3$) (major isomers): δ=207.55, 207.079, 69.411, 69.255, 68.689, 64.143, 52.774, 52.135, 43.757, 43.370, 40.371, 34.389, 30.379, 30.119, 29.695, 28.765, 28.571, 28.370. FTIR (cm^{-1})= 2957.56, 2875.02, 1704.14, 1674.93, 1359.27, 1171.61. HRMS (CI^+): calc. 233.0129 found 233.0130.

2-Methyl-2-(3,4,5-trithia-tricyclo[5.2.1.0^{2,6}]dec-8-yl)-[1,3]dioxolane (2.35): In a 50 mL RBF equipped with Dean-Stark trap and reflux condenser, **2.34** (4.42 g, 19.02 mmol), ethylene glycol (1.34 g, 21.59 mmol), 25 mL benzene and cat. *p*-TSA were combined and

heated to vigorous reflux for 12 h. The reaction was cooled, concentrated and isolated from a 1" silica gel plug with hexanes as eluent. Concentration led to a viscous yellow-orange liquid (5.09 g, 18.41 mmol, 96.8%). ^{1}H NMR ($CDCl_3$): δ= 4.0-3.7 (m, 4H), 3.7-3.5 (m, 2H), 2.5-2.2 (m, 2H), 2.0-1.4 (m, 4H), 1.3-1.2 (m, 3H), 1.2-1.0 (m, 1H). ^{13}C NMR ($CDCl_3$): δ= 110.608, 109.774, 71.033, 69.002, 68.719, 65.557, 64.649, 64.203, 64.054, 62.930, 49.382, 47.038, 42.120, 40.565, 34.040, 30.855, 30.148, 28.363, 23.742, 22.872. FTIR (cm^{-1})= 2953.83, 2877.55, 1372.79, 1246.55, 1038.45. HRMS (CI^{+}): calc. 277.0391 found 277.0390.

5-(2-Methyl-[1,3]dioxolan-2-yl)-bicyclo[2.2.1]heptane-2,3-dithiol (2.36): To a flame dried 100 mL RBF was added LAH (1.24 g, 32.67 mmol) and 50 mL dry ether. To this was added **2.35** (3.85 g, 16.57 mmol) in 10 mL dry ether:DCM (4:1) drop-wise. After stirring 2 h the reaction was quenched with sat. aq. $MgSO_4$. The solution was washed with 50 mL sat. aq. Rochelle's salt. The aqueous was extracted 2 x 50 mL ether and the combined organics were washed with water and brine, dried over $MgSO_4$, filtered, concentrated to yield a colorless foul smelling liquid (2.35 g, 11.73 mmol, est. 71%) which was used without further characterization.

1-(5,6-Dimercapto-bicyclo[2.2.1]hept-2-yl)-ethanone (2.37): In a 100 mL RBF, 50 mL H_2O, 5 mL conc. HCl and **2.36** (2.35 g, 11.73 mmol) were combined and heated to 60 ^{o}C overnight. After cooling to RT, the reaction mixture was washed with sat. aq. sodium bicarbonate, water and brine, dried over $MgSO_4$, filtered and concentrated to yield an odiferous, highly viscous odiferous yellow liquid (2.14 g, 10.55 mmol, 89.9%). ^{1}H NMR ($CDCl_3$): δ= 3.2-3.1 (m, 2H), 2.5-2.3 (m, 1H), 2.2-2.1 (m, 1H), 2.0 (br s, 3H), 1.9-1.7 (m, 2H), 1.7-1.2 (m, 4H), 1.05 (m, 1H). ^{13}C NMR ($CDCl_3$): δ= 207.354, 53.504, 50.483,

47.380, 47.016, 46.539, 31.071, 30.163, 28.504. FTIR (cm^{-1})= 2960.66, 2875.47, 2549.78, 1705.09. HRMS (CI^+): calc. 203.0564 found 203.0567.

Bicyclo[2.2.1]hept-5-ene-2,3-diol (2.38): In a 500 mL RBF, 100 mL *t*-BuOH, 6 mL TEA, 50 mL H_2O and NMO (25.54 g, 218.01 mmol) were combined with bicyclo[2.2.1]hepta-2,5-diene (9.00 g, 97.68 mmol) and heated to gentle reflux overnight. The reaction mixture was concentrated and isolated from a 1" silica gel plug (eluent 1:1 EA:Hex). The eluent was concentrated to brownish solid which was sublimed to an off white solid (10.82 g, 85.76 mmol, 41.6%). MP= 118-119 ^oC. ^1H NMR ($CDCl_3$): δ= 5.981 (t, *J*= 1.830 Hz, 2H), 3.795 (br s, 2H), 3.630 (d, *J*= 1.678 Hz, 2H), 2.638 (p, *J*= 1.678 Hz, 2H), 1.820 (br d, *J*= 9.303 Hz, 1H), 1.566 (dp, J_1= 9.302 Hz, J_2= 1.678 Hz, 1H). ^{13}C NMR ($CDCl_3$): δ= 136.246, 68.594, 47.715, 42.086. FTIR (cm^{-1})= 3373.78, 3064.36, 2974.91, 1396.66, 1060.98. HRMS (CI^+): calc. 127.0759 found 127.0757.

4,4-Dimethyl-3,5-dioxa-tricyclo[5.2.1.$0^{2,6}$]dec-8-ene (2.39): In a 100 mL RBF, **2.38** (1.78 g, 14.11 mmol) was combined with excess 2,2-dimethoxypropane in 50 mL benzene with cat. *p*-TSA. The reaction was heated to remove the MeOH-benzene azeotrope. The reaction was cooled to RT, concentrated and product isolated on a 1" silica gel plug with hexanes as eluent. Upon concentration a colorless liquid (2.00 g, 12.03 mmol, 85.2%) was obtained. ^1H NMR ($CDCl_3$): δ= 5.984 (t, *J*= 1.754 Hz, 2H), 4.120 (d, *J*= 1.525 Hz, 2H), 2.695 (p, *J*= 1.677 Hz, 2H), 1.90 (m, 1H), 1.611 (dp, J_1= 8.997 Hz, J_2= 1.677 Hz, 1H), 1.400 (s, 3H), 1.261 (s, 3H). ^{13}C NMR ($CDCl_3$): δ= 136.549, 113.440, 80.278, 45.012, 42.701, 25.998, 24.258. FTIR (cm^{-1})= 3064.91, 2984.33, 2933.51, 1206.20, 1059.62. HRMS (CI^+): calc. 167.1073 found 167.1072.

4,4-Dimethyl-3,5-dioxa-tricyclo[5.2.1.$0^{2,6}$]decane-8,9-diol (2.40): In a 50 mL RBF **2.39** (2.00 g, 12.03 mmol) and NMO (1.62 g, 13.83 mmol) were combined in 10 mL *t*-BuOH,

1 mL H_2O and 1 mL TEA with 0.5 mL 2.5 wt% OsO_4 in *t*-BuOH. The reaction was heated to reflux overnight. After cooling to RT the reaction was concentrated and isolated from a 1" silica gel plug using 2:1 hexanes:EA as eluent to yield a tacky black solid. The solid was twice sublimed to yield an off white solid (1.63 g, 8.14 mmol, 67.7 %). MP= 112-113 ^{o}C. ^{1}H NMR ($CDCl_3$): δ= 3.943 (d, *J*= 1.368 Hz, 2H), 3.556 (d, *J*= 1.368 Hz, 2H), 3.052 (br s, 2H), 2.234 (m, 2H), 1.66-1.56 (m, 2H), 1.409 (s, 3H), 1.237 (s, 3H). ^{13}C NMR ($CDCl_3$): δ= 110.117, 78.444, 69.431, 47.366, 25.752, 25.232, 23.896. FTIR (cm^{-1})= 3421.78, 2987.22, 2903.68, 1210.78. HRMS (CI^{+}): calc. 201.1127 found 201.1125.

CHAPTER 3 DEGRADABLE ACETAL CROSS-LINKED MATERIALS FOR IMPRINT LITHOGRAPHY

INTRODUCTION

The drive towards miniaturization of microelectronics comes with a large capital investment and increased production costs. As exposure tool complexity has increased so has price. Among other driving forces, the cost of retooling has served to drive many of the smaller players in the microelectronics industry to extinction or acquisition by larger entities. Additionally, the miniaturization drive has pushed the physical boundaries of resolution for optical lithography. The search for new technologies has pushed lithographers to examine radical departures from traditional projection lithography. Extreme-UV (EUV) utilizing 13.4 nm light has received much attention in spite of the fact that at this wavelength there are neither transparent materials for mask synthesis nor a light source capable of sufficient power to be utilized in production! Electron beam lithography is a high resolution but slow direct write process but methods to employ up to 13,000 beams working simultaneously have been proposed.[35] From this group nanoimprint lithography (NIL) has emerged as a potential low-cost high-resolution alternative to traditional projection optical lithography.

NANOIMPRINT LITHOGRAPHY

The upcoming 32 and 22 nm nodes on the ITRS roadmap[25] are in the process of becoming reality but they may represent the limit to which optical lithography can be pushed. A new method is almost certainly going to be needed to replace optical lithography for production of sub-20 nm features. A potential candidate is NIL, which was first introduced at Minnesota in 1996 by Chou.[36] Using a thermal process, Chou patterned 10 nm features in poly(methyl methacrylate) (PMMA) films on silicon wafers.

This was an important proof of concept and thermal imprinting is of great utility for some applications but polymeric films due to their high viscosity require relatively high temperatures and pressures to achieve template filling. The need for a heating and cooling cycle causes long processing times and thermal expansion, which occurs on heating, causes layer to layer alignment to be difficult if not impossible.

STEP AND FLASH

In 1999, Colburn *et al*. at the University of Texas introduced Step and Flash Imprint Lithography (SFIL).[37] SFIL is a lithography process in which the mask system used in traditional projection lithography is replaced with an optically transparent three-dimensional template. The quartz template is etched such that it contains the inverse relief images of those desired on the wafer. A photopolymerizable liquid prepolymer solution is dispensed onto the wafer. The template is then brought contact with the wafer forcing the resist to fill the recesses in the template. Once the template has filled, the system is flood exposed with UV light curing the solution into a cross-linked solid material. The template is then removed leaving an inverse relief image of itself. Subsequently this image is transferred to the underlying substrate with an RIE as in traditional photolithography. (Figure 3.1) Due to the use of a low viscosity liquid, SFIL, unlike thermal imprint, may be performed at low pressure and the photochemical transformation from liquid to solid can be done isothermally at room temperature.

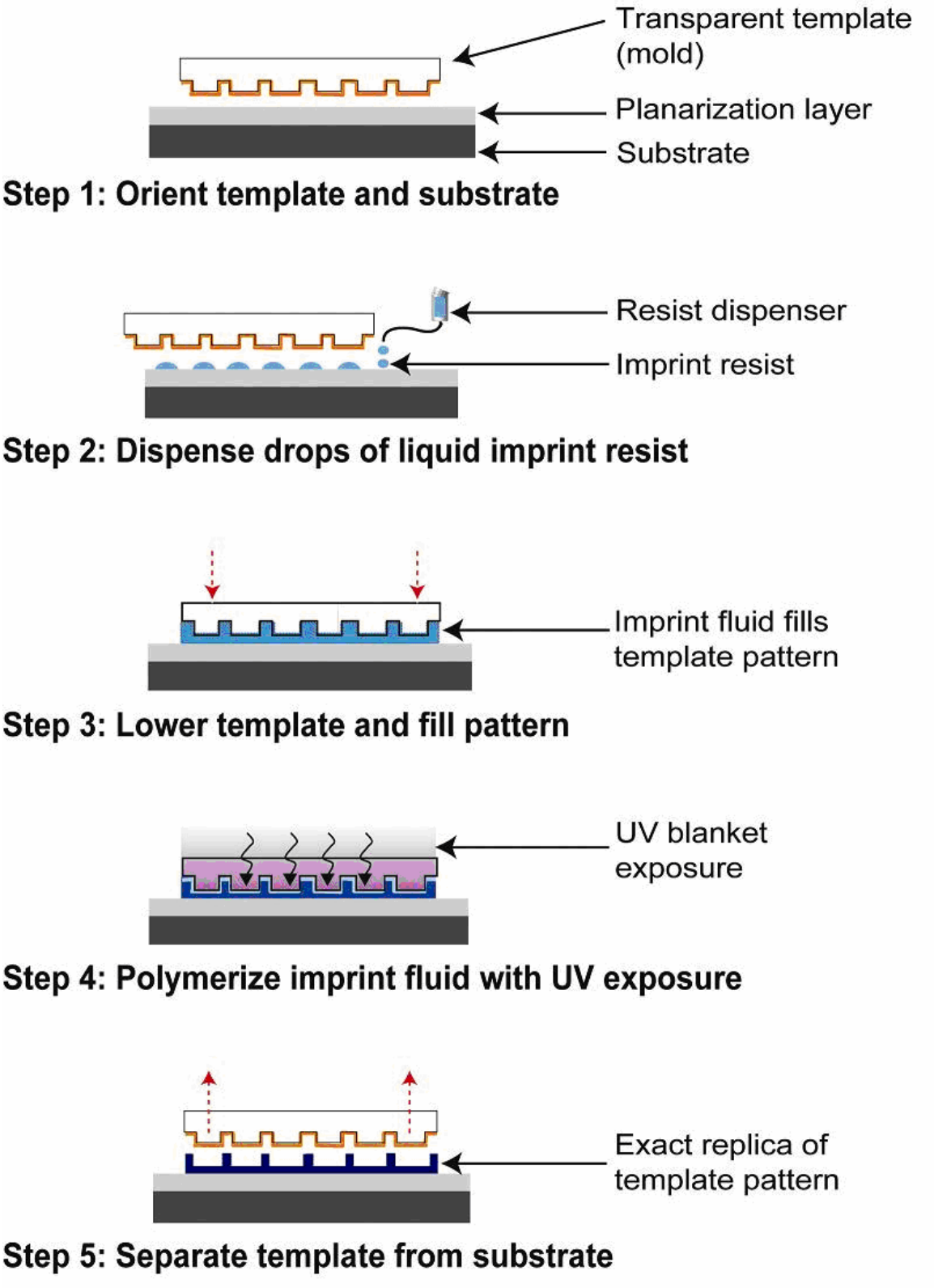

Figure 3.1 The SFIL process

In less than a decade, SFIL has moved from the research laboratory to a legitimate procedure for use in the production of microelectronics. Early generation SFIL tools produced by Molecular Imprints, Inc. of Austin, Texas have printed sub-20 nm features with high fidelity[38] and the resolution limit of SFIL appears to be governed by the ability to produce templates on small enough scales. To demonstrate this concept, Rogers has replicated the shape of a carbon nanotube (2.3 nm diameter) utilizing an imprint process.[39]

THROUGHPUT LIMITATIONS

Despite these encouraging results, adoption of this technology has been slow throughout the lithography community. This is largely due to the fact that these early tools suffer from low throughput, producing less than 20 wafers per hour while projection lithography tools can process closer to 100 wafers per hour depending on individual requirements. Within the microelectronics industry producing a better product is largely irrelevant if it can't be produced in sufficiently large quantities to account for a significant market share.

COST BENEFITS

If low throughput concerns can be adequately addressed, the low cost of ownership for SFIL tools would make NIL a highly attractive option for sub-22 nm nodes, thus, raising throughput capacity is a challenge that has been actively pursued within the engineering community. First generation imprint tools were introduced at a commercial cost of less than $8 million.[38] This low cost is largely reflective of the relative simplicity of the systems of SFIL tools when compared to optical systems in projection tools. Further, exposure is performed utilizing a mercury arc lamp as opposed to the more expensive excimer lasers currently utilized in projection tools. Recent developments in ink-jet

dispensing for SFIL resists have allowed dramatic reductions in the amount of resist formulation dispensed on the wafer relative to the spin coating process necessary for projection lithography representing a further cost saving measure. A recently developed process which provides a significant advantage for SFIL is the ability to pattern in three-dimensions.[40] This requires the use of multilevel templates to produce features allowing for a reduction of over 100 process steps in the manufacture of integrated devices and an accompanying reduction in cost. All of these factors have led to improved throughput in recent years aiding SFIL to gain a larger foothold in the microelectronics industry. While throughput is still lagging behind optical projection lithography, the low cost of ownership for a state of the art SFIL tool is sufficient to overcome the barrier to FAB introduction for some applications.

TEMPLATE-RESIST INTERACTION

Unlike projection lithography which utilizes 4:1 feature reduction from mask to printed feature, SFIL prints 1:1 features from template to resist. This naturally requires features on the SFIL template to be smaller than the features on a comparable photomask. While simpler to write than photomasks because they have no assist features, templates are still very expensive parts. Due to the necessity of utilizing the direct write technology of electron beam lithography for high precision writing of these tiny features templates costs can soar to as much as $70,000.[41] Avoidance of template fouling is therefore of utmost interest as extending template lifetime distributes cost thereby decreasing the effective cost per unit produced. Also unlike projection lithography, SFIL necessitates contact between the resist solution and the expensive template. This contact leaves the template susceptible to contamination from debris on the wafer or residual resist material left by incomplete release upon separation of template and cured resist. This is a major concern

due to both the high cost of the templates and the high fidelity with which features are replicated in SFIL as defects could then be transferred to subsequently processed wafers.

SFIL RESISTS REQUIREMENTS

A set of parameters necessary for an effective SFIL resist were presented by Kim *et al.*[42,43] Resist formulations must be cross-linkable with low viscosity and low vapor pressure. They must also contain monomers that rapidly polymerize to a high degree of conversion such as acrylates and vinyl ethers. After exposure induced curing these materials must be tough, with a tensile modulus over 100 MPa and contain greater than 9% silicon for sufficient etch resistance. To achieve all of these requirements, SFIL resists are multi-component systems in which each component imparts certain desired characteristics. The components of a typical SFIL resist formulation are shown in Table 3-1.

Table 3-1 Example of a Typical SFIL Formulation

Compound	Wt%	Function
Cyclohexyl methacrylate	28	Low vapor pressure linear monomer, provides high T_g polymer
isobutyl acrylate	20	Low viscosity, reactive diluent: improves monomer flow
ethyleneglycol diacrylate	20	Crosslinker: improves mechanical properties
acryloxypropyl-tris(trimethylsiloxy)silane	30	Silicon containing monomer: provides oxygen etch resistance
2-hydroxy-2-methyl-1-phenyl-1-propanone	2	Photoinitiator: generates free radicals upon exposure to UV radiation

Approaches to cleansing fouled templates are complicated due to the resist composition. SFIL resists rely on cross-linking to sufficiently harden the resist to maintain feature

dimensions and minimize resist separation from the wafer leading to template fouling. In addition to being cross-linked SFIL resists incorporate a high silicon content. For these reasons imprint resists are largely insoluble in organic solutions and possess etch characteristics similar to the template. Ultrasonic agitation and blasting with jets of solvent can damage small features. This renders physical and chemical approaches to template cleansing largely useless as resist removal would damage the template. As additional motivation, it is common industrial practice to 'rework' wafers which acquire defects during the printing process. If defective wafers cannot be easily recycled, another expense diminishes the advantage of this money saving technology.

DESIGNING DEGRADABLE RESISTS

Inducing a chemical change within a cross-linked resist to break the cross-links could render the insoluble resist as soluble (Figure 3.2). This would make it possible to simply wash the resist with an appropriate solvent such that previously insoluble resists could be removed from fouled templates or errant wafers.

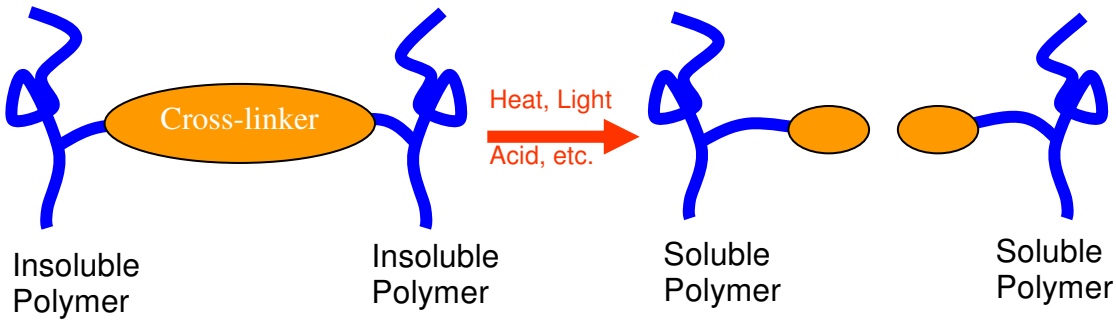

Figure 3.2 Generalization of breaking cross-links to form a soluble polymeric network

DEGRADABLE FUNCTIONALITIES

A number of organic functionalities can be imagined as the cross-linking group in materials that would allow for thermal or acid catalyzed cleavage. These include o-carbamoxyloximes, commonly referred to as blocked isocyanates, which thermolyze to isocyanate and oxime, Diels-Alder adducts of furans, which undergo thermally induced retro-Diels-Alder, have been studied extensively as so called 'mendable' polymeric systems.[44] Hydrogen-bonding units are thermally labile and have been used for reversible cross-linking.[45] *Tert*-butyl esters undergo thermal acid catalyzed cleavage.[46] Each of these linkages has been investigated as a possible decross-linkable unit for NIL materials.[47]

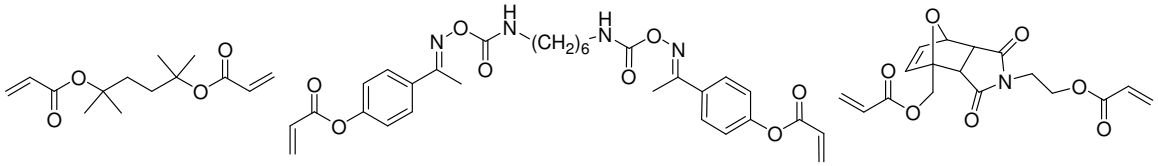

Figure 3.3 Compounds reported as potential decross-linkable NIL materials

ACETAL CROSS-LINKERS

Acetals are attractive because they are stable to both neutral and alkaline condition, but undergo ready hydrolysis in aqueous acidic solutions. Dimethacrylate acetals have been successfully incorporated into polymer networks and these networks have been shown to undergo acid catalyzed hydrolysis to produce linear polymers that are soluble in organic solvents.[48,49,50]

The dimethacrylate acetal (ADMA) **3.1** was synthesized through transketalization of 2,2-dimethoxypropanone with 2-hydroxyethylacrylate in the presence of *p*-TSA catalyst and hydroquinone radical inhibitor in benzene.[51] Methanol was continuously removed by

distillation of the benzene-methanol azeotrope (58°C) and the crude product was purified by flash column chromatography.

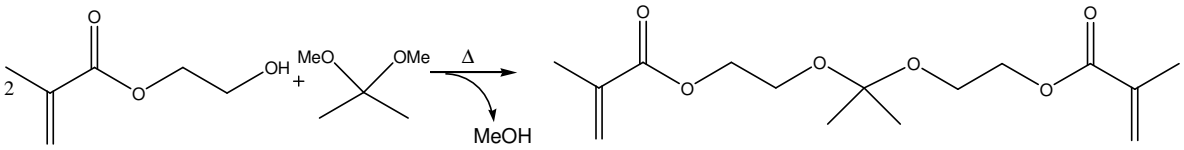

3.1

Figure 3.4 Synthesis of dimethacrylate acetal cross-linker (ADMA)

A high degree of cross-linking in the cured film is necessary to ensure high fidelity image transfer to the wafer with minimal distortion upon template removal. The cross-linker must therefore be freely soluble in the monofunctional acrylate in the range of 10-20 % (wt/wt). The ADMA cross-linker was obtained as a colorless liquid that is freely soluble in various alkyl acrylates. Initial tests substituting this material for EGDA as the cross-linking material in an SFIL resist formulation showed the ability to produce hardened films which were susceptible to acidic degradation.

PREPARATION OF ADA CROSS-LINKER

Acrylates demonstrate higher photopolymerization rates than their methacrylate analogues and are therefore more attractive for SFIL where photospeed is critical. Many reaction conditions that favor acetal formation result in thermally induced polymerization of the less stable acrylate functionality due to the high temperature required for water removal. The lower temperature and short reaction times required for transketalization removing methanol minimize this effect. As such ADA was synthesized in the same manner as ADMA.

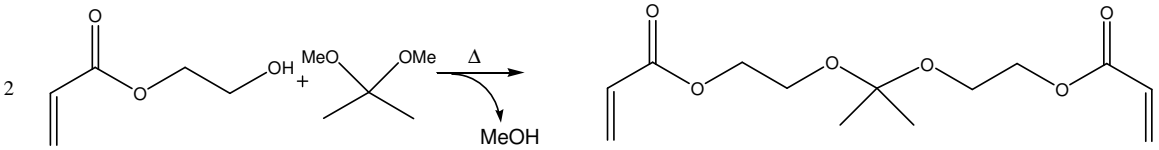

3.2

Figure 3.5 Synthesis of dimethacrylate acetal cross-linker (ADA)

RESIST PERFORMANCE

All performance and mechanical data collected for ADA were compared with commercially available 2,5-di(acryloyloxy-1-ethoxy)-2,5-dimethylhexane (TBDA) (Figure 3.3) as performed by Palmieri.[52] Data for TBDA is presented here solely for comparitive purposes.

PHOTOPOLYMERIZATION PERFORMANCE

The rate and extent of photopolymerization of the ADA cross-linker was investigated by real-time FT-IR spectroscopy. A neat solution of the monomer was irradiated and the conversion of monomer was determined by monitoring the decrease in the C=C stretch at ~1680 cm^{-1}. The extent of conversion for the ADA (~70% @ 2 min) was greater than that of TBDA (~60% @ 2 min.) under identical exposure conditions and initiator formulations. Ober observed a similar phenomena when photopolymerizing diacrylates with differing cross-linker lengths.[53] He found the extent of polymerization increased with the number of methylene spacers and attributed this to increased accesibility of the propogating radical. The diethyl acetal spacer of the ADA is 7 units long whereas the TBDA spacer is only 4 methylene units long so these data are in agreement with Ober's findings. As expected, ADA provides a substantial increase in reactivity relative to ADMA (Figure 3.6).

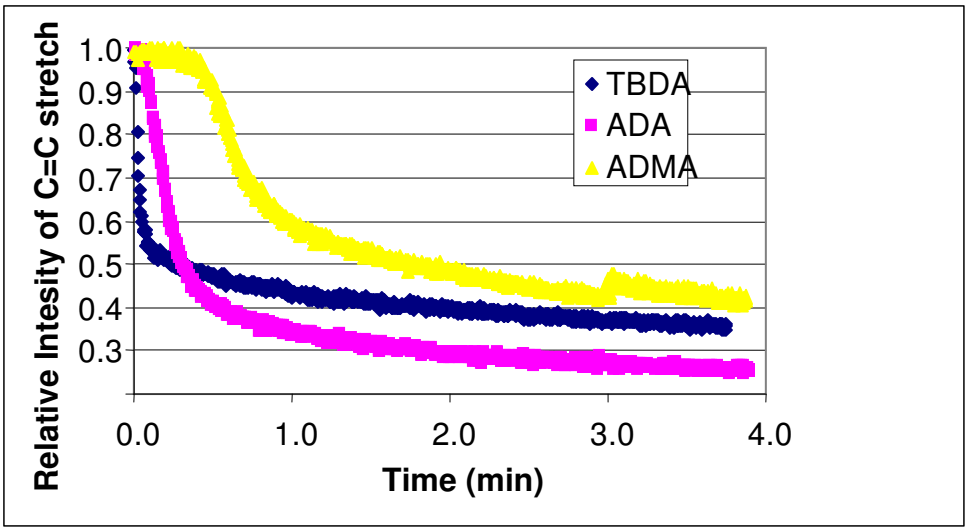

Figure 3.6 Alkene conversion monitored by FT-IR as a function of exposure time

FEASABILITY OF IMPRINTING

The properties listed in Table 3-2 show the comparative compatibility of TBDA and ADA with SFIL processing. The low molecular weight and viscosity of ADA maximizes cross-link density while improving template filling dynamics. The photospeed achieved during free radical polymerization of the acrylate functional groups, while lagging behind TBDA, is sufficiently rapid to facilitate good process throughput and ultimately yield a higher conversion percentage. Due to its compatibility and favorable properties, ADA was able to be implemented in existing imprint formulations and processes with minimum development work.

Table 3-2 Material properties of the degradable crosslinking monomers

Name	MW (g/mol)	Viscosity (cP)	Dose to cure (mJ/cm^2)
Desired Values	NA	< 20	< 90 @ > 50% conv.
TEDA	272.29	21.1	13.5 @ 52% conv.
ADA	254.32	12.3	58.3 @ 63% conv.

Experimental imprint resist formulations were prepared from the acid degradable cross-linkers TBDA and ADA and the linear monomers shown in Table 3-1. These formulations were photopolymerized and their physical properties and stripping characteristics were studied at cross-linker concentrations between 5 and 20 wt%. The concentration of isobutyl acrylate ranged from 20 to 35 wt% to compliment changes in cross-linker concentration.

STRIPPING EXPERIEMENTS

A control die was imprinted on a silicon wafer using the imprint resist formulation in Table 3-1, an experimental formulation including the decross-linking chemisty was imprinted next to the control die and then the wafer was cleaved in half. The wafer stripping process was applied on one half of the wafer to demonstrate the effectiveness of the cross-linking and decross-linking chemistry. The difference is dramatic as can be seen in Figure 3.7.

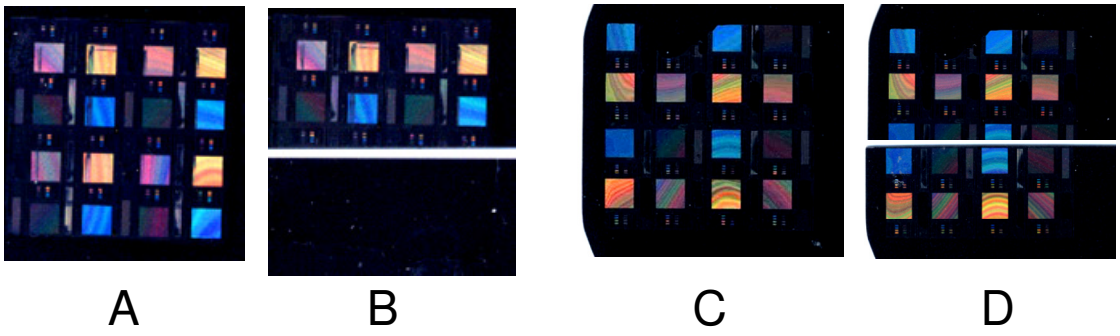

Figure 3.7 A) Wafer patterned with ADA cross-linker B) Cleaved wafer, bottom half refluxed in acidic THF C) EGDA patterened wafer D) Cleaved wafer, bottom half refluxed in acidic THF

The decross-linking reaction must achieve high conversion before the polymer is rendered soluble; therefore, iterative experiments were used to find the maximum concentration of crosslinker which produced easily strippable polymers. TBDA

containing films were successfully stripped with cross-linker concentrations less than 10 wt%. Above 10 wt%, the cross-linked films would swell, crack, and delaminate, but did not become completely soluble. ADA cross-linked films gave similar results with a maximum strippable cross-linker concentration of 15 wt% with trifluoroacetic acid at room temperatures. Higher degrees of cross-linking were able to be removed when the ADA patterns were stripped by submerging the wafer in acidic aqueous THF. The patterns dissolved very slowly at room temperature, however increasing the temperature to reflux the THF solution provided clean wafers in less than five minutes. Polymer films containing up to 40% (wt/wt) cross-linker swelled immediately upon submersion and dissolved completely to produce a homogenous solution. Films prepared with ethylene glycol diacrylate (EGDA) were used to confirm that hydrolysis of the acetal, not the ester, was responsible for dissolution of the cross-linked film. EGDA cross-linked films remained insoluble after refluxing for 18 hours in both acidic THF and NMP.

TEMPLATE CLEANING

Cleaning templates with imprint resist contamination is difficult and expensive to demonstrate due to small feature sizes, difficulty in cross-sectioning and examining of quartz template substrates and prohibitive costs of cleaving templates. To demonstrate template cleaning, silicon wafers coated with 1 micron film of silicon oxide (similar to template quartz) with contact holes as small as 130 nm in diameter and a 7:1 aspect ratio were imprinted with ADA formulation. Figure 3.8 shows deep contact holes filled with cross-linked resist and fully opened contacts holes after subjecting these structures to the room temperature template cleaning process. Even the highest aspect ratio patterns on the simulated template were completely cleaned as shown in the cross-section view. The via sidewalls show no residue of imprint resist polymer. This provides strong evidence

towards the conclusion that recessed template features contaminated with an inorganic-containing imprint resist can be completely cleaned through the decross-linking mechanism under appropriate and stripping conditions.

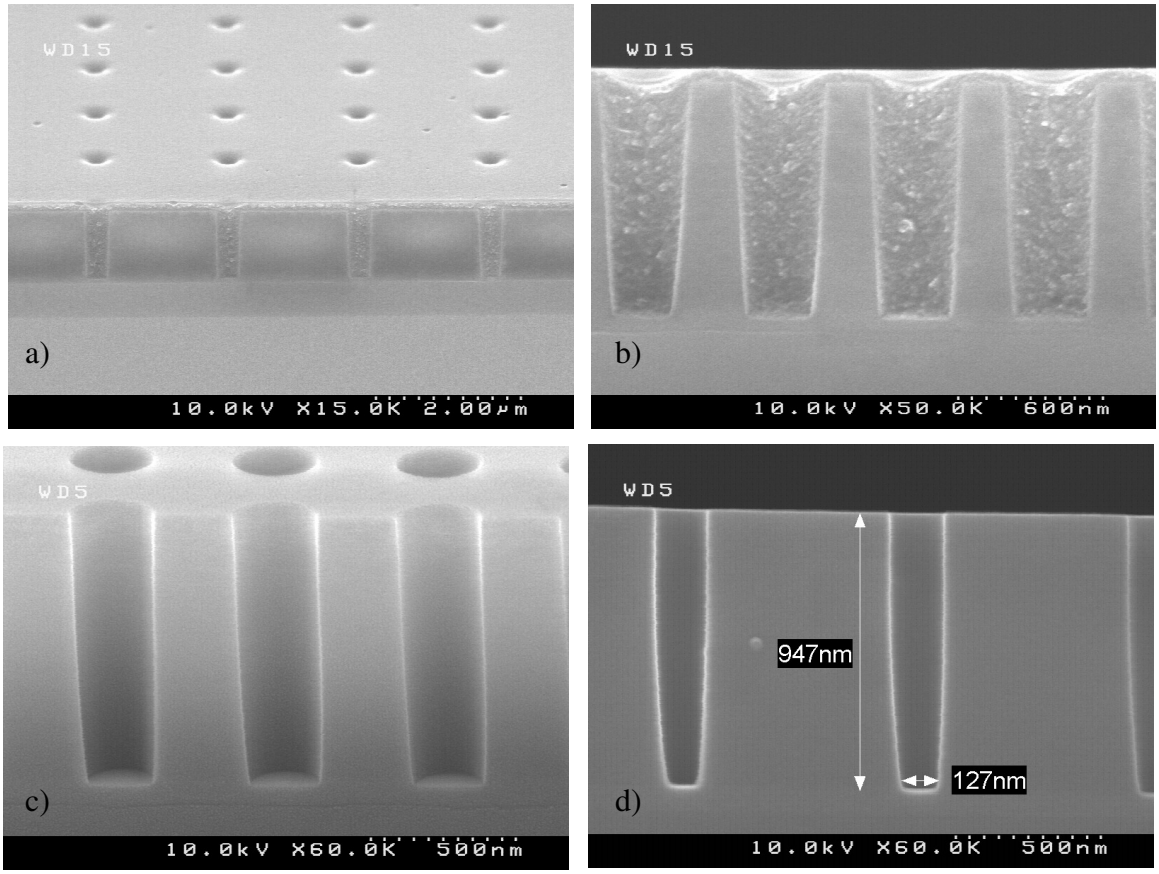

Figure 3.8 Simulated template cleaning results: a) and b) show contact holes filled with cured, degradable imprint resist c) and d) show clean contact holes after performing the stripping process

MECHANICAL STRENGTH OF DECROSS-LINKABLE SYSTEMS

The bulk tensile moduli of formulations containing TBDA and ADA are shown in Figure 3.9. ADA shows a reduced tensile modulus when compared to TBDA with the strain to yield recorded as 0.38 ± 0.002% for TBDA and 0.21 ± 0.003% for ADA. This result leads to the expectation that ADA films will likely result in poorer resolution than TBDA crosslinked films. Indeed, it is likely that the favorable extended spacer length attributed

to an increassed photopolymerization speed is at least partially at fault for a reduction in mechanical properties.

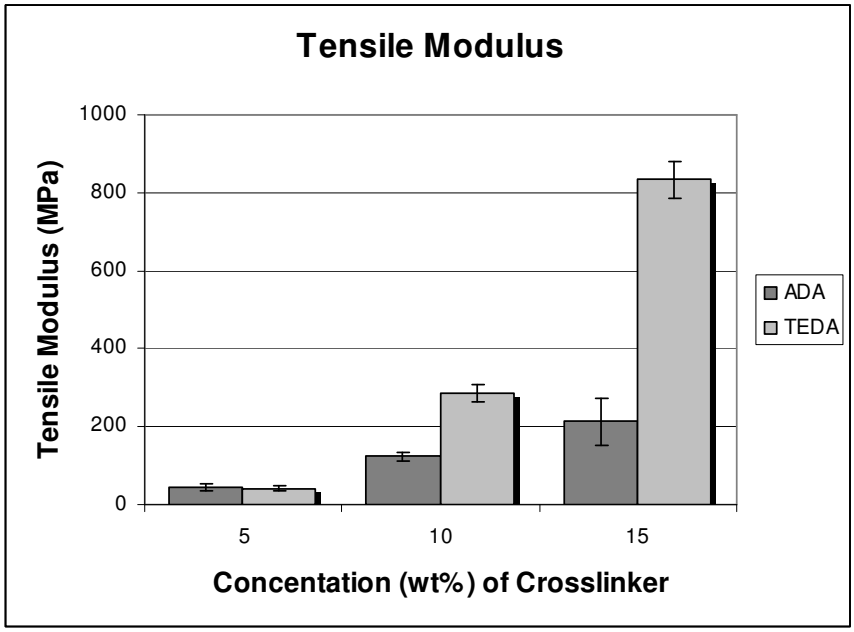

Figure 3.9 Tensile moduli of TBDA and ADA formulations

High fidelity replication of the high resolution template patterns is a key function of the imprint resist formulation. Scanning electron micrographs (SEMs) of imprinted experimental formulations were examined for imprint quality. The control and TEDA imprints show similar corner rounding and sidewall angles, which indicates that these are properties of the template. The image made using the 15 wt% ADA formulation in Figure 3.10 c) shows slightly bent and deformed posts. Plastic deformation of ADA cross-linked features occurs due to its lower strain to yield point relative to the 10 wt% TBDA formulation and the control. This problem may represent a limitation to this material at small dimensions however for patterning larger, more mechanically robust feature geometries with low aspect ratios this effect becomes less significant.

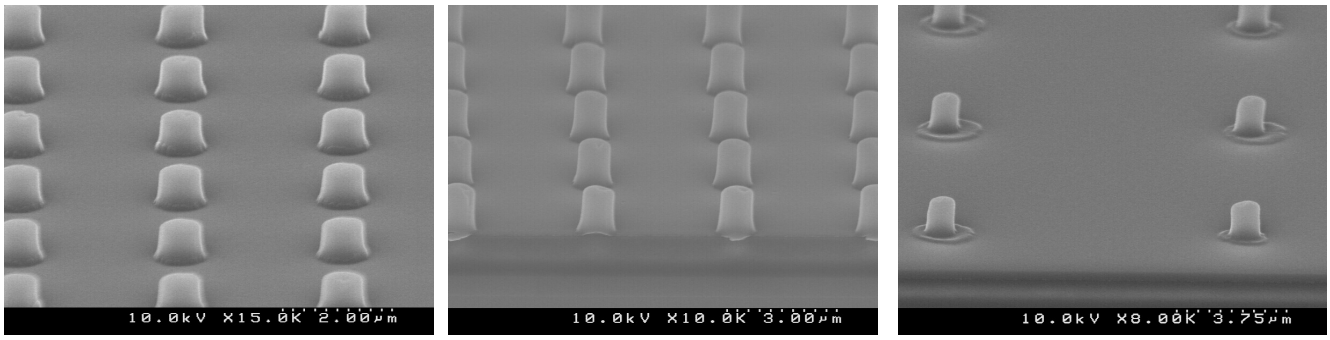

a) b) c)

Figure 3.10 Tilt SEM images of posts printed with: a) control formulation (Table 3-1), b) 10% TEDA experimental formulation and c) 15% ADA experimental formulation showing tilted and bent posts

EXPERIMENTAL METHODS

General materials

All solvents and reagents were obtained from Aldrich or Fisher Scientific and were used without further purification except where noted.

Measurement of dose to cure

Thin films of neat ADA were examined by reflectance-mode, FT-IR spectroscopy by pressing a drop of the liquid monomer between an aluminum coated silicon wafer and a sodium chloride window. The dose to cure was measured by real time FT-IR spectroscopy utilizing the acrylate double bond to monitor monomer conversion.[54] Dose to cure energies were obtained from the fractional conversion during polymerization as a function of time.

Imprinting

The SFIL process was used to prepare samples for decross-linking and stripping demonstrations. An Imprio 55, automated imprint tool manufactured by Molecular Imprints Inc., was used to prepare thin film samples (50 nm to 200 nm) and high

resolution patterns (< 1 μm).[55,56] Some samples were produced using a manual imprint process by pressing a drop of monomer between a quartz plate and silicon wafer. Wafers were treated with an adhesion promoter, AP410 obtained from Silicon Resources Inc., and templates were treated with a 0.2 wt% solution of phase fluorinated self-assmebled monolayer (tridecafluoro-1,1,2,2-tetrahydrooctyl)dimethylchlorosilane in toluene to aid in adhesive release from the template.[57] The formulation was cured through a quartz plate with a 300 mW/cm^2 i-line source for four minutes. Templates used for making high resolution post structures were prepared using the standard chromium on quartz process.[58]

Stripping

Stripping ADA cross-linked films was accomplished by immersion in a solution of 10 wt% trifluoroacetic acid and 4-methyl-2-pentanone at room temperature. Complete dissolution of all films was achieved in less than five minutes.

Measurement of mechanical properties

The mechanical properties of cured films were measured using an Instron 4858 Micro Tester operating in tensile extension mode. Samples were prepared by photopolymerizing the experimental imprint formulations between glass microscope slides and quartz plates using 150 μm spacers to control the film thickness. Film samples were separated from the glass and quartz substrates then measured for thickness and width prior to tensile testing.

Experimental

2-Methyl-acrylic acid 2-{1-methyl-1-[2-(2-methyl-acryloyloxy)-ethoxy]-ethoxy}-ethyl ester (3.1): In a 250 mL RBF, 2-hydroxyethylmethacrylate (10.14 g, 77.92 mmol), 2,2-dimethoxypropane (3.69 g, 35.43 mmol) and hydroquinone (1 g) were stirred in benzene

and distilled to remove the methanol-benzene azeotrope (58 ^{o}C). Upon completion of the reaction, the remaining benzene was removed in vacuo. The resulting colorless liquid was purified via flash column chromatography using DCM as the eluent to provide the acetal linked dimethacrylate as a colorless oil (8.64 g, 28.57 mmol, 80.64%). ^{1}H NMR ($CDCl_3$): δ= 5.97 (d, *J*= 0.68 Hz, 2H), 5.43 (d, *J*= 1.71 Hz, 2H), 4.13 (t, *J*= 5.13 Hz, 4H), 3.57 (t, *J*= 5.13 Hz, 4H), 1.80 (s, 6H), 1.24 (s, 6H), ^{13}C NMR ($CDCl_3$): δ= 166.92, 135.91, 125.29, 99.80, 63.67, 58.54, 24.45, 18.00.

Acrylic acid 2-[1-(2-acryloyloxy-ethoxy)-1-methyl-ethoxy]-ethyl ester (3.2): In a 250 mL RBF, 2-hydroxyethylacrylate (8.82 g, 75.96 mmol), 2,2-dimethoxypropane (3.62 g, 34.76 mmol) and 1 g hydroquinone were stirred in benzene and distilled to remove the methanol-benzene azeotrope (58 ^{o}C) Upon completion of the reaction, the remaining benzene was removed in vacuo. The resulting colorless liquid was purified via flash column chromatography using DCM as the eluent to provide the acetal linked diacrylate as a colorless oil (3.78 g, 13.88 mmol, 39.93%). ^{1}H NMR ($CDCl_3$): δ= 6.25 (dt, J_1= 17.44 Hz, J_2= 1.37 Hz, 2H), 5.98 (m, 2H), 5.67 (dt, J_1= 10.26 Hz, J_2= 1.37 Hz, 2H), 4.12 (m, 4H), 3.53 (m, 4H), 1.21 (d, *J*= 1.03 Hz, 6H). ^{13}C NMR ($CDCl_3$): δ=165.67, 130.59, 127.98, 99.80, 63.49, 58.53, 24.41. FTIR (cm^{-1})= 2992.41, 2950.00, 2882.01, 1735.45, 1410.94, 1297.84, 1193.90, 1063.10, 985.33. HRMS (CI^{+}): calc. 273.1338, found 273.1339.

CONCLUSIONS

Incorporation of degradable acetal cross-linkers can provide strippable and re-workable imprint resist formulations. The properties of ADA are compatible SFIL imprint resist requirements. Imprint formulations of 15 wt% ADA were successfully cured, decross-linked, stripped from wafers and cleaned from high aspect ratio contact holes. The

mechanical properties of the system met SFIL resists requirements. The formulation containing 15 wt% ADA showed only minor pattern defects as observed by SEM inspection. High resolution imprint lithography has been successfully coupled with a convenient template and wafer reworking process.

CHAPTER 4 GAIN WITHOUT BIAS

EARLY NON-CHEMICALLY AMPLIFIED RESISTS

Prior to the transition from 365 nm to 248 nm lithography NCARs were exclusively utilized in the photolithographic process. NCAR formulations of the 365 nm generation typically relied upon an aqueous base soluble material, such as novolac, and a photoactive material, such as DNQ, which functions as a dissolution inhibitor (DI) in the unexposed state.[59] Upon exposure to i-line radiation from a mercury arc lamp DNQ outgases nitrogen and undergoes a photochemical Wolff rearrangement to form a ketene.[60] The ketene is susceptible to nucleophilic attack from water forming an acidic compound that no longer functions as a DI but actually serves to promote dissolution thus producing the desired solubility switch (Figure 4.1).

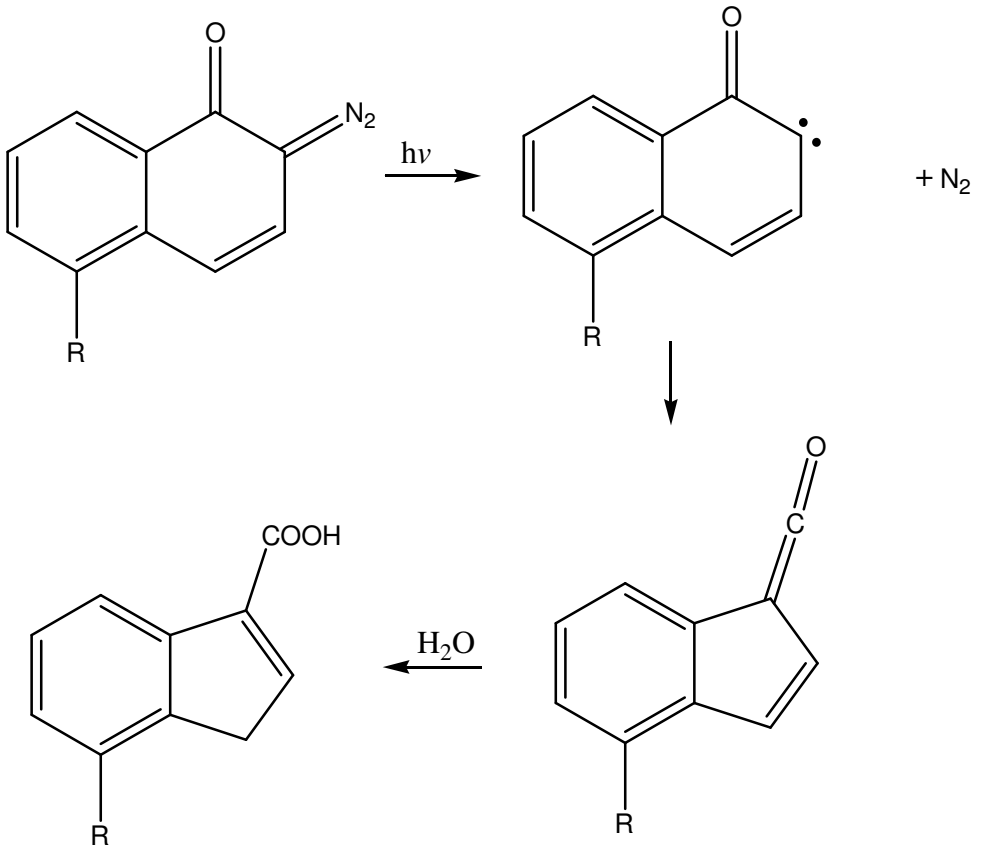

Figure 4.1 DNQ photochemical rearrangement from base dissolution inhibitor to base soluble material[59]

NCARs still find some applications in microelectronics; primarily in back end of the line applications, however they are not used to produce gate-level features on advanced devices. Available light sources for short wavelength photolithography cannot generate sufficient power to efficiently produce images utilizing NCARs (Figure 4.2). To utilize NCARs at shorter wavelengths processing speed would be sacrificed as longer exposure times would be required. Longer processing times would have lowered FAB outputs leading to higher unit costs and the drive to miniaturization would have ultimately ground to a halt. This economic reality necessitated the search for more

sensitive systems.

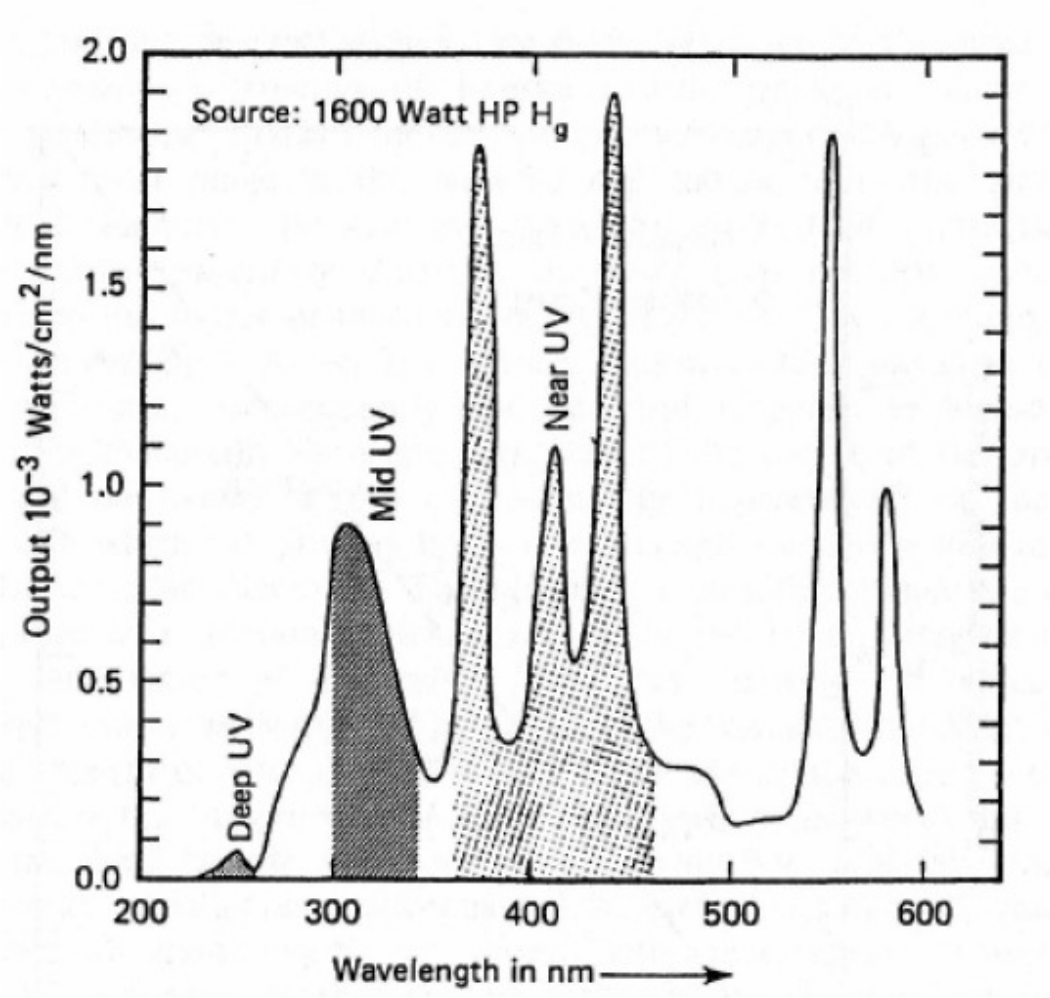

Figure 4.2 Power available at the wafer plane from mercury arc lamp demonstrating decreasing available power[59]

INTRODUCTION OF CARS

To deal with the lower power availability a system was needed in which a photochemically altered material proceeds to catalyze numerous reactions within the resist film. This type of material functions with a greater effective photoefficiency than its own quantum yield.[61] Within the microelectronics industry this principle is referred to

as gain. With gain the smaller amount of light power available is used more efficiently leading to decreased processing times.

Willson and Ito investigated systems which put the concept of chemical amplification into practice. One system utilized a polymeric dissolution inhibitor (PDI) that would undergo a catalytic backbone chain scission leading to the depropagation of the PDI to a non-DI species.[61] Another system used an aqueous base soluble polymer with an acid sensitive protecting group formulated with a PAG.[62] This was deemed the most viable system and ultimately spawned the CAR systems known today that revolutionized the microelectronics industry. The nomenclature of this system will seem odd to chemists who recognize the system as a simple catalytic reaction. However, for the benefit of their engineering colleagues at IBM Willson and Ito dubbed the process chemical amplification and hence the name.

Current generation technology is primarily produced utilizing CARs. Because these CARs rely on an acid-catalyzed side-chain deprotection to produce a solubility switch no DI is required. Small molecule PAGs are included in the resist formulation. Upon exposure to light, the irradiated PAG produces $PAGH^+$ and the PEB induces mass transport of the $PAGH^+$ through the film. This leads to some degree of diffusion into the unexposed regions.[63] This transit through the film allows $PAGH^+$ to catalyze multiple deprotections.[64] Due to the reliance on mass transport to produce gain, film thinning occurs where $PAGH^+$ diffuses into unexposed areas.[65] (Figure 4.3) This is referred to as bias.

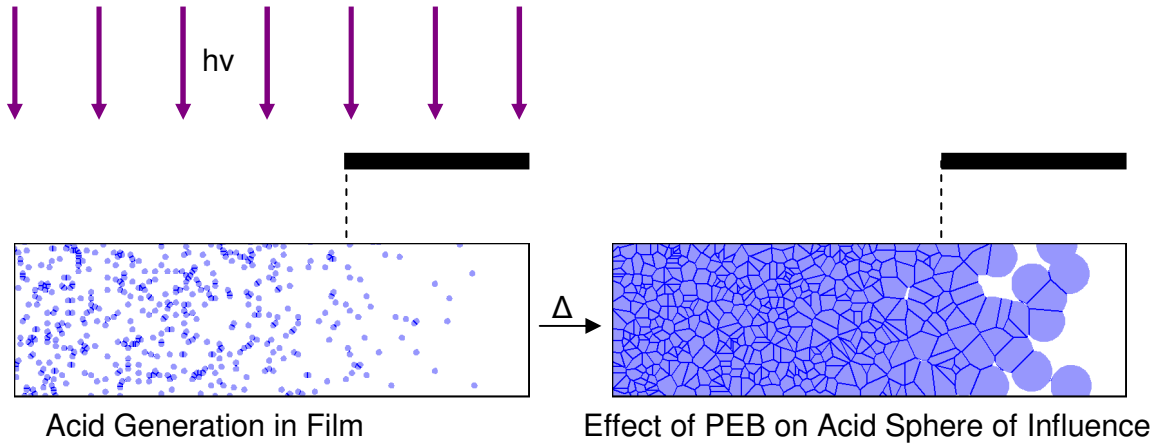

Figure 4.3 Acid diffusion in dark film[66]

LINE EDGE/WIDTH ROUGHNESS

As microelectronic devices have been miniaturized, the density of integrated circuits has necessarily increased. The error in line straightness incurred during imaging is known as line edge roughness (LER) or the more currently fashionable but perhaps more adeptly accurate misnomer, line width roughness (LWR). LER is typically evaluated by top-down SEM images and best fitting a line to the printed feature. The 3σ RMS deviation from that line is typically called the LER (Figure 4.4). Interestingly the actual roughness of an edge can be controlled by extending PEBs to smooth edges. This however results in a further increase in the deviation from the designed width of lines and thus increases LWR while decreasing LER. It is notable that the 'lines' are actually three-dimensional objects and as such LER is better observed by cross-section SEM and should be considered for the entire height of the line (Figure 4.5). LWR, also evaluated via SEM images, measures the deviation from width of the desired line to the printed line.

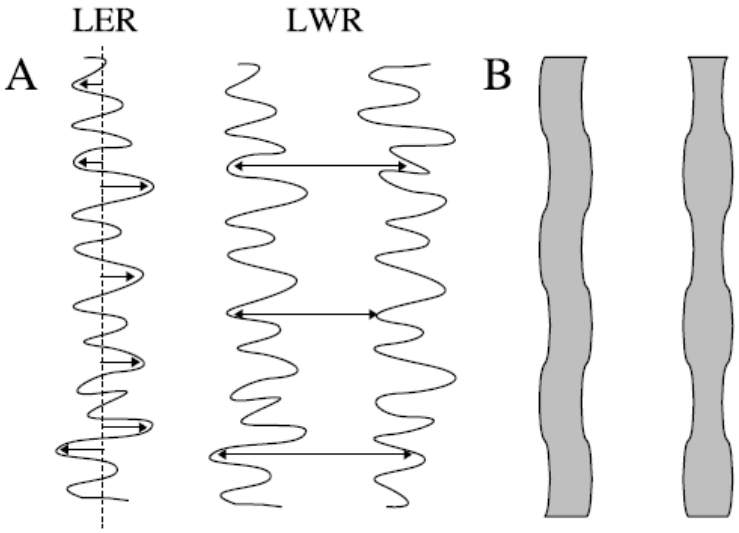

Figure 4.4 Representation of LER/LWR

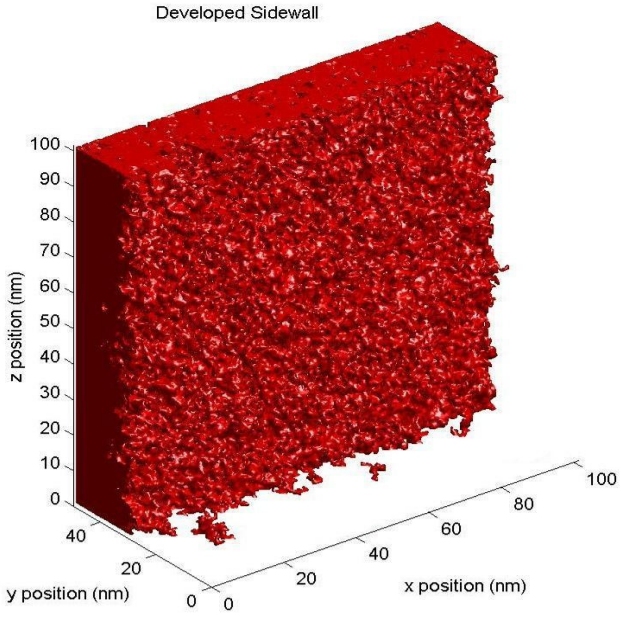

Figure 4.5 Computer model of side wall profile upon resist development[66]

Photolithographers have long been aware of the issues of LER and LWR. In early generations of CARs, the printed dimensions were so large relative to today's targets that these errors could be tolerated. As the critical dimension of resist features have begun to approach the radius of gyration of individual polymer molecules, it has become more necessary to address limiting LWR. It is important enough to the microelectronics industry to have been included on the ITRS with LWR less than the radius of gyration of polymeric materials has been targeted for the 32 nm and 22 nm nodes.[67]

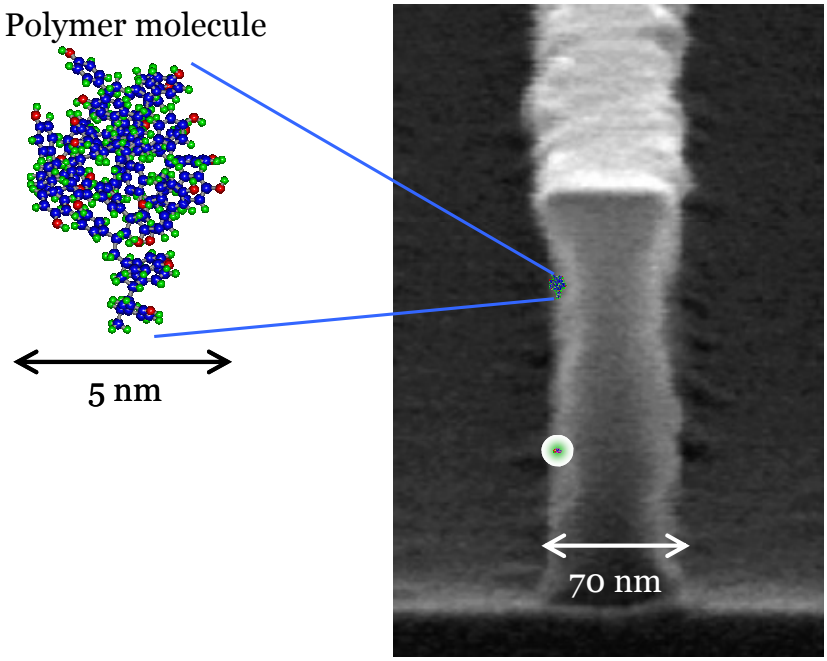

Figure 4.6 Polymer molecule relative to 70 nm feature

GAIN WITHOUT BIAS CONCEPT

As CARs reach the limit of their viability, it becomes necessary to explore the possibility of another fundamental overhaul in resist design. If a system could be designed in which chemical amplification or gain is used while removing the necessity for mass transport

the advantages of CARs and NCARs could be combined. Revisiting IBM's work[61] in the introduction of CARs the use of polyphthalaldehyde (PPHA) and poly (olefin sulfones) as a dissolution inhibitor for novolac represents an intriguing possiblity.

Coupling the gain of CARs to more efficiently exploit available light intensity and utilizing the principle of dissolution inhibition from NCARs to replace small molecule transport could lead to a photoresist featuring gain without bias (Figure 4.7).

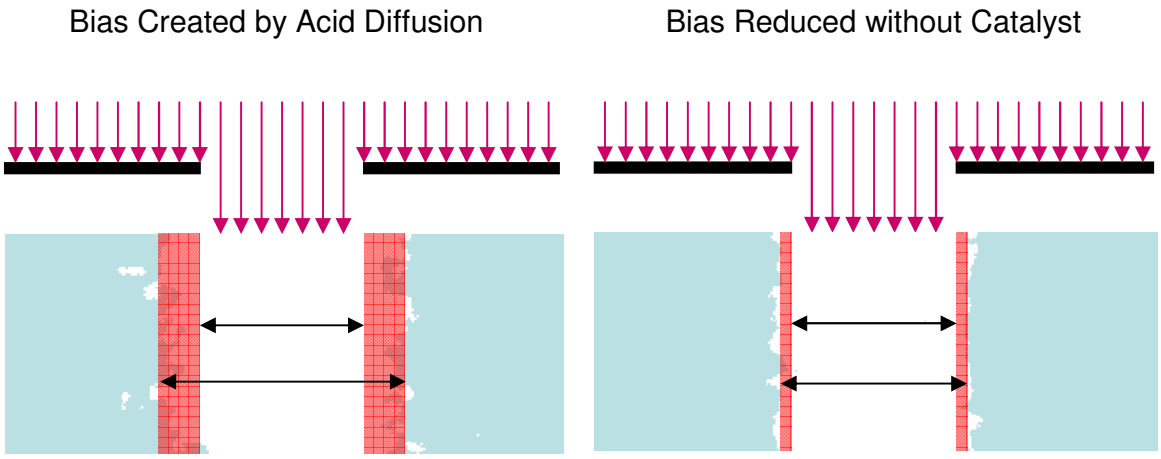

Figure 4.7 Pictorial representation of effect of dark loss due to mass transport

LOW CEILING TEMPERATURE POLYMERS

Polymers are entropicly disfavored relative to monomers. Indeed some polymers cannot be synthesized at room temperature due to the positive Gibbs free energy of the propagation reaction. Sufficiently lowering the temperature suppresses the negative entropic contribution allowing certain monomers that are otherwise not polymerizable at room temperature to be polymerized. For monomers of this sort, the temperature at which there is an equilibrium between the forward polymerization reaction and the

reverse depropagation or 'unzipping' is referred to as the ceiling temperature (T_c). Below the T_c the polymerization may freely occur in appropriate conditions.[68]

A notable example of a low T_c polymer is PPHA (Figure 4.8). PPHA can be formed through anionic polymerization at temperatures below -40 °C.[69] End-capping of the polymer terminates the polymerization. When the temperature of the system is raised above -40 °C, the end-cap prevents depropagation. The acetal backbone of the polymer makes the polymer susceptible to aqueous acid which causes a chain scission leading to depropagation.

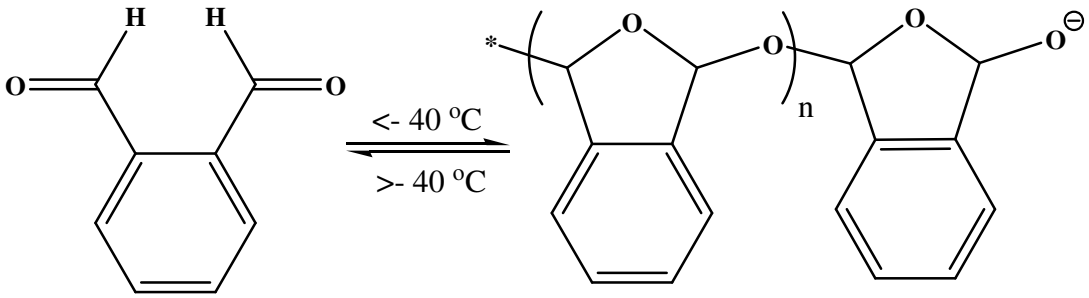

Figure 4.8 Equilibrium of phthalaldehyde and PPHA

FORMULATION OF PPHA WITH NOVOLAC

Due to its history of being successfully incorporated in resist formulations, novolac was targeted as a photoresist platform. Novolac and PPHA, which have been reported to be phase compatible by Ito,[70] were dissolved in PGMEA and spin coated on a silicon wafer. Early attempts failed to produce well blended polymers as phase separation was clearly evident upon inspection of the wafer. The fact that the polymers were phase compatible as reported by Ito is surprising in itself as phase incompatibility of two polymers is generally to be expected.[71] This result does not necessarily call into question Ito's

reports; the reason being two-fold. First, the system Ito reports incorporates either an triaryliodonium or diarylsulfonium salt which may effect polymer blending. Second, novolac consists of a large number of isomeric forms. Some of these forms are more favorable for use in photolithographic applications and as such processing changes targeting these forms have taken place in the time since the initial reports.

To overcome this obstacle, it was postulated that a comonomer would be necessary to induce phase compatibility. Initial copolymerizations were performed utilizing benzaldehyde bearing *para*- Lewis basic sulfones and more exotic *o*-nitro-containing aldehydes to induce photocleavage (Figure 4.9). It was hoped the basic copolymer would interact with the acidic novolac inducing blending by enthalpic contributions[72] and the acid-base interaction would cause the copolymers to behave as a DI.

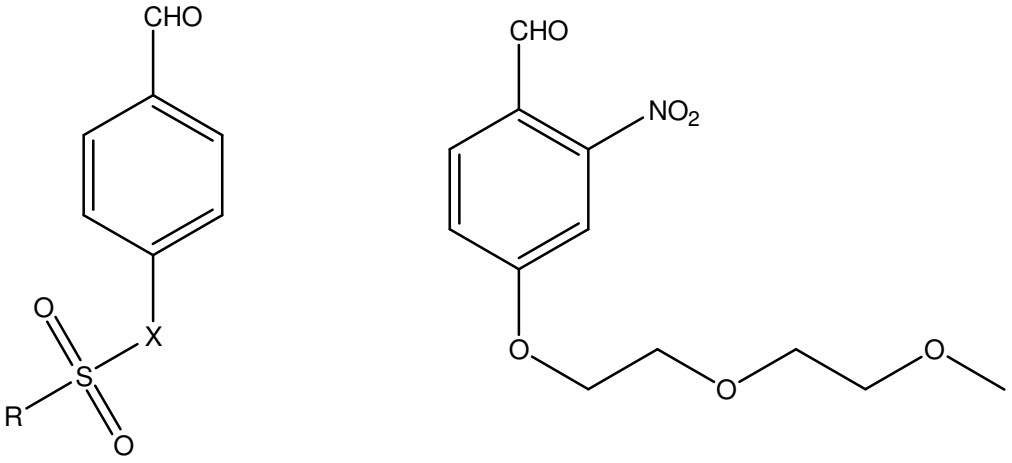

X = O, NH, CH_2
R= Me, C_4F_9

Figure 4.9 Examples of materials tested as comonomers

Ultimately this approach was not successful but significant reduction in the MW of PPHA enabled phase compatibility.

The reduction of MW changes the entropic interactions in the system and indeed does produce a phase compatible blend of PPHA with novolac.[77] As expected, PPHA of MW from ~800-3000 Da functioned as a DI without a comonomer. This result seemed to simplify the problem to be solved.

SWITCHING SOLUBILITY

Ito reported solubility switching in a novolac/PPHA system utilizing the introduction of a comonomer[61] which had been shown to undergo a photochemical rearrangement which induces unzipping of polymer chains.[73] Nitro substituted phenyl rings with a benzyl proton in the *ortho*- position will undergo a photochemical rearrangement oxidizing the benzyl position whilst reducing the nitro substituent to a nitroso group (Figure 4.10).[74] This rearrangement can be harnessed to produce a light catalyzed means of inducing depropogation while removing the necessity for catalytic acid. [75]

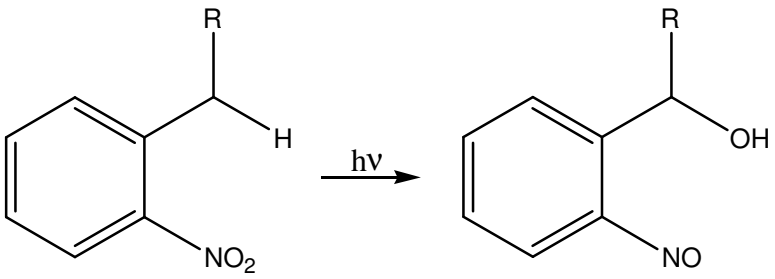

Figure 4.10 Photochemical rearrangement of *o*-nitrobenzyl groups

Incoroporation of *o*-nitrobenzaldehyde (NBA) as a copolymer does enable unzipping of the polymer. This has the notable benefit of removing the necessity for a PEB due to depropogation proceeding rapidly at room temperature. This material satisfied the

requirements of dissolution inhibition and gain without acid catalyst as the depropogation reaction produced non-DI small molecules. This method of incorporation of a photochemically active group is not ideal as unzipping only occurs in one direction.[61] Copolymerization results in some statistical distribution of NBA in the polymer chains. Some chains may have a higher percentage of photoactive sites and are therefore more likely to be cleaved and some may have no incorporation at all. This is particularly true of oligiomeric materials like the ones used.

This problem was overcome through the introduction of the anion of *o*-nitrobenzyl alcohol as an initiator for homopolymerization of phthalaldehyde. In this manner it is ensured that a single photolabile group is included on each polymer chain. It should be noted that as expected the film including PAG functioned at a much lower exposure dose (Figure 4.11). Further work also demonstrated the ability to end-cap the reaction with the chloroformate of NBA, thus providing three methods of incorporation for photolabile groups to PPHA.

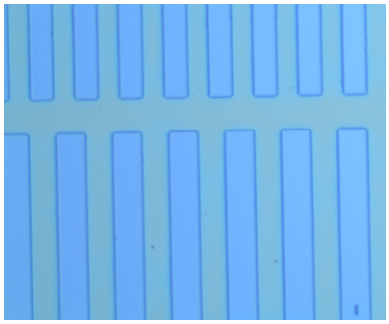

10 wt% with PAG
160 mJ/cm^2

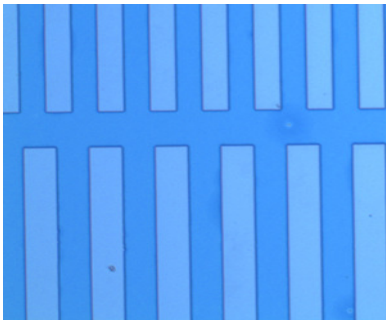

10 wt% without PAG
1800 mJ/cm^2

Figure 4.11 Contact printing of PPHA/novolac system A) with PAG B) without PAG, initiated by *o*-nitrobenzyl alcohol anion

Exposure of these films to light resulted in a disappointing result. Only 50% of the film thickness was reduced after exposure and development. Ito reported incomplete film development and attributed this to the incomplete depropagation due to the method of incorporation of the photoactive comonomer. Further study showed that upon subsequent re-exposure and development, 50% of the remaining film thickness could be developed. Tests revealed that phthalaldehyde is significantly more absorbing of UV light than PPHA (Figure 4.12) however the consistency of half film development regardless of exposure time or number of exposures has yet to be explained.

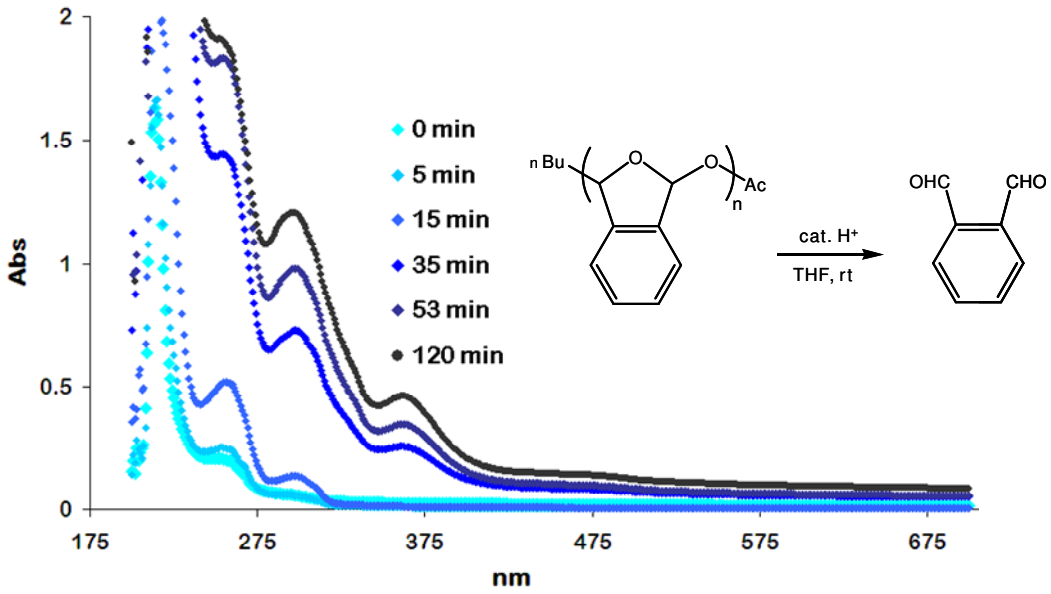

Figure 4.12 Change in absorbance with time for depropagation reaction

TARGETING STYRENIC BASED MATERIALS

While other polyacetals with less strongly absorbing side chains would seem to be the next attractive choice of material to investigate, in practice these materials are difficult to utilize as they form crystalline materials with little to no solubility.[76] Therefore, it was decided that another class of materials should be targeted.

A scan of available literature shows styrenic materials may be a potential replacement for polyacetals as increased electron density on the styrenic olefin rapidly decreases the T_c of those materials (Table 4-1).[77,78]

Table 4-1 Effect of increasing electron density on styrenic materials T_c

Monomer	T_c (^oC)
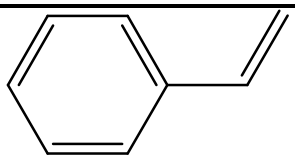	310
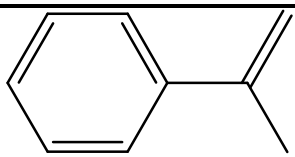	61
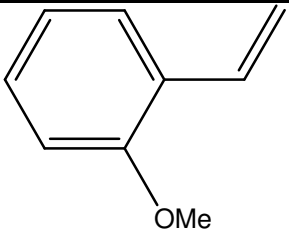	-25

A notable limitation to the use of styrenic materials as PDIs is that they undergo cross-linking upon homolytic chain scission thus increasing the MW and preventing dissolution.[59] Styrenic materials with a methyl group in the *alpha-* position do not undergo cross-linking and the methyl group has the additional positive effect of reducing the T_c. This is particularly important as initial testing of PDIs can be conducted with electron beam lithography (EBL), which causes homolytic chain scissions in a polymer backbone.

CATIONIC POLYMERIZATION

Extremely electron rich olefins are capable of functioning as nucleophiles and are generally not susceptible to radical or anionic polymerization. Many of these materials

will polymerize with cationic initiators. The most common cationic initiators are either protic acids or Lewis acids that typically require a proton donor as coinitiator.[79] The coinitiating systems require only trace amounts of the proton donor and water is typically present in sufficient quantities in systems which were not prepared in an inert atmosphere. Cationic systems may be polymerized in a living manner as first shown by Sawomoto, which gives promise to the ability to control MW and produce materials of similar molecular weights the PPHA described above.[80]

TARGETING MATERIALS

Initial synthetic efforts targeted α,*p*-dimethoxystyrene[81] **4.1** as a potential low T_c material. **4.1** was synthesized in one step from commercially available materials (Figure 4.13).

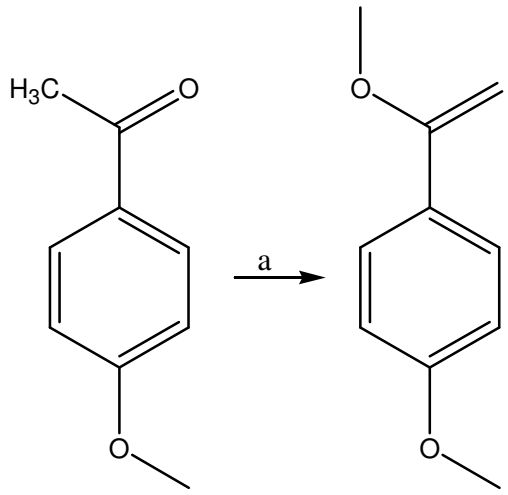

4.1

a. 2.25 eq. trimethylorthoformate, cat. H_2SO_4, MeOH.

Figure 4.13 Synthesis of α,*p*-dimethoxystyrene

It was not surprising that **4.1** failed to polymerize at temperatures as low as -110 ^oC, considering the dramatic effect of only a methyl group in the *alpha*-position. As the

processing requirements only call for depropagation to occur below room temperature, *p*-methoxy-α-methyl styrene (PMMS) **4.2** became the next target. **4,2** is accessible in one step from commercially available, 1-(4-methoxy-phenyl)-ethanone (Figure 4.14).

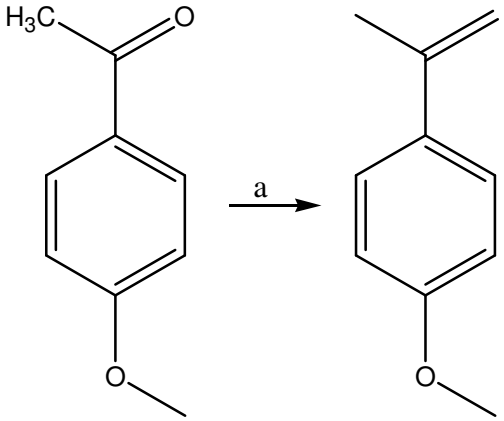

4.2

a. 1.5 eq NaH, 1.3 eq Ph_3PCH_3Br, 0 ^oC, THF, 30 min.

Figure 4.14 Synthesis of *p*-methoxy-*α*-methyl styrene

PMMS was successfully polymerized to form PPMMS via cationic polymerization using boron trichloride as catalyst. It was expected that a comonomer would likely be necessary both to induce both phase compatibility and to cause the material to function as a DI. Additionally, it was expected that living cationic techniques would be required to produce a polymer of sufficiently low MW such that blending could occur. Neither of these expectations was necessary as PPMMS was not only phase compatible but was a highly effective DI. PPMMS was effectively an off-switch for dissolution at 10 wt% relative to novolac in standard 0.26 N TMAH developer.

Because of the effectiveness of the PDI it was necessary to use a different base. Aqueous KOH was used in a series of developments performed to find the maximum

concentration that an unexposed system of PPHA/novolac could resist dissolution. To determine this concentration, wafers were coated with ~400 nm thick PPMMS/novolac films and unexposed films were immersed in various concentrations of KOH for 60 s. At concentrations greater than 0.25 M, rapid and complete film dissolution was observed. At concentrations as low as 0.16 M film erosion and flaking of resist from wafer edges was noticed. It was therefore determined that exposed wafers should be developed with concentrations just less than 0.16 M.

EBL exposures were performed in a 1 mm^2 area on several wafers. An exposed wafer was immersed in 0.14 M KOH. A visual inspection of the wafer revealed the exposed area however profilometry measurements revealed no change in film thickness. Using more concentrated 0.15 M KOH resulted in a clearly visible exposed area with an 80 nm difference in film thickness between unexposed and exposed area. The exposed area was thicker than the unexposed area, which is generally indicative of swelling and therefore high MW polymers. This result has yet to be explained.

CONCLUSIONS/FUTURE WORK

PPHA has been reinvestigated as a PDI for novolac. It was modified from an acid catalyzed switchable system to photo catalyzed system through the incorporation of *o*-nitrobenzaldehyde as a comonomer or alternately utilizing an NBA based initiator or end-capping agent. Photoswitching of the system has been demonstrated however incomplete dissolution of films has not been fully understood. PPMMS has been shown to function as an effective DI of novolac. Future work includes looking into control of the MW of PPMMS to determine the effect of low MW material on solubility switching.

EXPERIMENTAL METHODS

General polymerization of phthalaldehyde: Phthalaldehyde (0.5 g, 3.73 mmol) was dissolved in THF (5 mL) in a 50 mL RBF. The flask was cooled to -78°C. Lithium *tert*-butoxide (1 M in THF, 0.76 mL) was added to the solution via syringe. The reaction mixture was stirred for 8 h. Cold acetic anhydride (1 M in THF, 0.76 mL) was added to the solution via syringe. The mixture was stirred for 1 h at -78°C then warmed to rt. The solution was precipitated in MeOH (50 mL). The white precipitate was filtered, washed with MeOH and dried to yield a white powder (0.433g, 86%). M_n = 2000 Da.

Copolymerization with *o*-nitrobenzaldehyde: The same procedure was followed for incorporation of *o*-nitrobenzaldehye with ~ 5 mol% of the comonomer added. Comonomer incorporation was verified by ^{1}H NMR.

Initiation by *o*-nitrobenzyl alcohol anion: *o*-Nitrobenzyl alcohol (0.114g, 0.746mmol) in THF (10 mL) was deprotonated with 1 eq *n*-BuLi. To this was added phthalaldehyde (1.0g, 7.46mmol) in THF (10 mL). The aforementioned procedure was followed to produce and purify polymer. M_n = 2000 Da.

1-Methoxy-4-(1-methoxy-vinyl)-benzene (**4.1**): 1-(4-Methoxy-phenyl)-ethanone (11.9 g, 79.3 mmol) and trimethylorthoformate (20 mL, ~ 180 mmol) were combined in MeOH (40 mL). Four drops of conc. H_2SO_4 were added and the reaction stirred 12 h. TEA was added to neutralize the reaction and it was then concentrated and distilled (64 °C, 0.34 torr) to yield a colorless liquid (7.83 g, 47.7 mmol, 60.1%). ^{1}H NMR ($CDCl_3$): δ= 7.61 (d, *J*= 9.0 Hz, 2H), 6.90 (d, *J*= 9.0 Hz, 2H), 4.61 (d, *J*= 2.7 Hz, 2H), 4.18 (d, *J*= 2.7 Hz, 2H), 3.81 (s, 1H), 3.76 (s, 1H). ^{13}C NMR: δ=160.50, 159.71, 129.02, 126.49, 113.29, 80.01, 55.04, 54.98. FTIR (cm^{-1})= 3000.18, 2955.20, 2836.87, 1511.30, 1249.01.

1-Isopropenyl-4-methoxy-benzene (**4.2**): Sodium hydride (5.4 g, 225.0 mmol) was placed in a flame dried 1 L RBF to which was added THF (200 mL). The stirred suspension was cooled to 0 ^{o}C. To this was added bromomethyl triphenylphosphine (64.57 g, 180.8 mmol). The reaction was stirred for 30 min before warming to rt followed by addition 1-(4-methoxy-phenyl)-ethanone (21.5 g, 143.2 mmol). After stirring overnight 100 mL H_2O and 100 mL ether were added. The layers were separated and the aqueous layer was extracted 2 x 50 mL ether. The combined organics were washed with brine, dried over $MgSO_4$, filtered and concentrated. The yellow concentrate was purified via column chromatography using 4:1 Hex:EA as eluent. A light yellow solid (8.87 g, 59.5 mmol, 41.5%) was recovered upon concentration. Mp=39-40 ^{o}C. ^{1}H NMR: δ=7.59 (d, *J*= 9.0 Hz, 2H), 7.03 (d, *J*= 8.8 Hz, 2H), 5.52 (s, 1H), 5.20 (s, 1H), 3.90 (s, 3H), 2.32 (s, 3H). ^{13}C NMR: δ=158.95, 142.25, 133.38, 126.34, 113.31, 110.29, 54.71, 21.56. FTIR (cm^{-1})= 3004.62, 2955.25, 2837.55, 1513.40, 1250.92. HRMS (CI^{+}): calc. 149.0966 found 149.0969.

Polymerization of 4.2: In a 50 mL RBF, **4.2** was dissolved in dry DCM (10 mL). The solution was cooled to -78 ^{o}C and 2 drops of di-*tert*-butyl pyridine were added. BCl_3 solution (0.1 mL, 1 M in DCM) was injected and the reaction was quenched after 1 min with MeOH. And the reaction was poured into MeOH (100 mL). The white precipitate (M_n = 16.3-58.3 kDa, PDI = 1.2-1.35) was filtered on a coarse fritted funnel.

Appendix A NMR observation of acid catalyzed Equilibrium

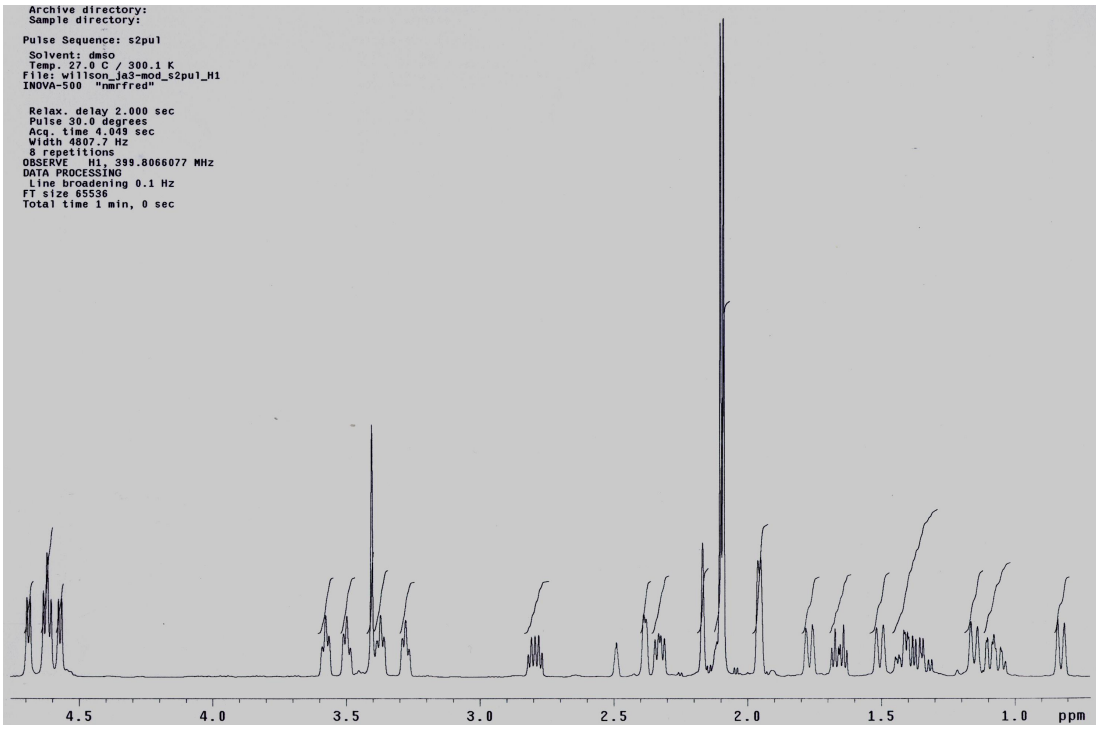

Figure A.1 ^{1}H NMR of **2.1**

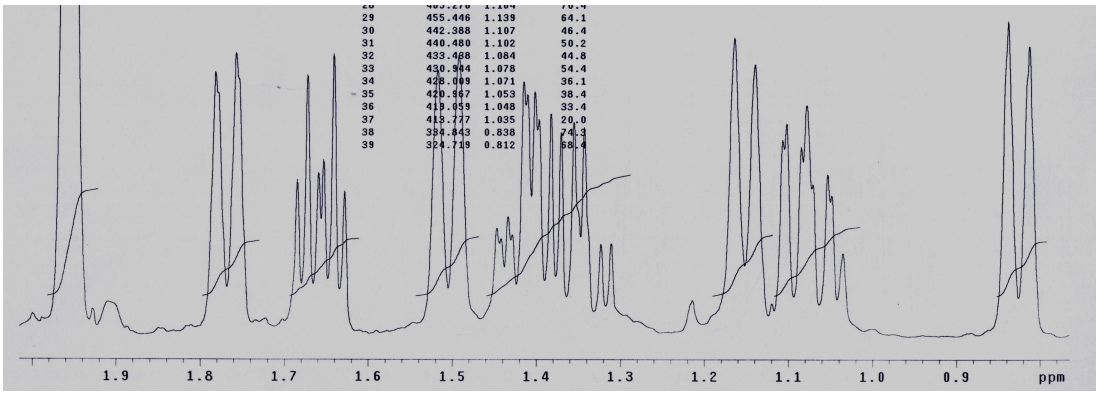

Figure A.2 Expansion of 2.0-0.8 ppm of ^{1}H NMR of **2.1**

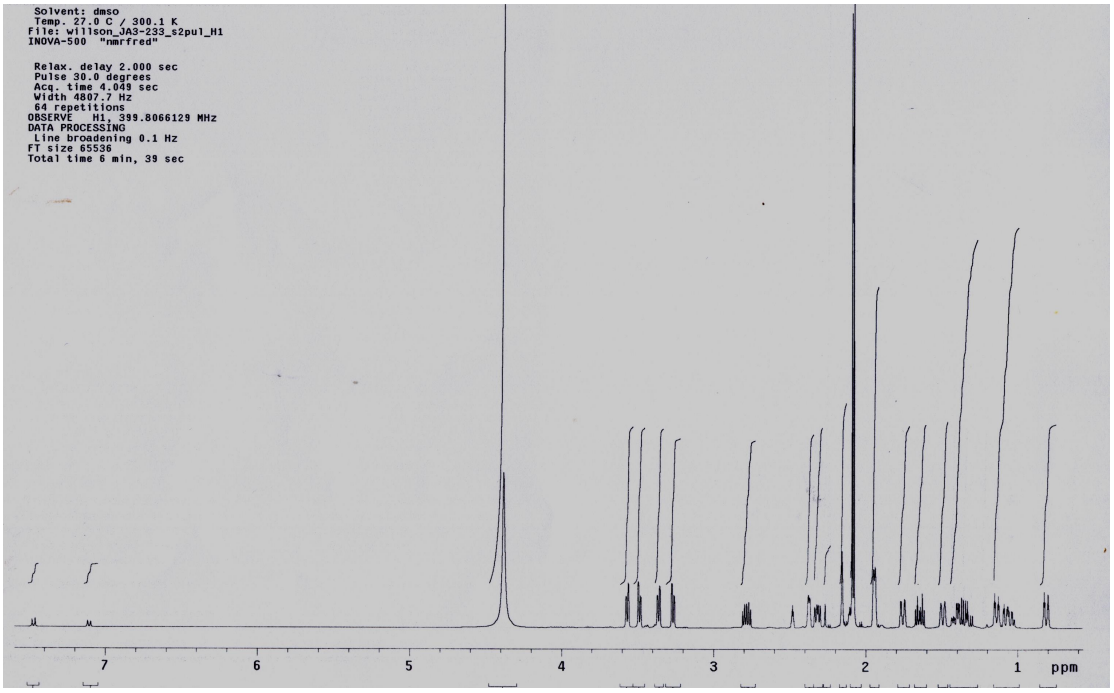

Figure A.3 ^{1}H NMR of 2.1 with catalytic *p*-TSA

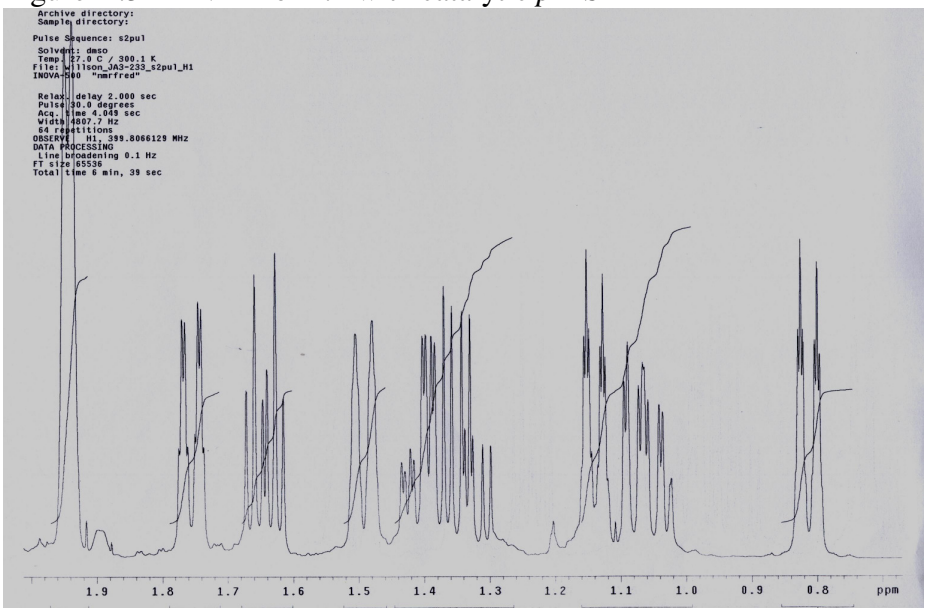

Figure A.4 Expansion of 2.0 -0.8 ppm of ^{1}H NMR of **2.1** with catalytic *p*-TSA showing no change

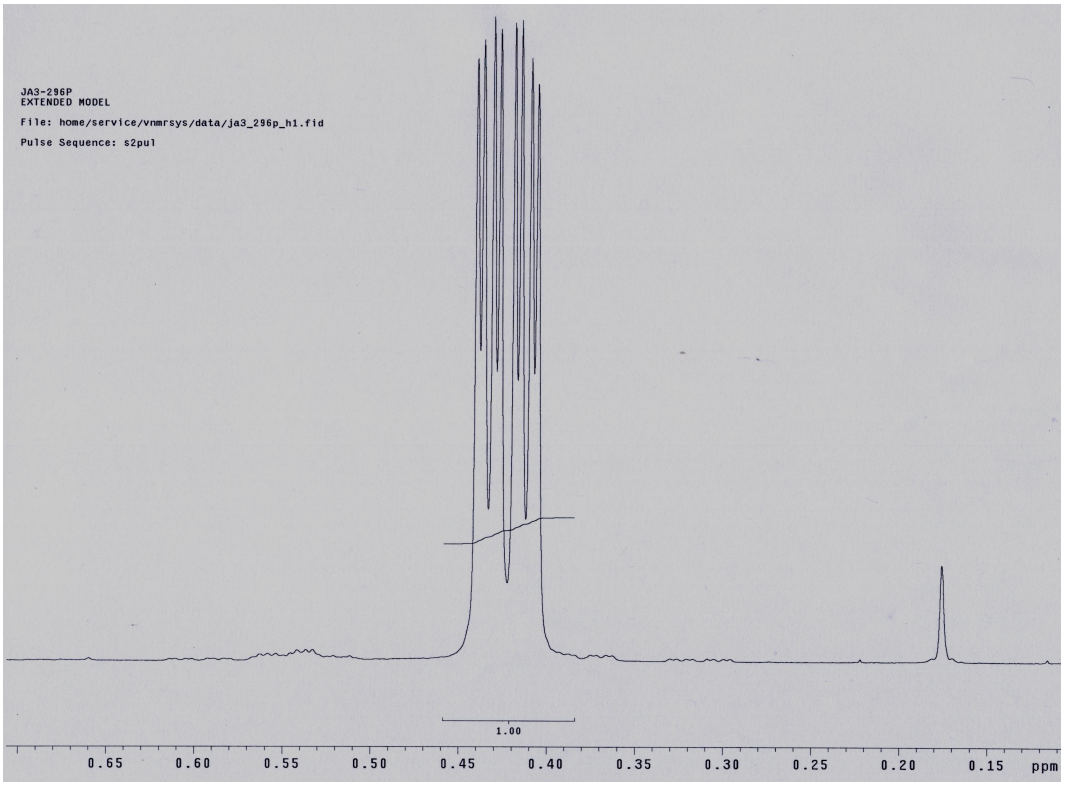

Figure A.5 ^{1}H NMR of methylene spaced **2.31** 0.7-0.2 ppm

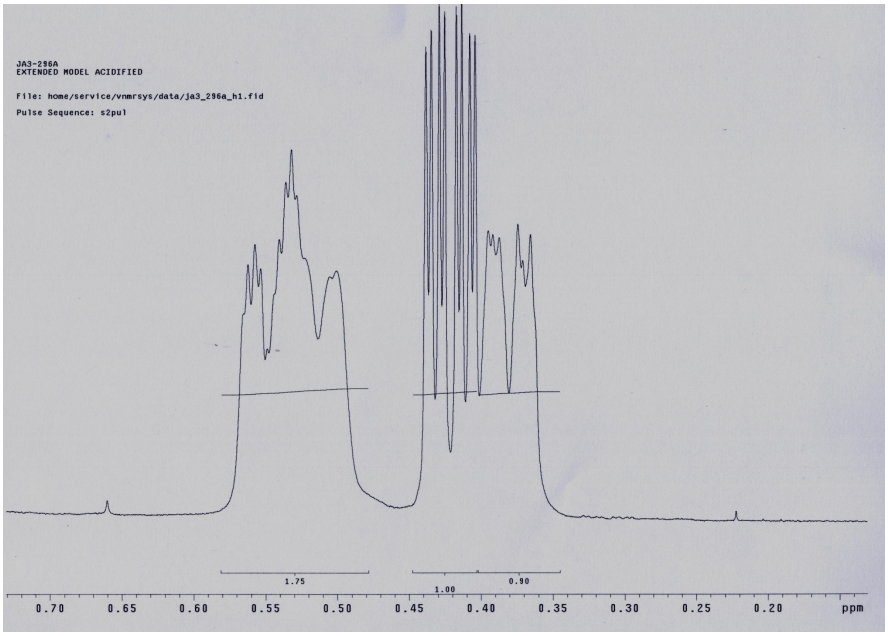

Figure A.6 ^{1}H NMR of methylene spaced **2.31** 0.7-0.2 ppm with catalytic *p*-TSA

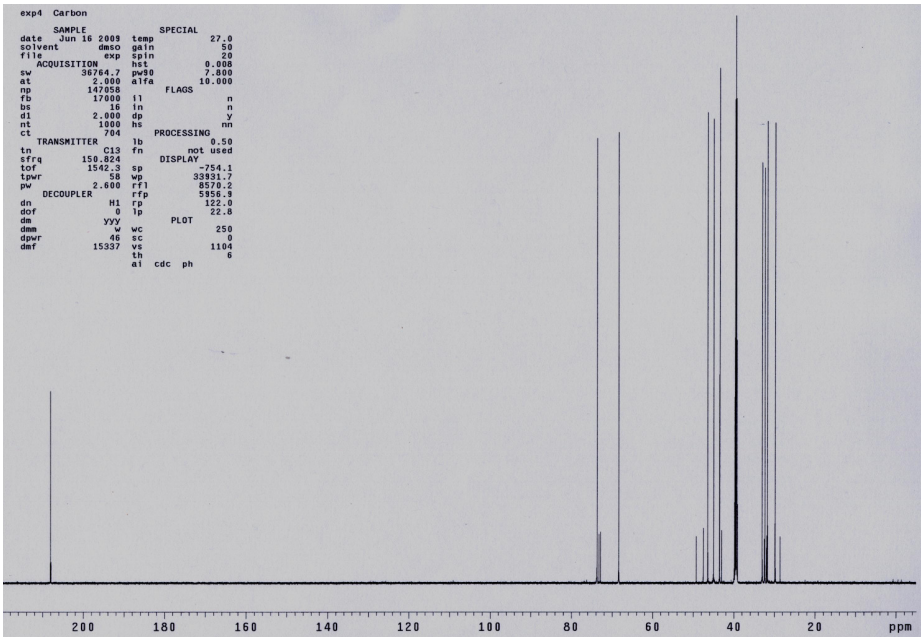

Figure A.7 ^{13}C NMR of **2.31**

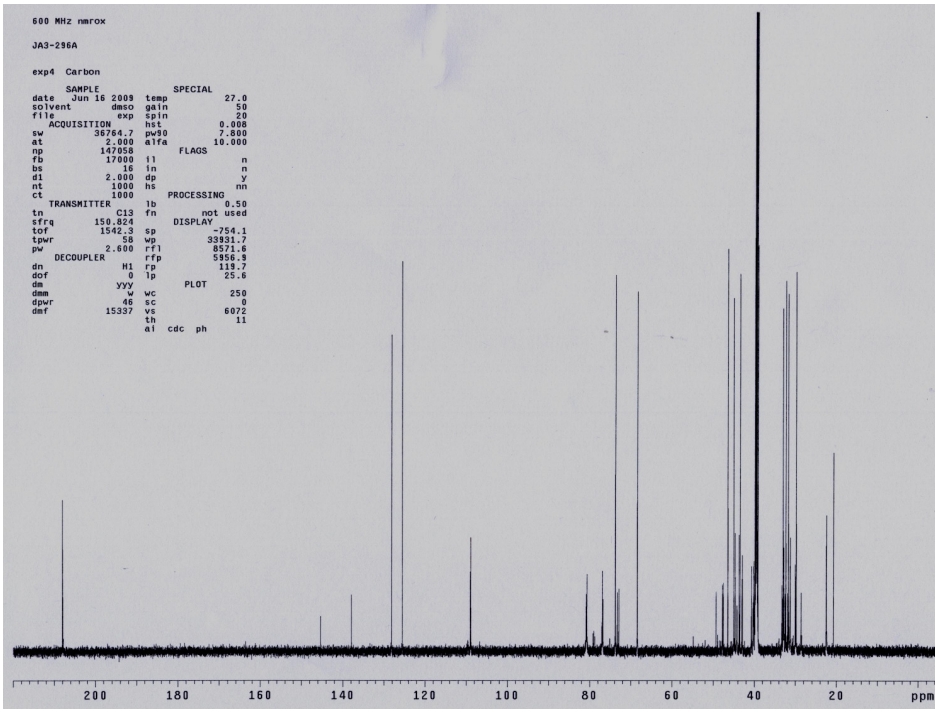

Figure A.8 Figure A-7. ^{13}C NMR of **2.31** with catalytic *p*-TSA demonstrating emergence of additional ethereal carbons and peaks between 100-110 ppm typical of acetal carbons

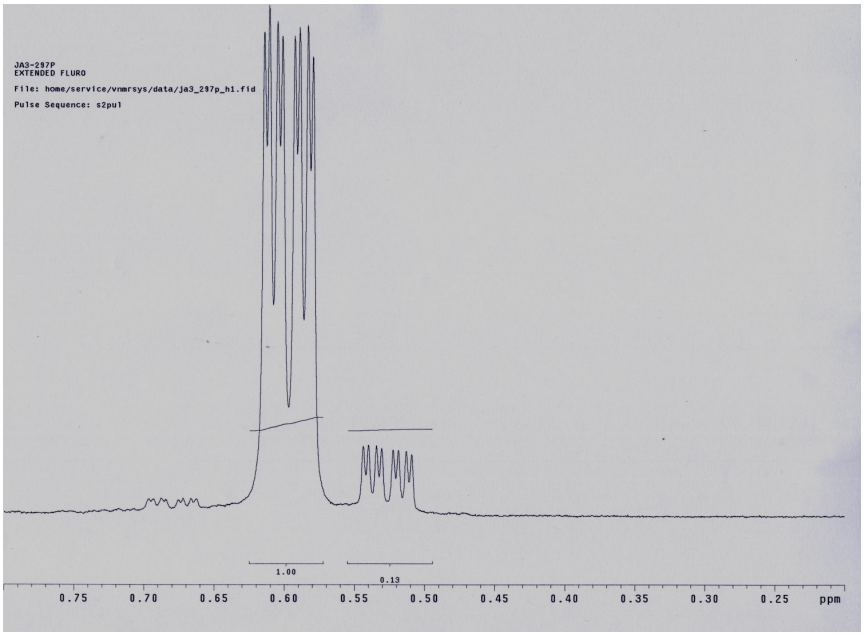

Figure A.9 ^{1}H NMR of trifluoromethyl compound **2.33,** 0.8-0.3 ppm showing additional ddd emerging

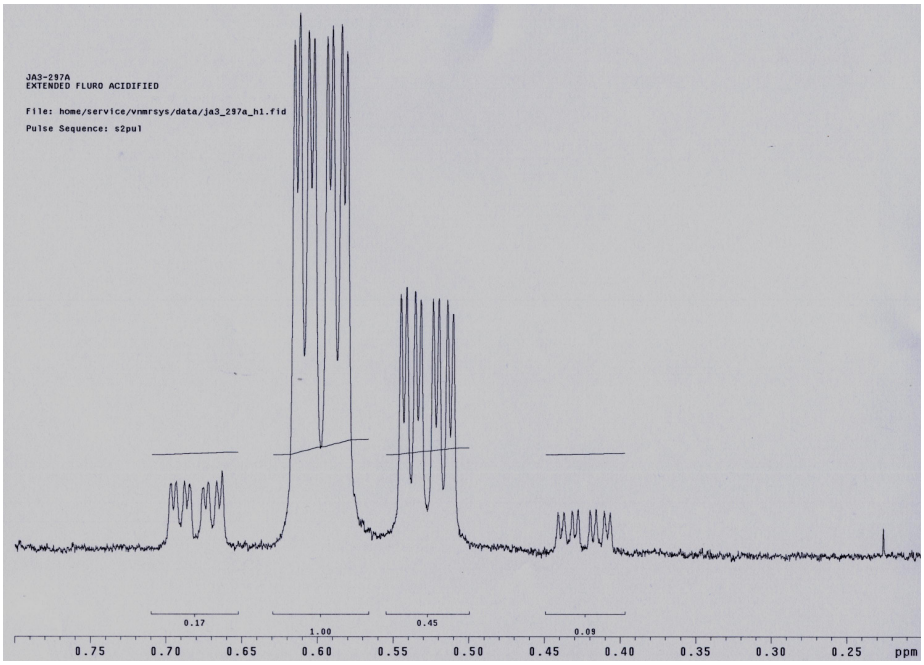

Figure A.10 ^{1}H NMR of trifluoromethyl compound **2.33,** 0.8-0.3 ppm with catalytic *p*-TSA showing emergence of an additional ddd and strengthening of minor ddds

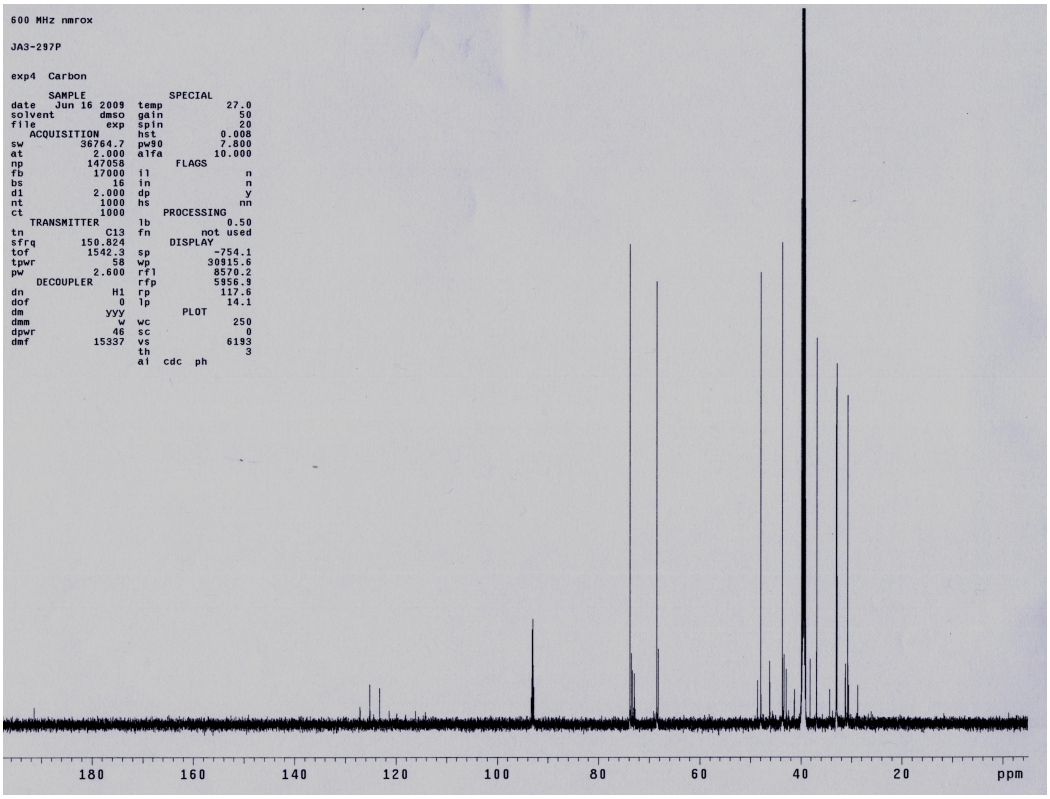

Figure A.11 ^{13}C NMR of trifluoromethyl compound **2.33**

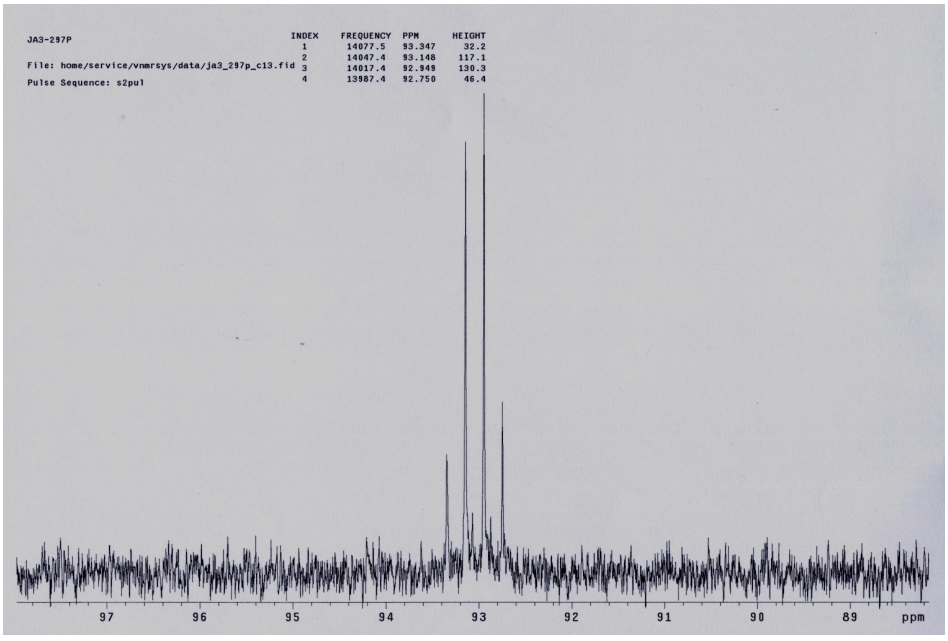

Figure A.12 ^{13}C NMR of trifluoromethyl compound **2.33**, acetal peaks

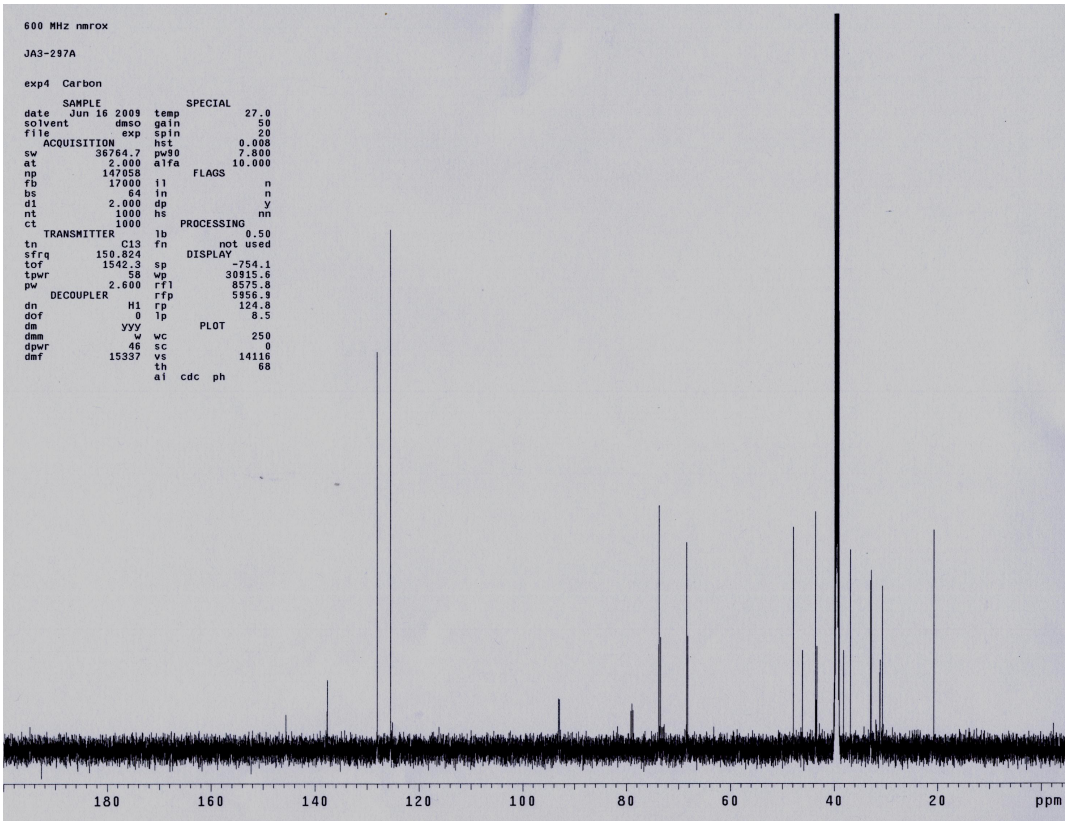

Figure A.13 ^{13}C NMR of trifluoromethyl compound **2.33** with catalytic *p*-TSA

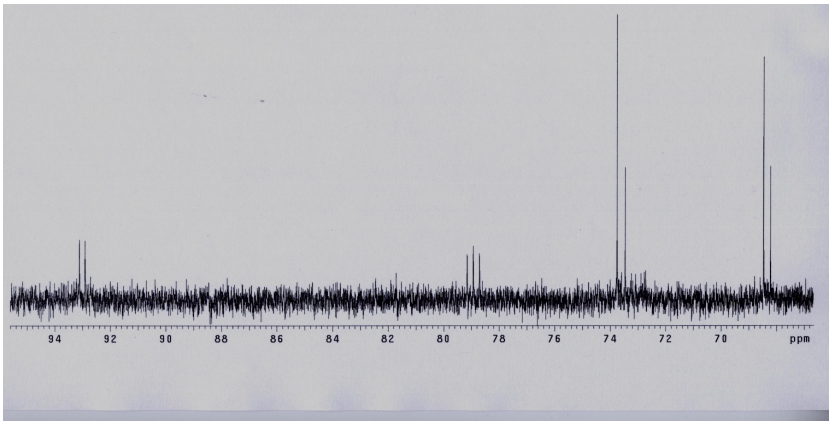

Figure A.14 ^{13}C NMR of trifluoromethyl compound **2.33** with catalytic *p*-TSA expansion

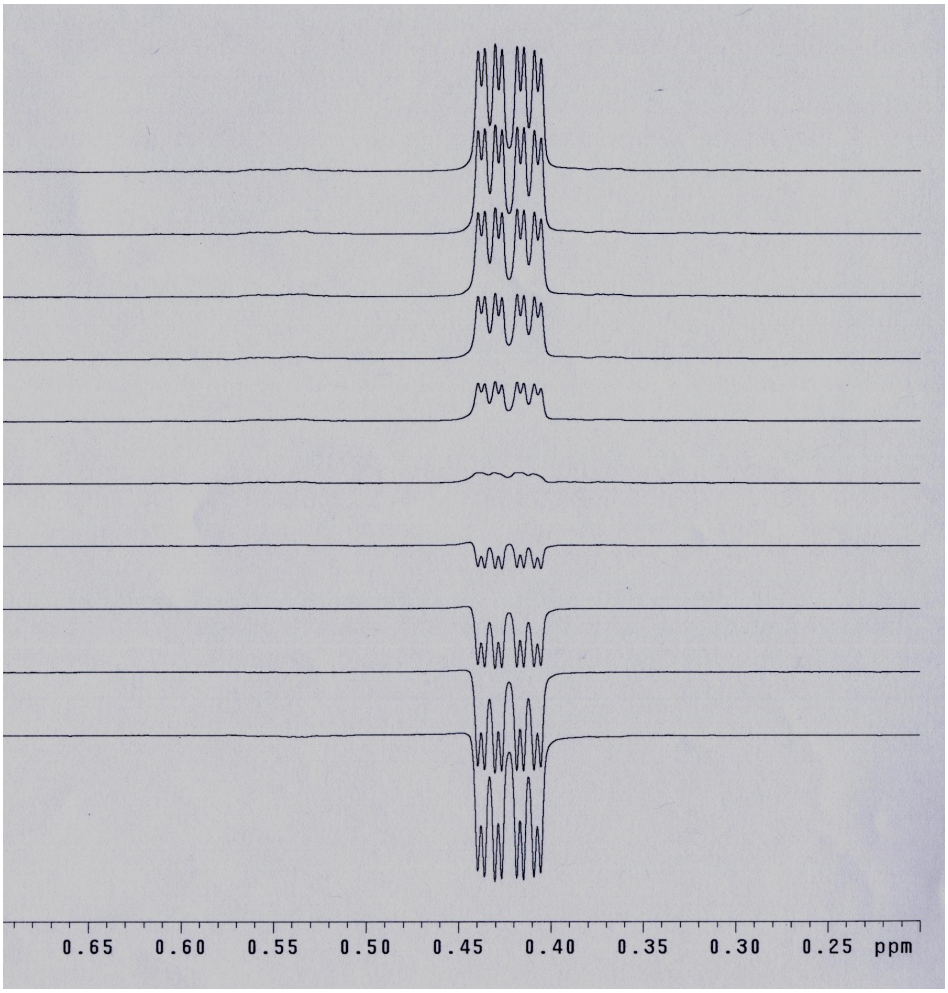

Figure A.15 T_1 Calculation of methylene spaced **2.31**

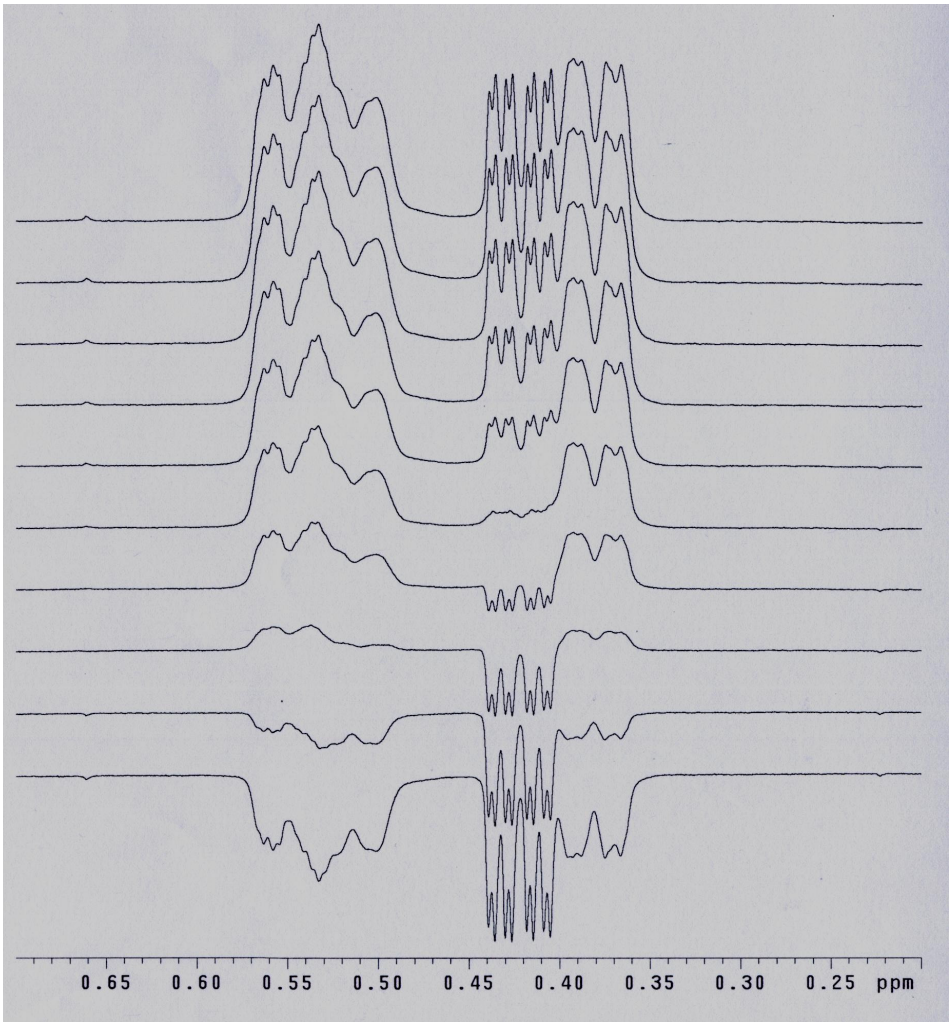

Figure A.16 T_1 Calculation of methylene spaced **2.31** with catalytic *p*-TSA

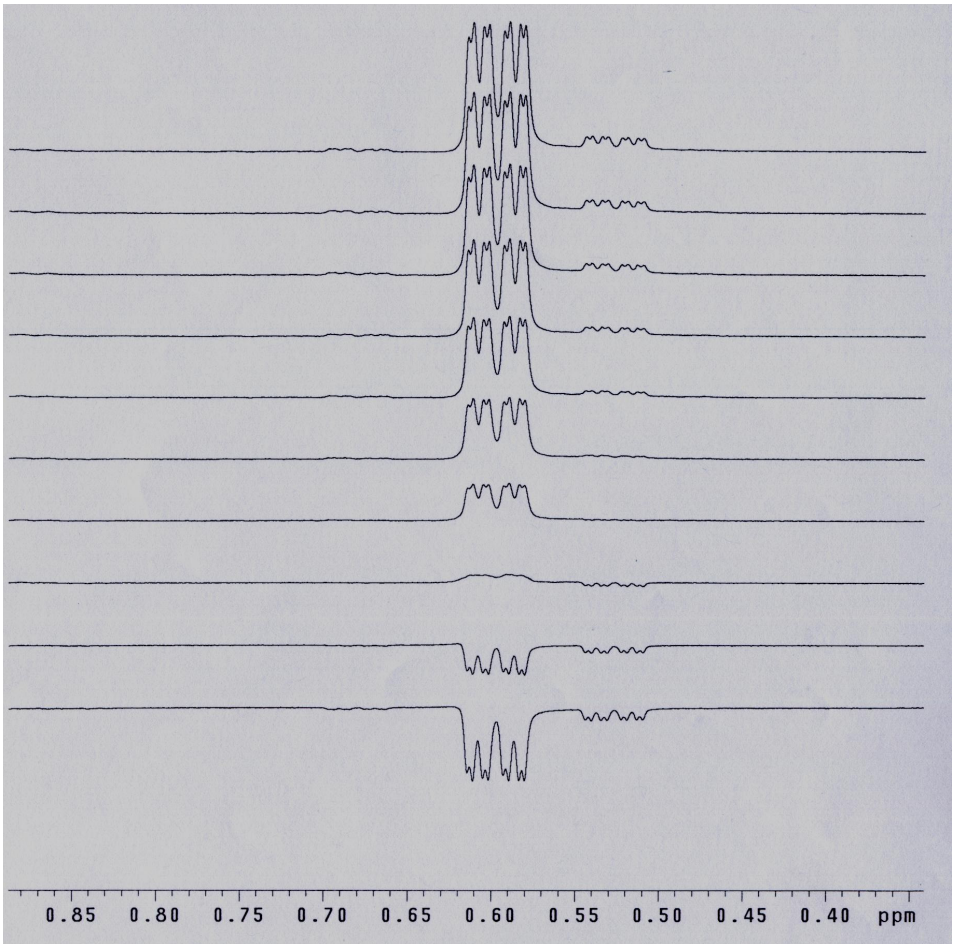

Figure A.17 T_1 Calculation of trifluoromethyl **2.33**

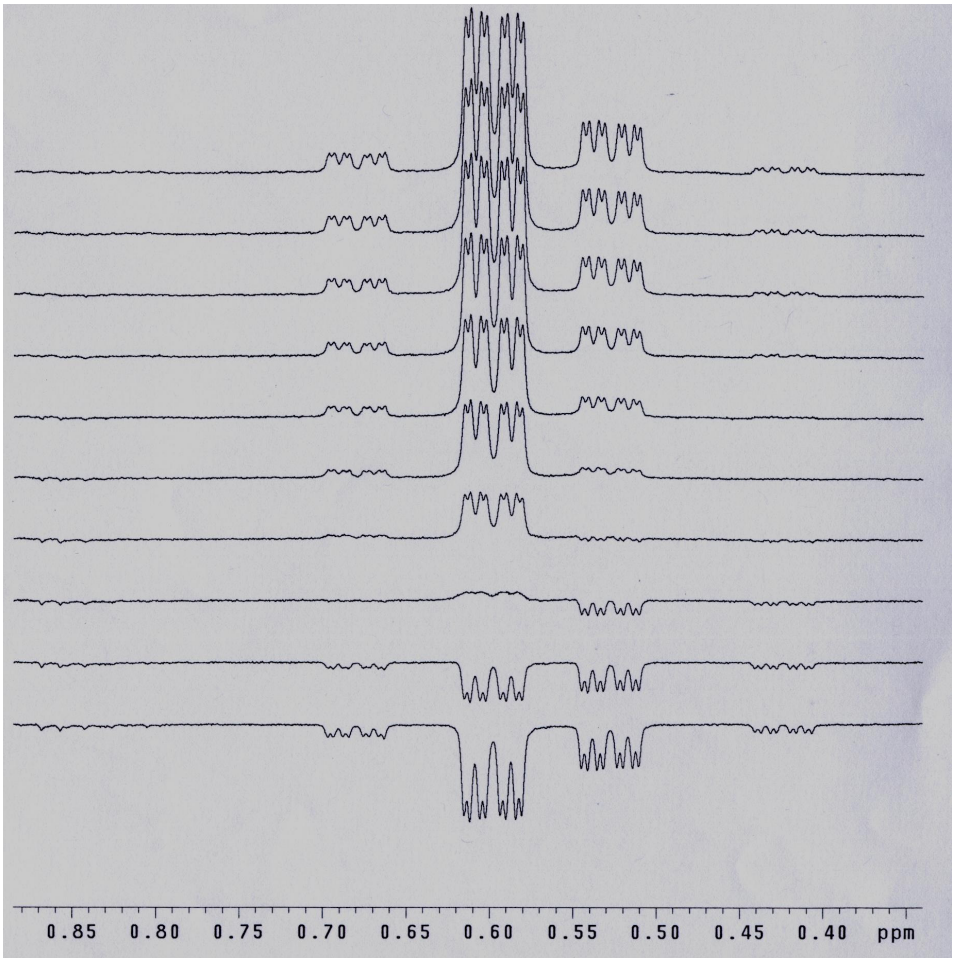

Figure A.18 T_1 Calculation of trifluoromethyl **2.33** with catalytic *p*-TSA

Appendix B Frequently Used Acronyms

ADA	Acetal diacrylate
ADMA	Acetal dimethacrylate
CAR	Chemically amplified resists
CPD	Cyclopentadiene
DI	Dissolution inhibitors
DNQ	Diazonapthoquinone
DSC	Differential scanning calorimetry
DUV	Deep ultraviolet
EGDA	Ethylene glycol diacrylate
EUV	Extreme ultraviolet
HFIPA	Hexafluoroisopropanol
IC	Integrated circuit
ITRS	International technology roadmap for semiconductors
LER	Line edge roughness
LWR	Line width roughness
MW	Molecular weight
NCAR	Non-chemically amplified resists
NIL	Nanoimprint lithography
PAB	Post apply bake
PAG	Photoacid generator
PDI	Polymeric dissolution inhibitor
PEB	Post exposure bake
PHOST	Poly(hydroxy styrene)
PPHA	Polyphthalaldehyde
RI	Refractive index
RIE	Reactive ion etch
ROMP	Ring opening metathesis polymerization
SEC	Size exclusion chromatography
SEM	Scanning electron microscope
SFIL	Step and flash imprint lithography
t-BOC	*tert*-Butyl carbonate
TMAH	Tetramethyl ammonium hydroxide
T_c	Ceiling temperature
T_g	Glass transition temperature
TGA	Thermal gravimetric analysis
UV	Ultraviolet

REFERENCES

[1] Moore, G. E. *Electronics* **1965**, *38(8)*.

[2] http://www.intel.com/technology/timeline.pdf

[3] Summary of fuel economy performance **2004** U.S. DEPARTMENT OF TRANSPORTATION Washington, DC 20590 NHTSA, NVS-220

[4] Gokan, H.; Esho, S.; Ohnishi, Y. *J. Electrochem. Soc.* **1983**, *130(1)*, 143-46.

[5] Patterson, K.; Yamachika, M.; Hung, R.J.; Brodsky, C.J.; Yamada, S.; Somervell, M. H.; Osborn, B.; Hall, D.; Dukovic, G.; Byers, J.; Conley, W.; Willson, C.G. *Proc. SPIE-Int. Soc. Opt. Eng.* **2000**, *3999*, 365-374.

[6] Kunz, R.R.; Bloomstein, T.M.; Hardy, D.E.; Goodman, R.B.; Downs, D.K.; Curtin, J.E. *J. Vac. Sci. Technol. B* **1999**, *17*, 3267-3272.

[7] Chiba, T.; Hung, R. J.; Yamada, S.; Trinque, B.; Yamachika, M.; Brodsky, C.; Patterson, K.; Vander Heyden, A.; Jamison, A.; Lin, S. H.; Somervell, M.; Byers, J.; Conley, W.; Willson, C. G. *J. Photopolymer Sci. Technol.* **2000**, *13*, 657-664.

[8] Partridge, R. H. *J. Chem. Phys.* **1966**, *45 (5)*, 1685-90.

[9] Trinque, B. C.; Chambers, C. R.; Osborn, B. P.; Callahan, R. P.; Lee, G. S.; Kusumoto, S.; Sanders, D. P.; Grubbs, R. H.; Conley, W. E.; Willson, C. G. *J. Fluorine Chem.* **2003**, *122(1)*, 17-26.

[10] Dammel, R.R.; Sakamuri, R.; Kudo, T.; Romano, A.; Rhodes, L.; Vicari, R.; Hacker, C.; Conley, W.; Miller, D. *J. Photopolymer Sci. Technol.* **2001**, *14*, 603-12.

[11] Ito, H., Reichmanis, E., Nalamasu, O., Ueno, T., Eds. *ACS Symposium Series*; American Chemical Society: Washington, DC, **1998,** 208-223.

[12] Somervell, M. H.; Fryer, D. S.; Osborn, B. P.; Patterson, K.; Byers, J.; Willson, C. G. *J. Vac. Sci. Technol., B* **2000***, 18(5),* 2551-2559.

[13] Tran, H.V. "Materials for advanced microlithography: polymers for 157 nm lithography and acid diffusion measurements," *Ph.D. Thesis,* Univ. of Texas, Austin, TX, USA, **2002,** 251 pp.

[14] Hung, R. J-P. "Organic materials for microelectronics: 157 nm photoresists and electrooptic liquid crystals." *Ph.D. Thesis.* Univ. of Texas, Austin, TX, USA. **2001**, 230 pp.

[15] Sanders, D. P.; Connor, E. F.; Grubbs, R. H.; Hung, R. J.-P.; Osborn, B. P.; Chiba, T.; MacDonald, S. A.; Willson, C. G.; Conley, W. *Macromolecules* **2003**, *36(5)*, 1534-1542.

[16] Pinnow, M. J.; Noyes, B. F.; Tran, H. V.; Tattersall, P. I.; Cho, S.; Klopp, J.M.; Bensel, N.; Fréchet, J. M. J.; Sanders, D. P.; Grubbs, R. H.; Willson, C. G. *Polym. Mater. Sci. Eng.* **2002**, *87*, 403-404.

[17] Six C.; Beck, K; Wegner A.; Leitner, W. *Organometallics,* **2000***, 19(22),* 4639-42.

[18] Osborn, B. P. "Vacuum ultraviolet directed design, synthesis and development of 157 nm photoresist materials." *Ph.D. Thesis.* Univ. of Texas, Austin, TX, USA. **2001**, 202 pp.

[19] Grayson, S. M.; Long, B. K.; Kusomoto, S.; Osborn, B. P.; Callahan, R. P.; Chambers, C. R.; Willson, C. G. *JOC* **2006**, *71*(1), 341.

[20] Nagai, T.; Hama, M.; Yoshioka, M.; Yuda, M.; Yoshida, N.; Ando, A.; Koyama, M.; Miki, T.; Kumadaki, I. *Chemical & Pharmaceutical Bulletin* **1989**, *37*(1), 177.

[21] Park, H.; Jang, J.; Sin, K. S. *Archives of Pharmacal Research* **2000**, *23*(3), 202-05.

[22] Romack, T. J.; Harrison, Z. J.; French, D. V.; Amin, D. H.; Hartsell, J. L.; Meyer, J. D. *Macromolecules* **2007**, *40*(20), 7180-83 (2007).; Netopilik, M.; Kratochvil, P. *Polymer* **2003** *44*(12), 3431-36.

[23] Scott, W. J.; Zuman, P. *J. Chem. Soc., Faraday Trans. I* **1976**,*72*, 1192-1200.

[24] Quarterly Reports of Michael Lin.

[25] International Technology Roadmap for Semiconductors 2004 Update Lithography.

[26] Loh, T.-P.; Li, X.-R. *Chem. Comm.* **1996**, *16*, 1929-30.

[27] Dolman, S. J.; Hultzsch, K. C.; Pezet, F.; Teng, X.; Hoveyda, A. H.; Schrock, R. R. *JACS* **2004**, *126*(35), 10945-53.

[28] Claridge, T. *High-Resolution NMR Techniques in Organic Chemistry*; Pergamon, New York, N. Y. **2000**, pp-16-20.

[29] Tatemoto, M. "Polymeric Materials Encyclopedia"; Salamone, J. C., Ed.; CRC: Boca Raton, FL, **1996**; Vol. 5, pp 3847-3860.

[30] Miyamoto, M.; Sawamoto, M.; Higashimura, T. *Macromolecules* **1984**, *17(3)*, 265-68.

[31] Karimi, B.; Golshani, B. *Synthesis* **2002**, 784; Basu, M. K.; Samajda, S.; Becker, F. F.; Banik, B. K. *Synlett* **2002**, 319.

[32] Sun, J.; Dong, Y.; Cao, L.; Wang, X.; Wang, S.; Hu, Y. *JOC* **2004**, *69*(25), 8932-34.

[33] Poulain, S.; Julien, S.; Dunach, E. *Tet Lett* **2005**, *46*, 7077-79.

[34] Luethje, S.; Bornholdt, C.; Luening, U. *Eur. J. Org. Chem.* **2006**, *4*, 909-15.

[35] Slot, E.; Wieland, M. J.; de Boer, G.; Kruit, P.; ten Berge, G. F.; Houkes, A. M. C.; Jager, R.; van de Peut, T.; Peijster, J. J. M.; Steenbrink, S. W. H. K.; Teepen, T. F.; van Veen, A. H. V.; Kampherbeek, B. J. *Proc. SPIE Int Soc. Opt. Eng.* **2008**, *6921*.

[36] Chou, S. Y.; Krauss, P. R.; Zhang, W.; Guo, L.; Zhuang, L. *J. Vac. Sci. Technol., B* **1997**, *15(6)* 2897–2904.

[37] Colburn, M.; Johnson, S.; Stewart, M.; Damle, S.; Bailey, T. C.; Choi, B.; Wedlake, M.; Michaelson, T.; Sreenivasan, S. V.; Ekerdt, J.; Willson, C. G. *Proc. SPIE Int Soc. Opt. Eng.* **1999** *3676* 379-389.

[38] Stewart, M. D.; Johnson, S. C.; Sreenivasan, S. V.; Resnick, D. J.; Willson, C. G. *J. Microlith., Microfab., Microsyst.* **2005,** *4 (1)*, 011002-1-6.

[39] Hua, F.; Sun, Y.; Gaur, A.; Meitl, M. A.; Bilhaut, L.; Rotkina, L.; Wang, J.; Geil, P.; Shim, M.; Rogers, J. A.; Shim, A. *Nano Letters* **2004** *4(12)*, 2467–71.

[40] Schmid, G. M.; Stewart, M. D.; Wetzel, J.; Palmieri, F.; Hao, J.; Nishimura, Y.; Jen, K.; Kim, E. K.; Resnick, D.; Liddle, J. A.; Willson, C. G. *J. Vac. Sci. Technol. B* **2006**, *24(3)*, 1283-91.

[41] Sreenivasan, S. V.; Willson, C. G.; Schumaker, N. E.; Resnick, D. J. *Proc. SPIE Int Soc. Opt. Eng.* **2002**, *4608*, 187–94.

[42] Kim, E. K. "Development and study of nano-imprint and electron beam lithography materials for semiconductor devices." *Ph.D. Thesis*, The University of Texas at Austin, Austin, TX USA **2005**.

[43] Kim, E. K.; Stacey, N. A.; Smith, B. J.; Dickey, M. D.; Johnson, S. C.; Trinque, B. C.; Willson, C. G. *J. Vac. Sci. Technol., B*, **2004**, *22(1)*, 131–35.

[44] Chen, X.; Wudl, F.; Mal, A. K.; Shen, H.; Nutt, S. R. *Macromolecules* **2003**, *36(6)*,1802–07.

[45] Sijbesma, R. P.; Beijer, F. H.; Brunsveld, L.; Folmer, B. J.; Hirschberg, J. H.; Lange, R. F.; Lowe, J. K., Meijer, E. W. *Science* **1997**, *278(5343)*, 1601–04.

[46] Shirai, M.; Kawaue, A.; Okamura, H.; Tsunooka, M. *Chem. Mat.* **2003**, *15(21)*, 4075–81.

[47] Heath, W. H.; Palmieri, F.; Adams, J. R.; Long, B. K.; Chute, J.; Holcombe, T.; Zieren, S.; Truitt, M. J.; White, J. L.; Willson, C. G. *Macromolecules* **2008**, *41(3)*, 719-26.

[48] De Clercq, R. R.; Goethals, E. J. *Macromolecules* **1992,** *25 (3)*, 1109-13.

[49] Ruckenstein, E.; Zhang, H. *Macromolecules* **1999**, *32 (12)*, 3979-83.

[50] Themistou, E.; Patrickios, C. S. *Macromolecules* **2006,** *39 (1)*, 73-80.

[51] Lorette, N. B.; Howard, W. L. *JOC* **1960,** *25*, 521-25.

[52] Palmieri, F. L.. "Step and Flash Imprint Lithography: Materials and Applications for the Manufacture of Advanced Integrated Circuits." *Ph.D. Thesis*, The University of Texas at Austin, Austin, TX USA **2008**.

[53] Ogino, K.; Chen, J.-S.; Ober, C. K. *Chem. Mat.* **1998,** *10 (12)*, 3833-38.

[54] Dickey, M. D.; Burns, R. L.; Kim, E. K.; Johnson, S. C.; Stacey, N. A.; Willson, C. G., *AIChE Journal* **2005,** *51 (9)*, 2547-55.

[55] McMackin, I.; Choi, J.; Schumaker, P.; Nguyen, V.; Xu, F.; Thompson, E.; Babbs, D.; Sreenivasan, S. V.; Watts, M.; Schumaker, N. *Proc. SPIE_Int. Soc. Opt. Eng.* **2004**, *5374*, 222–31.

[56] McMackin, I.; Schumaker, P.; Babbs, D.; Choi, J.; Collison, W.; Sreenivasan, S. V.; Schumaker, N. E.; Watts, M. P. C.; Voisin, R. D. *Proc. SPIE Int Soc. Opt. Eng.* **2003**, *5037*, 178-86.

[57] Bailey, T.; Choi, B. J.; Colburn, M.; Meissl, M.; Shaya, S.; Ekerdt, J. G.; Sreenivasan, S. V.; Willson, C. G. *J. Vac. Sci. Technol., B* **2000**, *18*, 3572–77.

[58] Resnick, D. J.; Bailey, T. C.; Mancini, D.; Nordquist, K. J.; Dauksher, W. J.; Ainley, E.; Talin, A.; Gehoski, K.; Baker, J. H.; Choi, B. J. *Proc. SPIE_Int. Soc. Opt. Eng.* **2002**, *4608*, 176–81.

[59] Thompson, L. F.; Willson, C. G. Bowden, M. J. *Introduction to Microlithography*; 1st ed.; American Chemical Society: Washington, D.C. **1983**, Ch. 3.

[60] Pacansky, J.; Lyerla, J. R. *IBM J. Res. Develop.* **1979**, *23*, 42.

[61] Ito, H. Willson, C. G. *Poly. Eng. Sci.* **1983**, *23(18)*, 1012-18.

[62] Willson, C. G.; Ito, H.; Fréchet, J. M. J.; Tessier, T. G., Houlihan, F. M. *J. Electrochem. Soc*. **1986**, *133(1)*, 181-87.

[63] Postnikov, S. V. "Transport properties of photogenerated acid and silylating agent in polymer films" *Ph.D. Thesis*, The University of Texas at Austin, Austin, TX USA **1999**.; Stewart, M. D. "Catalyst diffusion in positive-tone chemically amplified photoresists" *Ph.D. Thesis*, The University of Texas at Austin, Austin, TX USA **2003**.

[64] Tsiartas, P. C.; Flanagin, L.W.; Henderson, C. L.; Hinsberg, W. D.; Sanchez, I. C.; Bonnecaze, R. T.; Willson, C. G. *Macromolecules* **1997**, *30*, 4656–64.

[65] Stewart, M.; Somervell, M.; Tran, H. V.; Postnikov, S.; Willson, C. G. *Proc. SPIE Int Soc. Opt. Eng*. **2000**, *3999*, 665-74.; Schmid, G. M.; Stewart, M. D.; Singh, V. K.; Willson, C. G. *J. Vac. Sci. Technol., B* **2002,** *20(1)*, 185-90.

[66] Meiring, J. E. "Mesoscale simulation of the photoresist process and hydrogel biosensor array platform indexed by shape" *Ph.D. Thesis*, The University of Texas at Austin, Austin, TX USA **2005**.

[67] "The International Technology Roadmap for Semiconductors-2007" Available online http://www.itrs.net/Links/2007ITRS/Home2007.htm, **2007**.

[68] Joshi, R. M.; Zwolinski "Heats of Polymerization and Their Structural and Mechanistic Implications," in *Vinyl Polymerizations* Vol 1, Part I, Chap. 8 G.E. Ham, ed., Marcel Dekker, New York, **1967**.; Sawada, H. *Thermodynamics of Polymerization*, Chaps. 1,2,5, Marcel Dekker, New York, **1976**.

[69] Aso, C.; Tagami, S.; Kunitake, T. *J. Poly. Sci., Part A-1*, **1969**, *7*, 497.

[70] Ito, H.; Willson, C.G. *Poly. Sci. Eng.* **1983**, *23(18)*, 1012-18; Ito, H. *Proc. SPIE-Int. Soc. Opt. Eng.* **1988**, *920*, 33-41.

[71] Coleman, M. M., Graf, J. F. and Painter, P. *Specific Interactions and the Miscibility of Polymer Blends*, Technomic, **1991**, p.20.

[72] Ting, E. P.; Pearce, E. M. and Kwei, T. K., *J. Polym. Sci. Polym. Lett. Ed.*, 1980, *18*, 201.; Pearce, E. M.; Kwei, T. K. and Min, B. Y., *J. Macromol. Sci. Chem.*, 1984, *21*, 1181.

[73] Petropoulos, C. C. *J. Poly. Sci. Poly. Chem. Ed.* **1977**, *15(7)*, 1637-44.

[74] Paola, P.A.; Wirz, J. *Photochem. Photobiol. Sci.* **2002**, *1(7)*, 441-458.

[75] George, M. V.; Scaiano, J. C. *J. Phys. Chem.* **1980**, *84*, 492-95.

[76] Vogl, O. *J. Poly. Sci.* **1960**, *46*, 241.

[77] Odian, G. *Principles of Polymerization*; 4th ed.; Wiley-Interscience: New York, **2004**.

[78] Okamoto, Y.; Takano, H; Yuki, H. *Polym. J.* **1970**, *1*, 403.

[79] Evans, A. G.; Meadows, G. W. *Trans. Faraday Soc.* **1950**, *46*, 327.

[80] Toshinobu, H.; Masakazu, M.; Mitsuo, S. *Macromolecules* **1979**, *12(2)*, 178-82.

[81] Loudon, G. M.; Smith, C. K., Zimmerman, S. E. *J. Amer. Chem. Soc.* **1974**, *96*, 465.

Vita

Jacob Robert Adams was born in Myrtle Beach, SC on 4 November, 1980 to Rusty and the late Patricia Adams. He graduated from The Georgia Institute of Technology in 2002 with a B.S. in Chemistry.

Permanent address: 103 Wind Tree Lane, Conway, SC 29526

This dissertation was typed by the author.